20 December 2023—Revision 1—*American Mineralogist (MS #9004R)*

An evolutionary system of mineralogy, Part VIII: The evolution of metamorphic minerals

SHAUNNA M. MORRISON,[1] ANIRUDH PRABHU,[1] AND ROBERT M. HAZEN[1,*]

[1]*Earth and Planets Laboratory, Carnegie Institution for Science,*

5251 Broad Branch Road NW, Washington DC 20015, U. S. A.

ABSTRACT

Part VIII of the evolutionary system of mineralogy focuses on 1220 metamorphic mineral species, which correspond to 755 root mineral kinds associated with varied metamorphic rock types, most of which likely formed prior to the Phanerozoic Eon. A catalog of the mineral modes of 2785 metamorphic rocks from around the world reveals that 94 mineral kinds often occur as major phases. Of these common metamorphic minerals, 66 are silicates, 14 are oxides or hydroxides, 8 are carbonates or phosphates, 4 are sulfides, and 2 are polymorphs of carbon. Collectively, these 94 minerals incorporate 23 different essential chemical elements.

Patterns of coexistence among these 94 minerals, as revealed by network analysis and Louvain community detection, point to six major communities of metamorphic phases, three of which correspond to different pressure-temperature (*P-T*) regimes of metamorphosed siliceous igneous and sedimentary rocks, while three represent thermally altered carbonate and calc-silicate lithologies.

Metamorphic rocks display characteristics of an evolving chemical system, with significant increases in mineral diversity and chemical complexity through billions of years of Earth history.

This is the peer-reviewed, final accepted version for American Mineralogist, published by the Mineralogical Society of America.
The published version is subject to change. Cite as Authors (Year) Title. American Mineralogist, in press.
DOI: https://doi.org/10.2138/am-2023-9004. http://www.minsocam.org/

Earth's first metamorphic minerals formed in thermally altered xenoliths and contact zones (hornfels and sanidinite facies) associated with early Hadean igneous activity (> 4.5 Ga). The appearance of new Hadean lithologies, including clay-rich sediments, arkosic sandstones, and carbonates, provided additional protoliths for thermal metamorphism prior to 4.0 Ga. Orogenesis and erosion exposed extensive regional metamorphic terrains, with lithologies corresponding to the Barrovian sequence of index mineral metamorphic zones appearing by the Mesoarchean Era (> 2.8 Ga). More recently, rapid subduction and rebound of crustal wedges, coupled with a shallowing geothermal gradient, has produced distinctive suites of blueschist, eclogite, and ultrahigh pressure metamorphic suites (< 1.0 Ga). The evolution of metamorphic minerals thus exemplifies changes in physical and chemical processes in Earth's crust and upper mantle.

***E-mail:** rhazen@carnegiescience.edu

ORCID: 0000-0003-4163-8644

Keywords: metamorphism; Barrovian sequence; philosophy of mineralogy; classification; mineral evolution; Hadean Eon; Archean Eon; network analysis; community structure analysis

This is the peer-reviewed, final accepted version for American Mineralogist, published by the Mineralogical Society of America.
The published version is subject to change. Cite as Authors (Year) Title. American Mineralogist, in press.
DOI: https://doi.org/10.2138/am-2023-9004. http://www.minsocam.org/

INTRODUCTION

Metamorphism: the word, itself, means change through time—"evolution" by that contentious word's most basic definition. Every metamorphic mineral assemblage derives from prior minerals. Each metamorphic rock has a history revealed in the varied attributes of its phases—deep-time stories of changing crustal and mantle environments that epitomize mineral evolution.

And yet, paradoxically, metamorphic minerals are among the most difficult to place into an unambiguous, historical narrative. Each new suite of metamorphic phases—generation after generation of prograde followed by retrograde transformations—may partially mask what came before. Unlike the holocrystalline igneous assemblages featured in Part VII of this series (Hazen et al. 2023), coexisting metamorphic minerals are often in disequilibrium. In this contribution, though not fully resolving those ambiguities, we attempt to add metamorphic minerals to the larger context of the evolving mineral kingdom.

The evolutionary system of mineralogy is an effort to place all of the more than 6000 mineral species approved by the International Mineralogical Association's Commission on New Minerals, Nomenclature, and Classification (IMA-CNMNC; https://rruff.info/ima, accessed 17 December 2023) into their historical and paragenetic contexts (Hazen 2019; Cleland et al. 2021; Hazen and Morrison 2022; Hazen et al. 2022). The initial five parts of the system cataloged almost 300 mineral kinds that occur as primary and secondary phases in meteorites (Hazen and Morrison 2020, 2021; Morrison and Hazen 2020, 2021; Hazen et al. 2021). Part VI focused on Earth's earliest mineralogy, including 262 species formed via a variety of igneous, hydrothermal, aqueous alteration, and other near-surface processes (Morrison et al. 2023).

Part VII on "The evolution of the igneous minerals" documented 1665 primary species that crystallized from a melt, with special attention to associations and antipathies among the most common 115 kinds of igneous minerals (Hazen et al. 2023).

Our exploration of the evolution of metamorphic minerals is organized into five main sections.

1. The first section considers the unusual character of metamorphic mineral evolution as a historical pursuit, while outlining four significant challenges to this effort.
2. Section 2 reviews the sources of mineralogical data employed in this study, while introducing eight major groups of metamorphic minerals that represent different formational environments and/or compositional ranges.
3. As in prior parts of the evolutionary system, extensive tabulations of metamorphic mineral co-existence data are particularly ammenable to mineral network analysis (Newman 2010; Morrison et al. 2017) and community structure analysis (Girvan and Newman 2002; Fortunato 2010). Therefore, the third section applies these methods to explore patterns of mineral coexistence in metamorphic rocks. We present a data resource that records patterns of coexistence among 73 relatively common metamorphic minerals in 2785 diverse metamorphic rocks, with a consideration of potential preservational and anthropogenic biases in the literature of metamorphic petrology.
4. Section 4, addressing the evolution of metamorphic minerals at a planetary scale, considers if there have been significant changes in the nature of metamorphism through more than 4 billion years of Earth history.

This is the peer-reviewed, final accepted version for American Mineralogist, published by the Mineralogical Society of America.
The published version is subject to change. Cite as Authors (Year) Title. American Mineralogist, in press.
DOI: https://doi.org/10.2138/am-2023-9004. http://www.minsocam.org/

5. Finally, Appendix I details the nature and distribution of 94 of the most common minerals in metamorphic rocks, as well as the modified nomenclature employed in this contribution for some mineral kinds.

1. On the nature of "metamorphic mineral evolution"

In Part VIII of the evolutionary system we consider metamorphic minerals, many of which first appeared prior to 2.5 Ga, though some high-pressure metamorphic lithologies appear to be confined to the past billion years (Carswell and Compagnoni 2003; Palin and White 2016; Brown and Johnson 2019). The strategy, as outlined in previous contributions, is to identify historical processes that produced minerals with diagnostic combinations of physical and chemical attributes—what we suggest are "historical natural kinds" (Boyd 1991, 1999; Hawley and Bird 2011; Magnus 2012; Khalidi 2013; Ereshevsky 2014; Godman 2019; Cleland et al. 2021; Hazen et al. 2022). By so doing, the evolutionary system complements standard taxonomic protocols of the IMA-CNMNC, which differentiate each mineral "species" based on its unique combination of major element chemistry and idealized atomic structure (e.g., Burke 2006; Mills et al. 2009; Schertl et al. 2018; Hatert et al. 2021; Hazen 2021; Hawthorne et al. 2021).

Here we consider the diversity, distribution, and ages of 1220 metamorphic minerals, all but five of which (*Fe-dolomite*, *olivine*, *phengite*, *plagioclase*, and *silicate glass*) are species approved by the IMA-CNMNC (https:rruff.info/ima; accessed 17 March 2023). We define a metamorphic mineral as a naturally occurring solid phase that forms by the transformation of one or more prior solid phases through the sustained action of temperature and/or pressure. This definition is consistent with that of Philpotts and Ague (2009): "Metamorphism is the sum

111 of all changes that take place in a rock as a result of changes in the rock's environment; that is,
112 changes in temperature, pressure (directed as well as lithostatic), and composition of fluids.
113 The changes in a rock may be textural, mineralogical, chemical, or isotopic." Note, however,
114 that we restrict the focus to mineralogical changes resulting from T > ~150 °C up to
115 temperatures that cause melting and magma genesis. By this definition, we include regional
116 metamorphism from zeolite to ultrahigh temperature (UHT) facies; contact (i.e., thermal)
117 metamorphism from hornfels and sanidinite facies; and ultrahigh pressure metamorphism from
118 blueschist, ecologite, and ultrahigh pressure (UHP facies). However, we do not consider
119 alteration by impacts, lightning, or other transient processes that are considered in other parts
120 of this series (e.g., Hazen et al. 2023; Morrison et al. 2023). Furthermore, alterations that result
121 from biological sources, notably pyrometamorphism by hydrocarbon combustion, as well as
122 metamorphism of biomediated protoliths such as coal and phosphorites, will be considered in a
123 subsequent part of this series.

124 Metamorphism might seem the quintessential example of mineral evolution because
125 metamorphic assemblages by definition require sequential mineralogical changes through time.
126 However, the conventions of the evolutionary system of mineralogy result in four inherent
127 difficulties related to: (1) determining the timing of metamorphism; (2) documenting the
128 sequence and environment of metamorphic mineral paragenesis; (3) dealing with the critical
129 importance of many mineral's variable compositions owing to solid solution; and (4)
130 deciphering the important roles of fluids in metamorphism. In this contribution we only
131 partially resolve these four challenges.

132

1. *The timing of metamorphic mineralization:* Mineral evolution, as originally presented by Hazen et al. (2008), considers the near-surface (< 3 km) mineralogy of terrestrial planets and moons. Three factors were cited to justify this depth criterion: (1) these are the minerals most easily documented on Earth, (2) they are the minerals we are most likely to observe on other terrestrial worlds, and (3) interactions with cellular life occur primarily in this near-surface domain. Any consideration of the mineral evolution of much deeper regimes must inevitably lead to increased degrees of speculation and uncertainty.

Complications may arise because Earth's near-surface mineral inventory originates both from near-surface paragenesis (e.g., volcanism, evaporation, biomineralization), and from much deeper processes (igneous intrusion, deep hydrothermal mineralization, regional and ultrahigh pressure metamorphism). In the latter instances, a mineral is included in our tabulations only if it subsequently appears in the shallow crust, usually through some combination of volcanic, tectonic, and/or erosional processes. Consequently, the timing of a metamorphic mineral's appearance in a relatively shallow crustal environment likely postdates its formation age by tens to as much as hundreds of millions of years (e.g., Ganade et al. 2023)—a vast interval during which retrograde compositional and structural alterations are common.

Evidence for this protracted history is provided by the observation that the volume of metasedimentary rocks *at Earth's surface* for different geological ages has significantly decreased over the past 600 Myr. An average of > 40 vol % of the exposed lithologies of Neoproterozoic age (1000 to 541 Ma) are metamorphic rocks, compared to < 20 vol % of surface lithologies from the subsequent Phanerozoic Eon (Bluth and Kump 1991; Peters

and Husson 2017; Peters et al. 2018; Lipp et al. 2021; https://macrostrat.org, accessed 31 December 2022). In spite of this disparity, we suggest that the total volume of metasediments, including those still buried deep within the crust, has likely not diminished significantly over the past billion years. The occurrences, extents, and ages of near-surface metamorphic minerals are as much functions of the rates of tectonic and erosional processes as they are of the deep transformation of protoliths at pressure and temperature. Therefore, somewhat paradoxically, the evolution of metamorphic minerals at once provides some of the clearest examples of an evolutionary sequence of mineralogical states, while defying any simple statistical evaluation of the changing diversity and distribution of metamorphic minerals through deep time.

2. *The sequence of metamorphic mineralization:* The inevitable extended time intervals required for a protolith's burial, metamorphism, and uplift are particularly challenging in any attempt to document the exact sequence of a metamorphic mineral's evolution. On the one hand, metamorphic minerals, in contrast to those from most other paragenetic processes, represent a true *sequential* and *congruent* evolutionary pathway. Every metamorphic mineral assemblage was derived by the stepwise alteration of an igneous, sedimentary, or metamorphic protolith (Goldschmidt 2011), often with multiple transformations that reflect changes in the mineralizing temperature, pressure, and/or fluid composition (Barrow 1893; Eskola 1920; Bowen 1940; Tilley 1951). One can thus visualize an evolutionary metamorphic pathway with successive prograde and retrograde chemical reactions, illustrated for example on pressure-temperature-time diagrams

(Philpott and Ague 2009, their Figure 16-6, and references therein) or through a series of tree or network graphs (e.g., Heaney 2016; Morrison et al. 2017).

On the other hand, the temporal details of a metamorphic rock's history may be scrambled and difficult to interpret. Many metamorphic processes occur deep in the crust or upper mantle; hundreds of millions of years may be required for tectonic processes and erosion to expose highly altered metamorphic terrains.

An additional conundrum relates to metamorphic rocks, particularly lower grade contact and regional metamorphic formations, with biologically-derived protoliths. The processes of contact and regional metamorphism likely commenced long before the first living cells, and many metamorphic formations are unambiguously abiotic—i.e., arising via purely chemical and physical processes. However, the burial and alteration of coal, phosphorites, and a wide range of fossil-bearing limestone, marl, shales, and other biogenic deposits must postdate their Phanerozoic origins. Furthermore, the resultant metamorphic minerals, even if representing the same IMA-CNMNC-approved species as those in much more ancient abiotic rocks, may preserve diagnostic biosignatures in their trace elements, isotopes, morphologies, and other attributes. If so, then by the conventions of the evolutionary system these metamorphic phases represent distinct and relatively recent biologically mediated mineral kinds. Consequently, we defer discussion of the metamorphism of biotic protoliths until the final part of this series.

3. *Mineral solid solution*: Most diagnostic metamorphic minerals display significant solid solution, ranging from binary systems [e.g., olivine $(Mg,Fe)_2SiO_4$], to minerals with 4 or

more chemical degrees of freedom [e.g., "hornblende" $(Na,K)Ca_2(Mg,Fe^{2+},Al,Fe^{3+})_5(Si,Al)_8O_{22}(OH,F,Cl)_2$]. Continuous compositional variations with changes in temperature, pressure, and/or fluid composition are central to understanding metamorphic processes, especially teasing out the evolution from one mineral assemblage to the next. However, the nomenclature adopted by the IMA-CNMNC, as well as in the evolutionary system in its present preliminary form, are ill-suited to describing such subtle yet critical shifts in element ratios.

For example, both the IMA and evolutionary systems employ the end-member olivine minerals forsterite (Mg_2SiO_4) and fayalite (Fe_2SiO_4), neither of which is particularly useful when dealing with the variable intermediate Mg-Fe compositions of olivine in metamorphosed mafic and ultramafic rocks. Consequently, we add *olivine* as a mineral kind defined as $(Mg,Fe)_2SiO_4$ with $0.3 < Fe/(Fe + Mg) < 0.7$. Similarly, while the IMA system names only end-member compositions in the ternary of Ca-Na-K feldspars as valid mineral species, most natural specimens have intermediate compositions along either the Ca-Na (plagioclase) or Na-K (alkali feldspar) binaries and, in the extreme case of ultrahigh temperature facies, feldspar compositions may lie well within the ternary region (e.g., Harley 2021, their Figure 20).

This situation is especially concerning when comparing the mineralogy of very different protoliths. For example, near end-member forsterite formed during the contact metamorphism of dolomite differs significantly from intermediate olivine in metabasalt with Mg > Fe. Both minerals are classified as "forsterite" in the IMA formalism, though we call intermediate Mg-Fe olivine compositions *olivine*. Until we have much more

information on the compositional idiosyncrasies associated with minerals from different metamorphic environments (i.e., the "metamorphic mineral kinds"), these ambiguities in nomenclature will limit our efforts.

An additional challenge with respect to mineral nomenclature is the use of some names in the metamorphic petrology literature that do not coincide with approved mineral species. For example, "breunnerite" is not an approved mineral name, yet it is commonly applied to intermediate compositions of the magnesite—siderite [$(Mg,Fe)CO_3$] solid solution, where $0.1 > Fe/(Mg+Fe) > 0.3$. In our study, all such occurrences are reported as the Mg end-member, *magnesite*. Ankerite, by contrast, is an IMA-approved name for minerals in which Fe > Mg on the dolomite—ankerite [$Ca(Mg,Fe)(CO_3)_2$] binary. However, "ankerite" has been traditionally employed in the metamorphic petrology literature for a range of ferroan dolomites, including the majority with $Fe/(Mg + Fe) < 0.5$ (e.g., Chang et al. 1996; Ferry 1996; Ferry et al. 2015)—all occurrences that IMA would designate as dolomite. Consequently, important information related to intermediate compositions is lost through standardized mineral nomenclature.

Accordingly, in this study we employ several names for solid solutions. *Augite* and *pigeonite* are anomalous IMA-approved names for broad solid solutions among Ca-Mg-Fe clinopyroxenes. In this contribution we adopt the non-approved names "*Fe-dolomite*" for *dolomite* with $0.15 < Fe/(Fe + Mg) < 0.50$, "*olivine*" for examples with $0.3 < Fe/(Fe + Mg) < 0.70$, and "*plagioclase*" for intermediate Ca-Na feldspar compositions with $0.15 < Ca/(Ca + Na) < 0.85$. We also employ a number of group names such as *biotite*, *hornblende*, *scapolite*, *serpentine*, and *tourmaline* to lump several closely related species—a

convention that is especially useful for mineral groups for which the exact species is rarely reported in the petrologic literature (see Appendix 1).

4. The *role of fluids*: Another ambiguity, as yet imperfectly resolved in our treatment, relates to the role of fluid alteration during metamorphic processes. Hydration/dehydration, carbonation/decarbonation, and other fluid-rock interactions are integral to many metamorphic reactions. However, metasomatic alteration, by which a protolith reacts with external fluids, introduces complexities. We define metamorphism as mineralogical changes induced by changes in temperature and/or pressure, whether or not a fluid of differing composition is also involved. By contrast, in metasomatism mineralogical changes are caused by an influx of fluids of differing composition, whether or not changes in temperature and/or pressure are involved.

The processes of metamorphism and metasomatism thus differ conceptually; however, sharp boundaries do not exist between the two (Ramberg 1952). For example, Joplin (1968) notes that their "division of contact metamorphism and contact metasomatism into separate chapters is an artificial one since the two processes are very closely associated and cannot readily be separated." Consequently, in some cases outlined below we attempt to include minerals that have likely been compositionally transformed by proximal fluids (e.g., boron-fluorine metasomatism in some skarns; Tilley 1951; Marincea and Dumitras 2019), whereas in other instances we exclude minerals for which the alteration to a new phase appears to be principally related to fluids derived from sources more distant in space and/or time. Note that weathering, lithification, and

This is the peer-reviewed, final accepted version for American Mineralogist, published by the Mineralogical Society of America.
The published version is subject to change. Cite as Authors (Year) Title. American Mineralogist, in press.
DOI: https://doi.org/10.2138/am-2023-9004. http://www.minsocam.org/

diagenesis, as well as seafloor alteration by serpentinization, will be considered in Part IX, even if temperatures may be significantly greater than 150 °C in some instances.

In spite of these four challenges, we adopt the strategy employed in Part VII (igneous mineral evolution; Hazen et al. 2023) by tabulating the modes of diverse metamorphic rocks and investigating observed patterns of mineral coexistence, both their associations and their antipathies.

2. On the distribution of minerals in metamorphic rocks

An examination of the varied formation processes of all mineral species approved by the IMA-CNMNC (Hazen and Morrison 2022; https://rruff.info/ima, accessed 17 January 2022) reveals 1220 minerals that have been reported as phases in metamorphic rocks. Accordingly, we tabulate 1215 metamorphic mineral species approved by the IMA-CNMNC, as well as *Fe-dolomite*, *olivine*, *phengite*, *plagioclase*, and *silicate glass* [see Supplementary Table 1 and associated Supplementary Read-Me File 1; see also Hazen and Morrison (2022; their Supplementary Table 1 and additions)]. Table 1 catalogs 5 Supplementary Tables and an interactive graphical figure associated with this contribution.

This is the peer-reviewed, final accepted version for American Mineralogist, published by the Mineralogical Society of America.
The published version is subject to change. Cite as Authors (Year) Title. American Mineralogist, in press.
DOI: https://doi.org/10.2138/am-2023-9004. http://www.minsocam.org/

Table 1. Catalog of 5 Supplementary Tables (see also 5 associated Supplementary Read-Me Files) and an Interactive Graphical Figure (see figure caption for links and instructions).

Supplementary Table 1. A list of 1220 metamorphic mineral species (including *Fe-dolomite*, *plagioclase*, and *silicate glass*), and their correspondence to 755 root mineral kinds, with compositions and distributions among 8 metamorphic rock types.

Supplementary Table 2. A list matching 652 IMA-approved species with their associated 187 mineral kinds, which are defined by lumping two or more species.

Supplementary Table 3. A matrix listing the modes of 2785 metamorphic rocks. We record the distribution of 94 of the most common metamorphic minerals among these rocks.

Supplementary Table 4. A 73 x 73 symmetrical matrix that records the numbers of co-occurrences among 73 of the minerals in Supplementary Table 3. We do not include 21 minerals that occur commonly in multiple types of metamorphic environments.

Supplementary Table 5. A 73 x 73 symmetrical matrix (derived from Supplementary Table 4) that records the percentage of the less common mineral that co-occurs with the more common mineral.

Interactive Figure 1. A unipartite network of coexistence among 73 of the most common metamorphic minerals, based on data in Supplementary Tables 3, 4, and 5. The nodes are colored according to 6 communities, based on Louvain Community Detection.

This is the peer-reviewed, final accepted version for American Mineralogist, published by the Mineralogical Society of America.
The published version is subject to change. Cite as Authors (Year) Title. American Mineralogist, in press.
DOI: https://doi.org/10.2138/am-2023-9004. http://www.minsocam.org/

Mineral natural kinds: The list of 1220 metamorphic mineral species is significantly modifed in the evolutionary system of mineralogy by rules for "lumping and splitting" (Hazen et al. 2022). We have thus consolidated the list of 1220 minerals to recognize 755 "natural kinds" (Hawley and Bird 2011; Magnus 2012; Bird and Tobin 2015; Hazen 2019; Cleland et al. 2021) of metamorphic minerals [Appendix I; Supplementary Table 2 and associated Supplementary Read-Me File 2; see also Hazen et al. 2022, their Supplementary Table 1 and additions)].

Of the 1220 metamorphic mineral species, 568 correspond exactly to 568 root mineral kinds, whereas the other 652 species are lumped into 187 root mineral kinds. The majority of the resulting 755 metamorphic root mineral kind names (each *iltalicized*) are the same as the corresponding IMA mineral species name; thus, the IMA species albite is equivalent to the root mineral kind *albite*. In 26 instances, we adopt the IMA-approved mineral name, minus its suffix or prefix, as the root mineral name for groups of two or more closely-related species; thus, *chabazite* is the root mineral name for the four lumped species chabazite-Ca, chabazite-K, chabazite-Mg, and chabazite-Na, whereas *apatite* is the root mineral name for fluorapatite and hydroxylapatite. In 18 instances (*androsite, apophyllite, biotite, chlorite, ellestadite, hogbomite, hornblende, kspar, leakeite, melilite, orthoenstatite, Os-Ru alloy, Pd-Pt-Rh alloy, scapolite, serpentine, taaffeite, tourmaline,* and *wolframite*), we employ an unapproved mineral kind name for a group of closely-related IMA-approved mineral species. Thus, for example, *tourmaline* is the root mineral kind name for 18 IMA-approved species formed by metamorphic processes in the tourmaline group.

As suggested above, this proposed nomenclature is a first step in developing a much richer mineral taxonomy related to historical mineral kinds. In the case of metamorphic minerals,

numerous additional subdivisions are suggested. For example, our approach has yet to recognize and name many of the intermediate compositions of such important metamorphic mineral groups as amphiboles, carbonates, feldspars, micas, olivines, or pyroxenes. Until large databases of mineral compositions and their petrologic contexts are interrogated with cluster analysis (e.g., Gregory et al. 2019; Boujibar et al. 2021; Hystad et al. 2021), any consideration of mineral associations will be limited.

Metamorphic paragenetic modes: One approach to understanding metamorphic mineral evolution lies in documenting the coexistence of phases in different groups of metamorphic rocks. Supplementary Table 1 lists the distribution of these phases among 8 distinctive groups of metamorphic rocks (see also Table 2), each with characteristic mineral assemblages and each designated by a 3-letter abbreviation, as well as the paragenetic mode number (*p##*) originally employed by Hazen and Morrison (2022). In the course of this work we have expanded and revised the list of paragenetic modes associated with metamorphic minerals. In Supplementary Table 1, as indicated in red highlights, we have added 273 new combinations of a mineral species and metamorphic paragenetic mode, while removing 7 entries for which no supporting information could be found.

This is the peer-reviewed, final accepted version for American Mineralogist, published by the Mineralogical Society of America.
The published version is subject to change. Cite as Authors (Year) Title. American Mineralogist, in press.
DOI: https://doi.org/10.2138/am-2023-9004. http://www.minsocam.org/

Table 2. Division of mineral species and "root mineral kinds" among eight metamorphic paragenetic modes as recorded in Supplementary Table 1, with estimated ages of occurrence.

Paragenetic Mode	Code[a]	Age (Ga)	# Species[b]	#Unique[c]	# Kinds[d]
Pyrometamorphism of xenoliths	XEN; p09	> 4.5	173	87	130
Contact metamorphism	CON; p31	> 4.0	424	241	264
Metamorphic Ba/Mn/Pb/Zn deposits	BAM; p32	> 3.0	449	375	310
Ophiolites	OPH; p38	> 3.0	109	69	96
High-pressure metamorphism	HPM; p39	< 1.0	113	29	89
Regional metamorphism	REG; p40	< 3.0	351	151	205
Mantle metasomatism	MET; p41	> 4.0	37	5	35
Shear-induced minerals	SHE; p43	> 4.0	30	2	29

[a] Paragenetic codes from Hazen and Morrison (2022).

[b] Number of IMA-CNMNC-approved species associated with this paragenetic mode.

[c] Number of IMA-CNMNC-approved species unique to this paragenetic mode.

[d] Number of root mineral kinds associated with this paragenetic mode.

In the following sections, we summarize the compositions, processes, diversity, and possible ages of the eight groups of metamorphic minerals considered in this contribution.

1. Pyrometamorphism of xenoliths (XEN; *p09*): Thermally altered xenoliths are derived from both crustal and mantle sources subjected to high-temperature, low-pressure hornfels and sanidinite facies metamorphism by igneous melts (Grapes 2006). Typically formed at temperatures above 900 °C and pressures less than 0.5 GPa, pyrometamorphic suites were likely the earliest of Earth's near-surface metamorphic lithologies. The first protoliths were mafic and ultramafic igneous rocks from the earliest Hadean Eon (> 4.5 Ga), though xenoliths from virtually all of Earth's diverse igneous, sedimentary, and metamorphic lithologies have been subsequently subjected to pyrometamorphic conditions.

This is the peer-reviewed, final accepted version for American Mineralogist, published by the Mineralogical Society of America.
The published version is subject to change. Cite as Authors (Year) Title. American Mineralogist, in press.
DOI: https://doi.org/10.2138/am-2023-9004. http://www.minsocam.org/

We identify 173 IMA-approved mineral species, corresponding to 130 mineral kinds, that formed by xenolith pyrometamorphism. Based on our surveys, 87 of these phases are unique to xenoliths. Of special note are the more than 50 Ca-bearing limestone xenolith minerals from the intensively studied lavas of the Somma-Vesuvius Complex, Naples, Italy (https::/mindat.org; accessed 06 January 2023).

Note that under this heading we do not include several groups of relatively recent (< 400 Ma) biologically-mediated pyrometamorphic assemblages, including minerals formed in coal mine fires or by hydrocarbon fires, notably from the Hatrurim Basin (Grapes 2006; https://mindat.org, accessed 17 March 2023). Similarly, pyrometamorphic minerals from coal and other carbon-rich lithologies altered as xenoliths in lava or through contact metamorphism are deferred until Part XII of this series.

2. Thermal alteration via contact metamorphism (CON; *p31*): Contact metamorphism occurs when an igneous intrusive body thermally alters the older host country rock, including sedimentary, igneous, and metamorphic lithologies. Contact metamorphism is similar in many respects to the thermal alteration of xenoliths. However, contact metamorphism often differs by the extent of reactions with proximal aqueous fluids, notably those rich in carbonate and phosphate, as well as sulfate, borate, halogens, and other solutes derived from both the magma and the country rock (Einaudi et al. 1981; Einaudi and Burt 1982; Button 1982; Falkowski et al. 2000; Klein 2005; Kappler et al. 2005). We tabulate 424 mineral species (264 mineral kinds) that form through contact metamorphism, including phases that arise through reactions with local fluids. We find

This is the peer-reviewed, final accepted version for American Mineralogist, published by the Mineralogical Society of America.
The published version is subject to change. Cite as Authors (Year) Title. American Mineralogist, in press.
DOI: https://doi.org/10.2138/am-2023-9004. http://www.minsocam.org/

395 that 241 of these species are unique to contact metamorphic environments. Note that
396 continents with deep roots and active hydrological cycles also formed minerals by high-
397 temperature aqueous alteration through metasomatism—processes to be considered
398 further in Part IX of this series.

399 Contact metamorphism is an ancient process that must have commenced as early as a
400 second generation of magma penetrated the first cooling Hadean crust. The subsequent
401 history of contact metamorphism and its expanding mineral diversity parallels the
402 evolution of ever more differentiated crustal lithologies. Of special interest are
403 limestones and dolomites, which are particularly susceptible to transformation by hot
404 fluids emanating from acid intrusions—assemblages known as skarns (Bowen 1940;
405 Harker 1950; Tilley 1951).

406

407 3. Metamorphic Ba/Mn/Pb/Zn deposits (BAM; *p32*): We distinguish metamorphic phases
408 rich in otherwise minor metal elements, including Ba, Mn, Pb, and/or Zn, because they
409 feature distinctive mineral assemblages in both contact metamorphic and regional
410 metamorphic contexts (Post 1999; Leach et al. 2005). With 449 species (310 mineral
411 kinds), 375 of which are unique to these environments, these deposits are the most
412 mineralogically diverse of any metamorphic group. Several classic localities, including
413 Broken Hill, Australia (Spry et al. 2008); Franklin, Sussex County, New Jersey (Peters et al.
414 1983; Frondel 1990); Fresno County, California (Alfors et al. 1965); and the Wessel
415 manganese mine, South Africa (Cairncross and Beukes 2013), highlight the role of a few
416 mineral-rich localities in enhancing Earth's mineral diversity. Note, however, that these

This is the peer-reviewed, final accepted version for American Mineralogist, published by the Mineralogical Society of America.
The published version is subject to change. Cite as Authors (Year) Title. American Mineralogist, in press.
DOI: https://doi.org/10.2138/am-2023-9004. http://www.minsocam.org/

417 deposits are volumetrically insignificant compared to regional and contact metamorphic
418 rocks of more common igneous and sedimentary protoliths. Consequently, these
419 uncommon phases do not appear in our lists of metamorphic mineral modes
420 (Supplementary Table 3 and associated Supplementary Read-Me File 3).
421
422 4. Ophiolites (OPH; *p38*): Ophiolites incorporate highly altered sequences of mafic and
423 ultramafic rocks from the deep oceanic lithosphere—phases that have been
424 subsequently obducted onto crustal formations. As such, they provide important insights
425 to the mineralogy and petrology of the crust-mantle boundary (Moores 2002; Dilek 2003;
426 Kusky 2004). Ophiolites are documented to hold at least 109 mineral species (96 mineral
427 kinds), some of which resemble those of ocean floor igneous rocks altered by
428 serpentinization. However, we consider them as a separate metamorphic group for their
429 unique subaerial exposures of mantle lithologies, because of the occurrence of the
430 mineralogically distinctive and enigmatic Luobusha ophiolite from the Shannan
431 Prefecture of Tibet (references in Litasov et al. 2019), as well as minealogically diverse
432 ophiolite localities in the Urals and other localities (references in Litasov et al. 2019).
433 Luobusha is of special interest for its puzzling suite of ultrahigh pressure minerals (e.g.,
434 *diamond* and *moissanite*) that co-occur with dozens of highly reduced phases, including
435 native elements (Al, Cr, Cu, Fe, Ti, W), carbides, nitrides, and phosphides that are unique
436 to this locality (Bai et al. 2011). In addition, the Luobusha occurrence features many PGE
437 metal alloys (including possibly as many as 30 undescribed metal phases) that are
438 associated with chromitite zones reminiscent of assemblages in layered intrusions

(references in Litasov et al. 2019; Hazen et al. 2023). We include these diverse, rare minerals under ophiolites, though details of their paragenesis, and especially their assignments to metamorphic processes, remain uncertain (Ballhaus et al. 2017; Litasov et al. 2019).

Extensive alteration of Earth's oldest rocks obscures the identity of the oldest ophiolites, which may have predated the Proterozoic Eon, significantly before 2.5 Ga (Kusky et al. 2001; Zhai et al. 2002; Furnes et al. 2007; Nutman and Friend 2007). Confident identifications of several altered ophiolites support an origin by at least 2.5 Ga (Kusky 2004)—an observation consistent with the establishment of some form of plate tectonics by the late Archean Eon.

5. High-pressure metamorphism (HPM; *p39*): So-called "high-pressure" metamorphic assemblages are distinguished by their formation in the deep crust and upper mantle under unusually low geothermal gradients of less than 10 °C/km. Such conditions are only possible during transient subduction and subsequent rapid buoyant uplift of crustal rocks (Chopin 1984; Carswell and Compagnoni 2003; Hacker 2006; Palin and White 2016; Zheng and Chen 2017). High-pressure metamorphic rocks include blueschist facies, typically with *glaucophane*, *jadeite*, and/or *lawsonite* (formed at depths to 30 km); eclogite with *omphacite* and *pyrope* (> 45 km); and ultrahigh pressure (UHP) formations, featuring the dense *coesite* form of SiO_2 (> 80 km), micro-*diamond*, and other dense phases that point to origins approaching depths of 200 km. We list 113 high-pressure metamorphic mineral species (89 mineral kinds), of which 29 species, including

461 *barioperovskite* ($BaTiO_3$), *ellenbergerite* [$Mg_6(Mg,Ti^{4+},Zr^{4+},\square)_2(Al,Mg)_6Si_8O_{28}(OH)_{10}$], and
462 *trinepheline* ($NaAlSiO_4$), are unique to these metamorphic environments.

463 The ages of the oldest known high-pressure metamorphic rocks (< 850 Ma), and even
464 younger ages for the oldest UHP occurrences (Ganade et al. 2023), reveal much about
465 Earth's evolving lower crust and upper mantle (Jahn et al. 2001; Brown 2007; Stern
466 2018). Thus, for example, several of the oldest recorded *lawsonite* occurrences are from
467 the Paleozoic Era (De Roever 1956). These Neoproterozoic and later developments are in
468 sharp contrast to ultrahigh temperature metamorphic rocks from the Archean and
469 Proterozoic Eons (Brown 2006; Harley 2021). In particular, there are no known examples
470 of blueschist or ultrahigh pressure metamorphism until after 700 Ma (Ernst 1972; Palin
471 and White 2016; Brown and Johnson 2019; Holder et al. 2019). These temporal
472 differences apparently reflect the cooling average geotherm over billions of years of
473 Earth history.

474

475 6. Regional metamorphism (REG; *p40*): Most metamorphic rocks fall under the broad
476 heading of regional metamorphism, which is associated with burial, alteration, and uplift
477 of thick accumulations of sediments, volcanic rocks, and intrusive igneous lithologies. We
478 list 351 regional metamorphic mineral species, representing 205 mineral kinds, with 151
479 species unique to this paragenesis. Most regional metamorphic minerals derive from
480 common sedimentary and igneous protoliths.

481 Regional metamorphic rocks, which typically formed under an average geothermal
482 gradient of 15 to 30 °C/km (Vernon 2008; Philpotts and Ague 2009), are subdivided into

Barrovian index mineral zones based on the appearance of new minerals with increasing temperature and/or pressure: *chlorite*, *biotite*, *garnet*, *staurolite*, *kyanite*, and *sillimanite*, as first outlined by Barrow (1893). Mineral zones also extend to lower pressures, though higher than shallow contact/thermal metamorphism (Miyashiro 1961), as well as to ultrahigh temperature environments (> 900 °C at P < 1.5 GPa; Harley 2021). Goldschmidt (1911) and Eskola (1920) proposed a series of facies of increasing metamorphic grades, originally based on the mineralogy of metabasalt, including greenschist facies (typically with *chlorite*, *epidote*, and *serpentine*), amphibolite facies (*hornblende* and *plagioclase*), and granulite facies (a pyroxene group mineral and *plagioclase*). Subsequent research extended metamorphism to the UHT facies (often with *orthopyroxene*, *osumilite*, and/or *sapphirine*). In this overview we have lumped these regional metamorphic zones, though future research may warrant splitting into multiple groups based on ranges of temperature, pressure, and/or composition. Regional metamorphism, unlike high-pressure metamorphism, was well established by the Neoarchean Era (> 2.5 Ga).

Regional metamorphic mineral zones may form by either prograde metamorphism during heating and/or burial, or retrograde metamorphism during cooling and/or unburial. If close to equilibrium conditions, metamorphic rocks rarely contain more than 4 or 5 major minerals, following Gibbs' phase rule. However, many metamorphic mineral assemblages have more than 6 coexisting major phases and therefore may not represent equilibrium mineral assemblages.

This is the peer-reviewed, final accepted version for American Mineralogist, published by the Mineralogical Society of America.
The published version is subject to change. Cite as Authors (Year) Title. American Mineralogist, in press.
DOI: https://doi.org/10.2138/am-2023-9004. http://www.minsocam.org/

7. Mantle metasomatism (MET; *p41*): Deep-seated metasomatism, including processes in both the lower crust and upper mantle (Luth 2003; O'Reilly and Griffin 2012), is a high-pressure process that combines aspects of metamorphism and metasomatism, thereby altering the chemistry of existing ultramafic/mafic minerals and producing new phases through interactions with deep C-O-H fluids (Manning and Frezzotti 2020). We identify 37 oxide and silicate mineral species (35 kinds) formed through mantle metasomatism, all but 5 of which (including *nixonite*, $Na_2Ti_6O_{13}$; Anzolini et al. 2019) are familiar minerals in other environments.

8. Shear-induced minerals (SHE; *p43*): Minerals that form while experiencing significant shear strain represent a distinct metamorphic paragenetic mode in our system. Shear-induced mineralization is most commonly associated with the polished fault surfaces known as slickensides that represent zones of mylonitization, typically with pyroxene converted to amphibole and plagioclase much reduced in grain size and spread out into layers (Harker 1950; Passchier and Trouw 2005; Trouw et al. 2009).

Such shear zones can also act as fluid conduits (Gates and Speer 2022). Minerals produced by strain/shear can be formed by purely mechanical action, or they may involve chemical changes. Shear phenomena include twinning, as commonly observed with *calcite* in marble; strain bending, for example of mica; inclusion trains; cracks; and recrystallization (Harker 1950).

In Supplemental Table 1 we tabulate 30 mineral species (29 kinds) known to form in shear zones, most of which are common oxides and silicates that recrystallize in silicate

This is the peer-reviewed, final accepted version for American Mineralogist, published by the Mineralogical Society of America.
The published version is subject to change. Cite as Authors (Year) Title. American Mineralogist, in press.
DOI: https://doi.org/10.2138/am-2023-9004. http://www.minsocam.org/

rocks during shearing. The "sericite" variety of *muscovite* is among the most common mylonite minerals, often in association with *albite*. In other reactions, *biotite* shears to form *chlorite*, at times with *magnetite*; *augite* or *hornblende* shears to *chlorite* plus *epidote* or *calcite*; *forsterite* shears to *tremolite* or *anthophyllite* plus *talc*; *andradite* transforms in part to *titanite* and *magnetite*; and the antigorite form of *serpentine* arises through shearing of other *serpentine* polymorphs. While most of these phases probably first appeared early in Earth's history, the rare chlorite group mineral *donbassite* [$Al_2(Si_3Al)O_{10}(OH)_2 \cdot Al_{2.33}(OH)_6$] has been reported uniquely from slickensides of coal (Anthony et al. 1990–2003), and therefore must have formed within the past 350 million years as a biologically-mediated phase.

These eight proposed groups of metamorphic rocks, though useful in the larger context of the evolutionary system and its consideration of paragenetic modes writ large, are subjective and fail to properly represent the diversity of metamorphic *P-T-X* environments. Inevitably, significant overlaps occur in the compositional, environmental, mineralogical, and temporal ranges of the eight broad categories of metamorphic rocks outlined above. Nevertheless, we suggest that each group is associated with its own characteristic mineral assemblages and environmental contexts (e.g., Deer et al. 1982-2013; Anthony et al. 1990-2003). Therefore, each of the eight processes plays its own distinctive role in the evolutionary system of mineralogy.

This is the peer-reviewed, final accepted version for American Mineralogist, published by the Mineralogical Society of America.
The published version is subject to change. Cite as Authors (Year) Title. American Mineralogist, in press.
DOI: https://doi.org/10.2138/am-2023-9004. http://www.minsocam.org/

3. METAMORPHIC MINERAL ASSOCIATIONS AND NETWORK ANALYSIS

Bowen (1928) employed patterns of "mineral associations and antipathies" in the development of his theory of igneous rock evolution, in which he recognized that some pairs of minerals are frequently encountered in equilibrium igneous assemblages, whereas as others never occur (Hazen et al. 2023). The same principles apply to metamorphic minerals, with the caveat that overlapping prograde and retrograde reactions often result in nonequilibrium assemblages.

In this section we amplify Bowen's approach by quantifying the extent of coexistence among pairs and larger groupings of 94 of the commonest minerals in metamorphic rocks (Table 3; Appendix 1). Of these metamorphic minerals, 66 are silicates, 14 are oxides or hydroxides, 8 are carbonates or phosphates, 4 are sulfides, and 2 are polymorphs of carbon. Collectively, these 94 minerals incorporate 23 different essential chemical elements, including oxygen (in 88 of 94 minerals), Si (71), Al (44), Fe (40), Ca (38), Mg (37), H (27), Na (14), C (10), F (8), K (8), Ti (7), S (5), Cl (4), Cr (3), Mn (2), Zr (2), and B, Ce, Cu, Ni, P, and Sr (all in only 1 of 94 minerals).

The core data of this study are found in Supplementary Table 3 (see also Supplementary Read-Me File 3), which details the distribution of these 94 metamorphic minerals among 2785 metamorphic rock modes. We employed 29 primary sources to assemble these metamorphic mineral modes: Augustithis (1985; 156 modes), Botha (1983; 95 modes), Carswell (1990; 198 modes), Carswell and Compagnoni (2003; 49 modes), Coleman et al. (1965; 13 modes), Grapes (2006; 218 modes), Harker (1950; 285 modes); Harley (2021; 121 modes); Joplin (1968; 345 modes); Philpotts and Ague (2009; 885 modes); Reverdatto and Sóbolev (1973; 71 modes); and Tilley et al. (1964; 50 modes), as well as 299 modes from contributions by Ferry and colleagues

569 (Davis and Ferry 1983; Ferry 1976, 1984, 1988, 1989, 1992, 1994, 1995, 1996, 2007; Ferry and
570 Rumble 1997; Ferry et al. 1987, 2001, 2002, 2005; Léger and Ferry 1993; Penniston-Dorland and
571 Ferry 2006).

572 Ideally, the extensive data on coexisting metamorphic minerals in Supplementary Table 3
573 would represent a wide range of equilibrium assemblages, while accurately documenting the
574 relative abundances of metamorphic minerals. However, even though we have surveyed 29
575 diverse compilations of metamorphic modes representing several geographic areas and most
576 distinct types of metamorphic environments, it is important to recognize at least four likely
577 sources of bias and error in the modal mineralogy data in Supplementary Table 3. Each of these
578 factors may distort the true distribution of mineral associations among metamorphic rocks.

579 (1) *Biases owing to disequilibrium*: Metamorphic mineral modes often represent non-
580 equilibrium assemblages, with prograde and retrograde phases of differing metastability
581 occurring together. Therefore, the coexistence data in Supplementary Table 3 cannot be
582 employed in the same way as the corresponding table of igneous modes in Part VII of this
583 series.

584 (2) *Biases related to optical petrography:* Most of our modal data come from studies that
585 employed optical petrography, but not electron microprobe analysis. Several inevitable biases
586 result.

587 • Euhedral vs. poorly crystallized phases: Well-crystallized minerals such as almandine
588 or staurolite are more likely to be identified than fine-grained assemblages
589 containing brucite, phyllosilicates, or zeolites. For example, Ferry (1994), Ferry and
590 Rumble (1997), and Ferry et al. (2002) document the widespread occurrence of

This is the peer-reviewed, final accepted version for American Mineralogist, published by the Mineralogical Society of America.
The published version is subject to change. Cite as Authors (Year) Title. American Mineralogist, in press.
DOI: https://doi.org/10.2138/am-2023-9004. http://www.minsocam.org/

591 brucite and serpentine—metamorphic minerals almost never recorded in modes
592 from earlier literature.

593 • Exotic versus common minerals: Our compilation likely over-represents certain rare
594 minerals, such as *coesite* and *diamond*, especially if they occur in optically distinctive
595 crystals.

596 • Optically similar minerals: A number of minerals are difficult to identify via optical
597 petrography. For example, distinguishing among *calcite*, *ankerite*, and *aragonite*, as
598 well as between fine-grained *quartz/albite* and *muscovite/paragonite*, is difficult and
599 may lead to errors in reported modes.

600 • *Opaque minerals*: Identification of opaque minerals is another petrographic challenge
601 that leads to omissions and biases in Supplementary Table 3. For example, electron
602 microprobe analyses indicate that *pyrrhotite* is extremely common in a wide variety
603 of metamorphic rocks (e.g., Ferry 1994), though it is often unreported (or perhaps
604 misidentified as *pyrite*) in earlier descriptions of metamorphic rock modes. Similarly,
605 some opaque Fe-Ti-Cr bearing oxides, including the oxide spinels *chromite* and
606 *hercynite*, as well as *ilmenite*, and *rutile*, may be under-represented in our
607 tabulations.

608 • Trace minerals: Detailed studies with electron microprobe analysis suggest that
609 minor phases, especially those with grain sizes < 5 micrometers, are much more
610 common than suggested by our survey. Examples of rarely reported trace
611 metamorphic minerals include *allanite* and *monazite* (Wing et al. 2003); *baddelyite*,

This is the peer-reviewed, final accepted version for American Mineralogist, published by the Mineralogical Society of America.
The published version is subject to change. Cite as Authors (Year) Title. American Mineralogist, in press.
DOI: https://doi.org/10.2138/am-2023-9004. http://www.minsocam.org/

612 *geikielite*, *qandilite*, and *sphalerite* (Ferry 1996); and *anhydrite*, *calzirtite*, and
613 *celestine* (Ferry et al. 2002).

614 (4) *Problems in nomenclature:* A number of petrographic terms lead to ambiguities when
615 listing minerals in Supplementary Table 3. General group names such as "garnet" encompass
616 several different mineral kinds in our study. Therefore, the relative abundances of *almandine*,
617 *andradite*, *grossular*, and *pyrope* may be in error. "Spinel" may refer to the mineral species
618 $MgAl_2O_4$, or to members of the oxide spinel group such as *magnetite*, *chromite*, or *hercynite*.
619 "Ankerite" is technically $CaFe(CO_3)_2$, but is often used to designate a Fe-bearing dolomite in the
620 literature of metamorphic petrology.

621 (5) *Missing recent research*: Metamorphic studies of the past 20 years are less likely to
622 tabulate numerous modes; fewer than a third of the modes in Supplementary Table 3 were first
623 published after 2003. As a consequence, our survey under-represents more recently
624 documented metamorphic lithologies, such as ultrahigh temperature metamorphism (Harley
625 2021).

626

627 *Metamorphic mineral coexistence*: Of the 94 minerals considered in Supplementary Table 3, 21
628 occur commonly in several different types of metamorphic rocks and therefore are not easily
629 grouped by community detection algorithms. Therefore, we tabulated the frequency of co-
630 occurrence of every pairwise combination of the remaining 73 mineral kinds, all of which are
631 more likely to be associated with only one or two metamorphic lithologies (Supplementary
632 Table 4; see also associated Supplementary Read-Me File 4). For each mineral pair we
633 calculated the percentage of the less common mineral that co-occurs with the more common

mineral (Supplementary Table 5; see also Supplementary Read-Me File 5). For example, consider matrix element W7, which relates to the coexistence of *andalusite* (with 146 occurrences, as listed in Supplementary Table 4) and *cordierite* (with 395 occurrences). In Supplementary Table 4, matrix element W7 reveals that 84 rocks (out of 2785 tabulated) contain both *andalusite* and *cordierite.* Therefore, in Supplementary Table 5, matrix element F7 = 84/146 x 100 = 58 %.

This protocol is especially important when considering the coexistence of a relatively rare mineral with a common one. For example, *baddeleyite* is a scarce metamorphic mineral, occurring in only 18 of 2785 metamorphic rocks recorded in Supplementary Table 3. However, 16 of those occurrences also contain the common metamorphic mineral *calcite*. Therefore, as recorded in matrix element Q14 of Supplementary Table 5, 16/18 = 89 % of *aegirine* occurrences also have *calcite*. Thus, *baddeleyite/calcite* is a common mineral pair whenever the rare mineral *baddeleyite* occurs. As Bowen emphasized for igneous minerals (Bowen 1928; Hazen et al. 2023), we find that a small percentage of all possible metamorphic mineral pairs commonly occur (e.g., *almandine/biotite; diopside/grossular; chloritoid/muscovite; quartz/staurolite*).

As demonstrated in our previous study of igneous minerals (Hazen et al. 2023), network analysis of mineral associations and antipathies reveals phase relationships and reaction sequences that may not be immediately recognized from tables of mineral modes. Therefore, we have applied two types of data visualization: unipartite networks that highlight Louvain community detection and bipartite networks representing relationships among minerals and their formational environments.

This is the peer-reviewed, final accepted version for American Mineralogist, published by the Mineralogical Society of America.
The published version is subject to change. Cite as Authors (Year) Title. American Mineralogist, in press.
DOI: https://doi.org/10.2138/am-2023-9004. http://www.minsocam.org/

Unipartite networks and Louvain community detection analysis of coexisting metamorphic minerals: Mineral network analysis reveals patterns among coexisting minerals (Morrison et al. 2017). Accordingly, Figures 1A and 1B display a unipartite network that illustrates the coexistence among 73 relatively common metamorphic minerals, as listed in Table 3. This graph was built on "Observable" (https://observablehq.com/), using D3js (Bostock et al. 2011). The networks use the D3-force algorithm (https://d3-wiki.readthedocs.io/zh_CN/master/Force-Layout/) for its network layout. The code and an interactive version of this network can be found at: (https://observablehq.com/@anirudhprabhu/revised-evolutionary-system-of-mineralogy-part-8-uni; for instructions, see Figure 1 caption).

Each of the 73 nodes in Figure 1 represents a metamorphic root mineral kind, with the size of the node in Figure 1A indicating the abundance of that mineral in our tabulations of 2785 metamorphic rock modes (Supplementary Table 3). Links between pairs of nodes indicate mineral coexistence. in Figure 1A, we illustrate the case where at least 6 % of occurrences of the less common mineral coexist with the more common mineral, based on percentages tabulated in Supplementary Table 5 (6 % is the highest percentage for which all 73 mineral nodes are still interconnected). Figure 1 is a static rendering of a dynamic interactive network in which the co-occurrence percentage, *P*, can be varied continuously from 1 to 100 %. This variable feature, as well as other interactive aspects of the online version of Figure 1, facilitates studies of mineral associations and antipathies.

This is the peer-reviewed, final accepted version for American Mineralogist, published by the Mineralogical Society of America.
The published version is subject to change. Cite as Authors (Year) Title. American Mineralogist, in press.
DOI: https://doi.org/10.2138/am-2023-9004. http://www.minsocam.org/

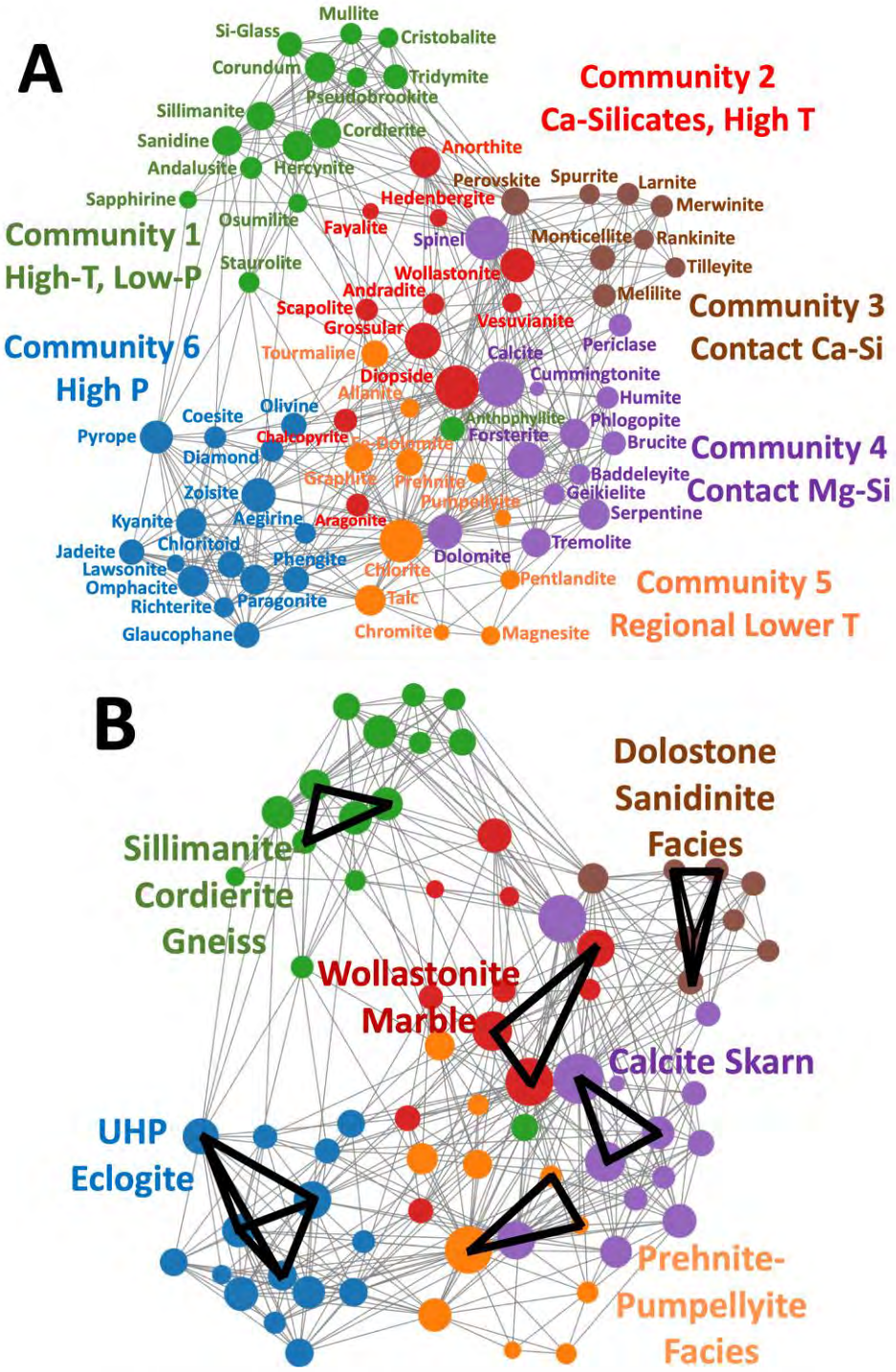

Figure 1. **(A)** A unipartite network of 73 common metamorphic minerals (colored circles), with links between pairs of coexisting minerals. Node sizes indicate the relative abundances of the minerals, while colors indicate 6 communities of metamorphic minerals that were determined using Louvain community

This is the peer-reviewed, final accepted version for American Mineralogist, published by the Mineralogical Society of America.
The published version is subject to change. Cite as Authors (Year) Title. American Mineralogist, in press.
DOI: https://doi.org/10.2138/am-2023-9004. http://www.minsocam.org/

683 detection (see text). Each of these communities corresponds to a different temperature-pressure-
684 composition regime. In this figure, links are drawn between two minerals if at least 6 % of rocks that
685 incorporate the less common mineral also incorporate the more common mineral (as tabulated in
686 Supplementary Table 3). One can vary this percentage in an interactive version of this graph at:
687 (https://observablehq.com/@anirudhprabhu/revised-evolutionary-system-of-mineralogy-part-8-uni).
688 Hover your cursor over any node to identify the corresponding mineral; click and hold your cursor to
689 move that node and identify links to other nodes; use your cursor to move the "Weight Threshold"
690 vernier to systematically eliminate links between nodes based on *P* values (see text). Adjust node
691 attributes by clicking on the "Size Nodes By" feature. **(B)** The unipartite network of 73 metamorphic
692 minerals embeds metamorphic rock types as sub-graphs. Highlighted subgraph examples include 6
693 common metamorphic lithologies.
694
695 Links in a mineral network are not uniformly distributed; they typically display sub-networks
696 of more closely connected nodes. We color mineral nodes in Figure 1 based on Louvain
697 community detection analysis (Girvan and Newman 2002; Fortunato 2010), which employs a
698 heuristic method based on modularity optimization to extract the community structure of large
699 networks (Blondel et al. 2008). This method identifies members of a group iteratively in two
700 phases: (1) starting with each node as its own distinct community, larger communities are
701 formed at a local level by maximizing modularity of certain nodes; (2) each small community is
702 aggregated into one "super node" to form a new "super node network." We repeat these steps
703 until the modularity has been optimized and there are no changes in the network. The Louvain
704 modularity approach reveals an optimal number of communities without requiring the user to
705 specify the number of clusters in a dataset. Consequently, Louvain community detection

706 removes some of the bias associated with some other clustering algorithms, while identifying
707 the most closely interconnected subsets of minerals.

708 The identification of community structures may be complicated by the inclusion of mineral
709 nodes that link to multiple communities. Such nodes typically plot near the center of a network
710 and "pull" more diagnostic nodes toward the middle while obscuring community structures
711 (Hazen et al. 2023). Therefore, we do not include 21 of the most common metamorphic
712 minerals in our networks, including such major phases as *albite*, *almandine*, *augite*, *biotite*,
713 *hornblende*, *kspar*, *muscovite*, *plagioclase*, and *quartz*, because they occur across a wide variety
714 of metamorphic rocks. In addition, *apatite*, *ilmenite*, *magnetite*, *pyrite*, *pyrrhotite*, *rutile*, *titanite*
715 and *zircon* are widespread accessory phases that we exclude from network analysis. By
716 contrast, each of the 73 metamorphic minerals illustrated in Figure 1 is more characteristic of a
717 restricted pressure, temperature, and/or compositional metamorphic regime. One
718 consequence of this exclusion of 21 of the most widespread metamorphic minerals is that the
719 classic Barrovian sequences of metapelite and metabasite zones are not well represented in
720 Figure 1. Rather, the subset of 73 less ubiquitous phases define six principal communities of
721 metamorphic phases, each with its own distinctive pressure-temperature-composition regime
722 (see also Table 3):
723
724 *Community 1:* Community 1 holds 15 high-temperature, low-pressure minerals, including
725 such pyrometamorphic and ultra-high temperature phases as *corundum*, *mullite,*
726 *osumilite, sanidine, sapphirine, silicate glass, sillimanite*, and *tridymite*, with mineral
727 assemblages typical of pyroxene hornfels, sanidinite, and ultrahigh temperature

This is the peer-reviewed, final accepted version for American Mineralogist, published by the Mineralogical Society of America.
The published version is subject to change. Cite as Authors (Year) Title. American Mineralogist, in press.
DOI: https://doi.org/10.2138/am-2023-9004. http://www.minsocam.org/

metamorphism. Community 1 is well separated from most minerals of Communities 2 through 6, which represent higher pressure and/or lower temperature environments. Note that within the adjacent Communities 2 and 6, the higher-temperature minerals appear closest to Community 1 in Figure 1. Thus, there is a temperature gradient from upper left to lower right in the network.

Community 2: Community 2 features 11 minerals, including *andradite, anorthite, diopside, grossular, hedenbergite, vesuvianite*, and *wollastonite*, all of which are typical of mid- to high-temperature contact and regional metamorphism of calc-silicates. Note that Communities 2 and 5 display significant overlaps in this network, with a prominent temperature gradient from the top to the bottom of the network. Communities 2 and 5 are thus relatively dispersed compared to Communities 1, 3, 4, and 6

Community 3: The eight minerals of Community 3—*larnite, melilite, merwinite, monticellite, perovskite, rankinite, spurrite*, and *tilleyite*—form a tightly clustered group of idiosyncratic phases typical of the highest temperature Ca-rich skarns. A number of petrologists have recognized sequences of metamorphic skarn minerals as a function of temperature and composition (Bowen 1940; Harker 1950; Tilley 1951). For example, Bowen (1940) listed 10 minerals in order of their increased temperature of formation: *tremolite, forsterite, diopside, periclase, wollastonite, monticellite,* åkermanite (e.g., *melilite*)*, spurrite, merwinite*, and *larnite*, whereas subsequent studies slightly rearranged the order of some of these phases (e.g., Weeks 1956; Ferry 1976). We see suggestions of such a sequence, with the highest temperature phases in Community 2 located in the upper right of Figure 1.

Community 4: Thirteen minerals, including Mg-bearing *brucite, cummingtonite, dolomite, forsterite, geikielite, humite, periclase, phlogopite, serpentine, spinel,* and *tremolite*, represent contact metamorphic environments of Mg-rich skarns, as well as regional metamorphism of Mg-Si-silicates. Mineral assemblages of Community 4 thus have close links to the higher temperature, more calcic environments of Communities 2 and 3.

Community 5: Community 5 incorporates 11 metamorphic minerals, including phases from two distinct environments. On the one hand, lower-temperature regional metamorphic lithologies are represented by *chlorite, prehnite,* and *pumpellyite*, which are characteristic of the prehnite-pumpelleyite and greenschist facies. Community 5 also includes a suite of minerals typical of ophiolites and metamorphosed ultramafic rocks, including *chlorite*, *chromite*, *magnesite*, *pentlandite*, and *talc.* Consequently, Community 5 is relatively dispersed and co-mingled with the higher temperature phases of Community 2.

Community 6: Diagnostic high-pressure metamorphic phases occur in Community 6. This well-defined cluster of 15 minerals in the lower lefthand region of Figure 1 holds typical high-pressure phases of blueschist (*glaucophane, lawsonite*), eclogite (*jadeite, kyanite, omphacite*), and ultrahigh pressure (*coesite, diamond, pyrope*) facies. These minerals are all characteristic of metamorphism under the relatively low geothermal gradients experienced by deeply subducted crustal wedges that buoyantly rebound.

The degree of connectivity, or network density, of the graph in Figure 1 varies signficantly with the percentage of co-occurrence, *P*. The density of a network (*D*) is defined as the fraction of all possible links that are observed; in the case of 94 minerals, there exist $[(94^2 - 94)/2] =$

4371 possible links. When P = 1 %, the density of the network has a value of D = 0.400 because 1747 (40.0 %) of the 4371 possible links between mineral pairs are observed to occur at least once. By contrast, when we restrict links to P = 25 % then 524 links remain (D = 0.120). And when we consider P = 50 %, only 198 links persist – a relatively sparse network with D = 0.045.

Note that at P > 6 %, one or more mineral nodes is no longer connected to the network. The first node to disconnect is *cummingtonite* at P = 7 %, while at P = 15 % *olivine* also becomes disconnected. At P = 25 %, 66 of the original 73 mineral nodes remain interconnected, including representatives of all 6 communities. However, at P = 50 %, only 39 nodes form a sparse network with all 13 minerals of Community 4 (Mg skarns) forming a hub with radiating suites of minerals from Community 2 (7 minerals), Community 3 (6 minerals), and Community 5 (10 minerals). By contrast, all but 2 minerals from Community 6 and 1 mineral from Community 1 remain connected at P = 50 %.

An important feature of the unipartite networks of metamorphic minerals is that every metamorphic rock, for example each of the 2785 examples in Supplementary Table 3, as well as every prograde or retrograde sequence of metamorphic rocks, is embedded as a multi-node subgraph of this network (Figure 1B). *P-T-X* series of lithologies can be represented by a sequence of subgraphs that wend their way across the larger network of Figure 1B. Thus, Figure 1 and related networks are useful visual approaches to comparing and contrasting aspects of metamorphic petrology for research and education.

In many respects, the topology of Figure 1 for common metamorphic minerals is reminiscent of the topology of the analogous network of 115 igneous minerals in Part VII of this series (Hazen et al. 2023; their Figure 1). In both instances, Louvain community detection reveals

794 several communities of mineral kinds, each from a distinct compositional and/or environmental
795 regime. Furthermore, every rock in extensive lists of mineral modes is represented by a
796 subgraph (compare Figure 1B to Hazen et al. 2023, their Figure 1B). Nevertheless, two
797 important differences exist between these two renderings.

798 1. In the case of igneous rocks, the majority of the minerals tabulated by Hazen et al. (2023)
799 are minor accessory phases (< 5 vol %), most of which incorporate relatively rare
800 elements. By contrast, reported modes of metamorphic rocks rarely include minor
801 phases. Consequently, the network for metamorphic minerals illustrates fewer mineral
802 kinds, but almost twice as many major phases spanning a much wider *P*-*T* range,
803 compared to the network for igneous mineral kinds.
804 2. In our study of the evolution of igneous minerals, we attempted to include only modes
805 based on equilibrium assemblages of primary minerals. Accordingly, we have suggested
806 that phase equilibrium for multi-component chemical systems (including myriad rare
807 elements) might be extracted from the topology of the igneous mineral network.
808 However, owing to often incomplete transformations during prograde or retrograde
809 metamorphism, the assumption of equilibrum assemblages cannot be applied to
810 metamorphic rocks. On the other hand, because most metamorphic rock modes are
811 embedded in Figure 1, it should be possible to illustrate any metamorphic sequence in *P*-
812 *T*-*X* space with an animated series that systematically moves across Figure 1, even if the
813 individual mineral assemblages are not in equilibrium.

814

This is the peer-reviewed, final accepted version for American Mineralogist, published by the Mineralogical Society of America.
The published version is subject to change. Cite as Authors (Year) Title. American Mineralogist, in press.
DOI: https://doi.org/10.2138/am-2023-9004. http://www.minsocam.org/

Unipartite network graph at P = 33 %: The unipartite graph of Figure 1 represents the co-occurrences of 73 different metamorphic minerals based on tabulations of 2785 modes at P = 6 %, which is the maximum value at which all minerals are still connected. However, Figure 1 may be visually misleading in three ways.

First, Figure 1 is a two-dimensional projection of a graph in 72 dimensions [any network with N nodes possesses (N – 1) dimensions]. Consequently, the proximity of two adjacent nodes does not necessarily imply that those two minerals are closely related. Thus, for example, *forsterite* (Community 4) and *prehnite* (Community 5) lie next to each other in Figure 1, yet those two minerals do not coexist in any rock in our survey.

Second, in some instances a mineral will be located in a position somewhat removed from its community. For example, the Mg-amphibole *anthophyllite* is included in Community 1, yet it appears near the center of Figure 1, closer to Communities 2, 4, and 5. This positioning results from *anthophyllite*'s close association with both *cordierite* (Community 1) and *forsterite* (Community 4)—a common situation when one node is closely associated with two or more communities.

Third, because Figure 1 represents all links between nodes with at least 6 % co-occurrence, some relatively weak connections (i.e., those with only 6 % to 10 % co-occurrence) will tend to intermingle some phases that only co-exist relatively infrequently with other minerals in two or more communities.

Figure 2 is a unipartite network similar to that of Figure 1 but with P = 33 %. Therefore, a link appears only if at least one-third of occurrences of the rarer mineral also features the more common mineral. The result is a much sparser network of 66 mineral nodes and 185 links.

This is the peer-reviewed, final accepted version for American Mineralogist, published by the Mineralogical Society of America.
The published version is subject to change. Cite as Authors (Year) Title. American Mineralogist, in press.
DOI: https://doi.org/10.2138/am-2023-9004. http://www.minsocam.org/

Seven minerals—*aegirine, anorthite, cummingtonite, fayalite, hedenbergite, olivine*, and *staurolite*—are no longer connected. The resulting graph retains the six communities of Figure 1, but they are much more tightly clustered, revealing well-separated groups of minerals.

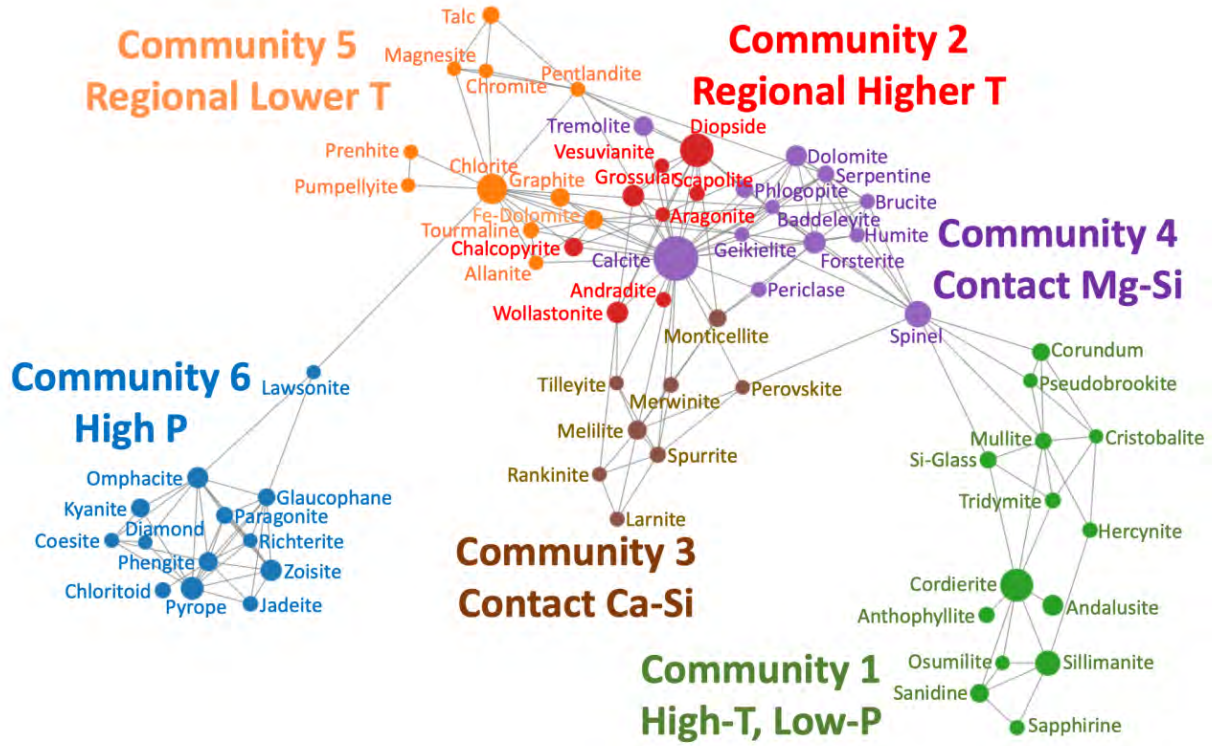

Figure 2. A unipartite network of 66 common metamorphic minerals (colored circles). Node sizes indicate the relative abundances of minerals, while colors indicate six communities of metamorphic minerals that were determined using Louvain community detection (see text). Each of these communities corresponds to a different temperature-pressure-composition regime. In this figure, links are drawn between two minerals if at least 33 % of rocks that incorporate the less common mineral also incorporate the more common mineral (as tabulated in Supplementary Table 3). One can vary this percentage in an interactive version of this graph at: (https://observablehq.com/@anirudhprabhu/revised-evolutionary-system-of-mineralogy-part-8-uni). Hover your cursor over any node to identify the corresponding mineral; click and hold your cursor to move that node and identify links to other nodes; use your cursor to move the "Weight Threshold" vernier to systematically eliminate links between nodes based on *P* values (see text). Adjust node attributes by clicking on the "Size Nodes By" feature.

This is the peer-reviewed, final accepted version for American Mineralogist, published by the Mineralogical Society of America.
The published version is subject to change. Cite as Authors (Year) Title. American Mineralogist, in press.
DOI: https://doi.org/10.2138/am-2023-9004. http://www.minsocam.org/

Figure 2 displays the same six communities (with 66 of the 73 minerals) that appear in Figure 1. However, the more stringent criteria of P = 33 % results in a network with far greater separation between communities. Community 1 now appears at the extreme right of the graph, retaining 14 of the original 15 minerals (only *staurolite* has been lost). The only link between Community 1 and the rest of the network is to Community 4 through *spinel*.

Community 4 has 12 of the original 13 minerals (*cummingtonite* disconnects at P = 7 %), which form a cluster in the upper right of the network. Note that *tremolite* is displaced from the main cluster because it forms only three links—to *calcite* (also in Community 4), *diopside* (Community 2), and *pentlandite* (Community 5). Community 4 is most closely linked to Communities 2 and 5, but has only 3 links to Community 3, 1 link to Community 1, and no connections to Community 6.

Community 3, which represents relatively high-temperature skarn minerals, retains all of its original 8 phases in an isolated cluster that is linked only to the lower-temperature skarn minerals of Communities 2 and 4. By contrast, Community 2 is the most intermingled cluster in this network. Only 8 of the original 11 minerals remain; *anorthite, fayalite*, and *hedenbergite* are disconnected by P = 25 %.

All 11 of the original Community 5 minerals appear in Figure 2, which reveals a well-defined cluster with three subgraphs. *Chlorite-prehnite-pumpelleyite* appear as a triangle corresponding to low-temperature metamorphism, while *chromite-magnesite-pentlandite-talc* form a quartet of ophiolite phases. In addition, *allanite, Fe-dolomite, graphite*, and *tourmaline* are commonly associated accessory minerals in regional metamorphic rocks. Community 6, with 13 of the original 15 high-pressure minerals (minus *aegirine* and *olivine*), is the most isolated cluster in

This is the peer-reviewed, final accepted version for American Mineralogist, published by the Mineralogical Society of America.
The published version is subject to change. Cite as Authors (Year) Title. American Mineralogist, in press.
DOI: https://doi.org/10.2138/am-2023-9004. http://www.minsocam.org/

Figure 2, with only a single link between *lawsonite* of Community 6 and *chlorite* of Community 5.

The resulting sparse network forms an arc, with the highest pressure minerals to the left and the lowest pressure minerals to the right. The central grouping of Communities 2, 3, and 4 represent metamorphosed Ca-Mg silicates and skarns, with higher temperature phases located toward the bottom of the graph. Thus, in spite of the continuous variations of temperature, pressure, and composition represented by metamorphic mineral assemblages, distinct clusters representing formational environments with idiosyncratic minerals are important characteristics of metamorphic rocks.

An unexpected result of this network analysis are the strong separtions among some mineral communities. By their nature, metamorphic rocks represent continua of *P-T-X* conditions. One might expect, therefore, to observe similarly continuous linkages in the network topology of Figure 2. However, we observe strong clustering into six communities with signifcant gaps. Most notably, Community 1 on the right and Community 6 on the left are isolated from Communities 2 through 5. In addition, we observe lesser gaps between Communities 2 and 5, as well as between Communities 3 and 4. Similar topologies in network graphs of igneous rocks correspond to known compositional trends, such as the Daly gap (Daly 1925; Hazen et al. 2023, their Figure 5). Is it possible that similar composition gaps exist among the diversity of metamorphic rocks?

Bipartite network of metamorphic minerals and their host lithologies: Figure 3 is a bipartite network (i.e., a network with links between two different kinds of nodes) that illustrates 1220

This is the peer-reviewed, final accepted version for American Mineralogist, published by the Mineralogical Society of America.
The published version is subject to change. Cite as Authors (Year) Title. American Mineralogist, in press.
DOI: https://doi.org/10.2138/am-2023-9004. http://www.minsocam.org/

897 diamond-shaped nodes representing metamorphic mineral species and their 1686 links to 8
898 nodes that represent the different groups of metamorphic rocks, as first described by Hazen
899 and Morrison (2022) and modified here in Supplementary Table 1. This bipartite network was
900 made using the "visNetwork" (Almende et al. 2021) and "igraph" (Csardi & Nepusz 2006) R
901 packages. The code for construction of this network can be found
902 at: https://github.com/anirudhprabhu/StellarNet/tree/master/PartVIII. The network layout
903 uses the "barnesHut" approximation algorithm (Barnes and Hut 1986).

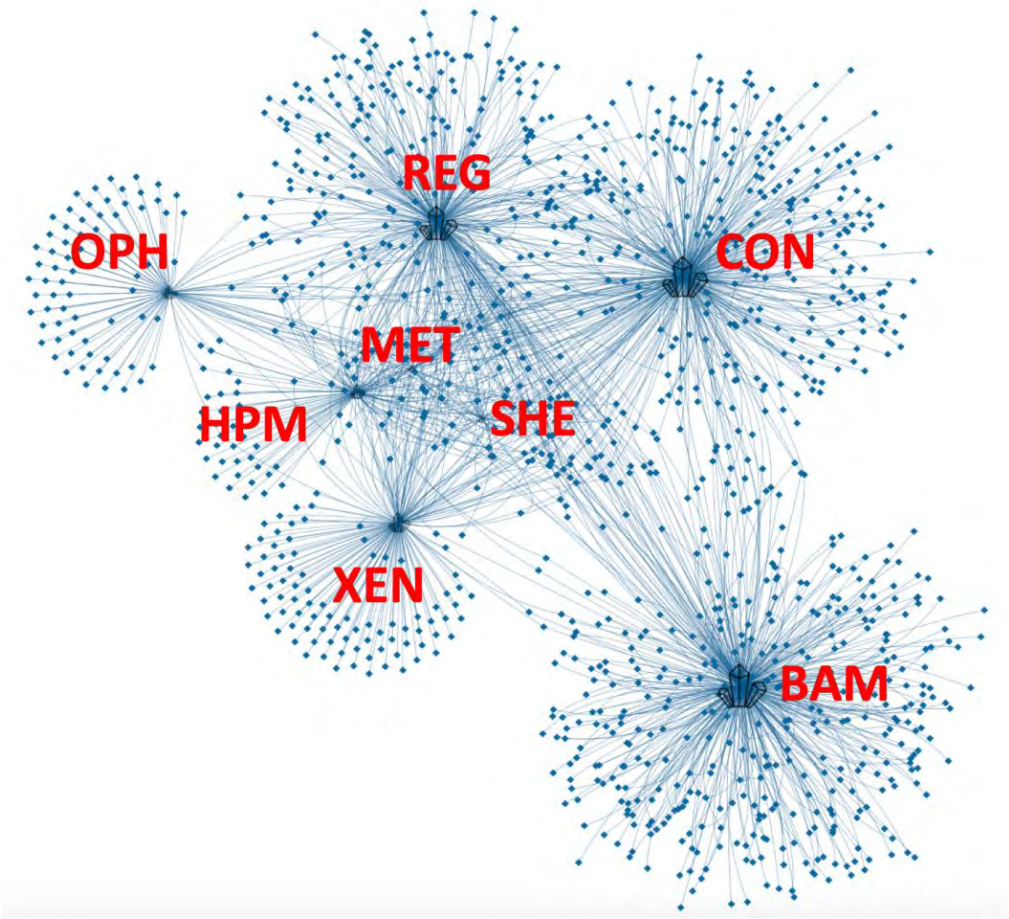

904

905 Figure 3. This bipartite network of 1220 metamorphic minerals (colored diamond-shaped nodes)
906 displays 1686 links to 8 icons representing different major groups of metamorphic rocks, as first
907 described by Hazen and Morrison (2022) and modified here (Table 2; Supplementary Table 1).
908 Three-letter identifiers are XEN = pyrometamorphism of xenoliths (with 173 minerals); CON =

contact metamorphism (424); BAM = metamorphic Ba/Mn/Pb/Zn deposits (449); OPH = ophiolites (109); HPM = high-pressure metamorphism (113); REG = regional metamorphism (351); MET = mantle metasomartism (37); and SHE = shear-induced minerals (30). The 6 "starburst" features around the periphery reflect 959 mineral species that are uniquely associated with only one paragenetic mode. Most of the other nodes, representing 261 mineral species that are connected to two or more nodes representing paragenetic modes, lie in the dense central region of the bipartite network.

This bipartite network displays several features that are common to other mineral systems (Morrison et al. 2017, 2020, 2022; Hazen et al. 2019). A minority of 261 relatively common metamorphic mineral species adopt central positions, where each is linked to two or more different groups of metamorphic minerals. Only 1 mineral species, *magnetite*, is linked to all 8 groups of metamorphic rocks. Six additional common minerals—*calcite, diopside, ilmenite, pyrite, rutile*, and *quartz*—are linked to 7 groups. These minerals from multiple metamorphic lithologies are less diagnostic in defining communities or clusters of closely-related minerals than minerals known from only one or two types of metamorphic rocks.

By contrast, a significant majority of mineral species are rare; 959 of these minerals are linked to a single metamorphic mineral group, thus creating six dramatic "starbursts" of nodes decorating the periphery of the bipartite network. Metamorphosed Ba-Fe-Mn-Pb deposits (node BAM) boast the greatest number of these single-node phases (375 species, or 31 % of the 1220 metamorphic minerals), which create the largest such display in the lower right of the network. Note that this concentration of relatively rare minerals, like the BAM node with which it is associated, forms a relatively isolated region of the bipartite network. Other prominent starbursts are connected to contact metamorphism (CON; 241 unique mineral species), regional metamorphism (REG; 151 unique species), xenoliths (XEN; 87 unique species), and

ophiolites (OPH; 69 unique species). Thus, as in many other mineral systems, most metamorphic minerals are rare, known from 5 or fewer localities and formed by a single process (Hazen and Ausubel 2016).

In addition, 160 minerals are associated with exactly two of the 8 metamorphic rock groups, 32 minerals are linked to 3 groups, and 30 minerals are linked to 4 groups. The most common connection from one mineral species to two metamorphic rock groups is for contact and regional metamorphic rocks (135 minerals), which explains the proximity of CON and REG nodes in the upper half of Figure 3. Other strong connections of a mineral to two groups of metamorphic rocks include regional and high-pressure metamorphic rocks (71 species); xenolith and contact metamorphic rocks (67 species); xenolith and regional metamorphic rocks (64 species); contact and high-pressure metamorphic rocks (55 species); regional and Ba-Mn deposits (47 species), and contact and Ba-Mn deposits (41 species). These varied mineral associations across several kinds of metamorphic lithologies are reflected in the distinctive topology of Figure 3.

This is the peer-reviewed, final accepted version for American Mineralogist, published by the Mineralogical Society of America.
The published version is subject to change. Cite as Authors (Year) Title. American Mineralogist, in press.
DOI: https://doi.org/10.2138/am-2023-9004. http://www.minsocam.org/

4. IMPLICATIONS: THE EVOLUTION OF METAMORPHIC MINERALS

Metamorphic rocks display characteristics of an evolving chemical system, with significant increases in diversity and average chemical complexity over 4.5 billion years of Earth history (Krivovichev et al. 2018). Tabulations of the earliest known ages for diagnostic metamorphic minerals have the potential to document these changes. The Mineral Evolution Database (MED: https://rruff.info/evolution, accessed 11 September 2023) records the ages of 200,000 mineral/locality pairs. While ages of metamorphic minerals were not the principal focus of the MED, most major metamorphic minerals are represented by multiple ages. Accordingly, Table 4 lists the oldest MED ages for 47 minerals that are most commonly found in metamorphic rocks.

Table 4. Oldest recorded ages of 47 select metamorphic minerals arranged chronologically. Ages are from the Mineral Evolution Database (https://rruff.info/evolution, accessed 11 September 2023) unless otherwise noted.

Mineral Kind	Chemical Formula	Age Range (Ma)[1]	Community[2]
Geikielite	$MgTiO_3$	4330—4310	4
Diopside	$CaMgSi_2O_6$	4330—4010	2
Hedenbergite	$CaFe^{2+}Si_2O_6$	4330—4010	2
Wollastonite	$CaSiO_3$	4330—4010	2
Andalusite	Al_2SiO_5	4000—3200	1
Anthophyllite	$\square Mg_2Mg_5Si_8O_{22}(OH)_2$	4000—3200	1
Cordierite	$(Mg,Fe^{2+})_2Al_4Si_5O_{18}$	4000—3200	1
Tremolite	$\square Ca_2(Mg_{5.0\text{-}4.5}Fe^{2+}{}_{0.0\text{-}0.5})Si_8O_{22}(OH)_2$	4000—3200	4
Chloritoid	$Fe^{2+}Al_2O(SiO_4)(OH)_2$	4000—3040	6
Grunerite	$\square Fe^{2+}{}_2Fe^{2+}{}_5Si_8O_{22}(OH)_2$	4000—2920	--
Cummingtonite	$\square Mg_2Mg_5Si_8O_{22}(OH)_2$	4000—2917	4
Kyanite	Al_2SiO_5	4000—2714	6
Sillimanite	Al_2SiO_5	3640—3200	1
Graphite	C	3640—3200	5
Corundum	Al_2O_3	3640—3040	1
Diamond[3]	C	3600—3600	6
Spessartine	$Mn^{2+}{}_3Al_2Si_3O_{12}$	3293—2874	--
Phlogopite	$[[KMg_2(Mg,Fe^{2+})(Si,Al)_2Si_2O_{10}(OH,F)_2]]$	3200—3200	4
Grossular	$Ca_3Al_2Si_3O_{12}$	2969—2969	2
Vesuvianite	$(Ca,Na)_{19}(Al,Mg,Fe)_{13}(SiO_4)_{10}(Si_2O_7)_4(OH,F,O)_{10}$	2918—2835	2

This is the peer-reviewed, final accepted version for American Mineralogist, published by the Mineralogical Society of America.
The published version is subject to change. Cite as Authors (Year) Title. American Mineralogist, in press.
DOI: https://doi.org/10.2138/am-2023-9004. http://www.minsocam.org/

	Staurolite	$Fe^{2+}_2Al_9Si_4O_{23}(OH)$	2906—2730	1
	Piemontite	$Ca_2Al_2Mn^{3+}(Si_2O_7)(SiO_4)O(OH)$	2906—2782	--
	Prehnite	$Ca_2Al(Si_3Al)O_{10}(OH)_2$	2900—2810	5
	Scapolite	$(Na,Ca)_4(Al,Si)_{12}O_{24}(CO_3,SO_4,Cl)$	2845—1930	2
	Glaucophane	$\square Na_2(Mg_3Al_2)Si_8O_{22}(OH)_2$	2845—1700	6
	Andradite	$Ca_3Fe^{3+}_2Si_3O_{12}$	2742—2670	2
	Baddellyite	ZrO_2	2742—2670	4
	Brucite	$Mg(OH)_2$	2742—2700	4
	Pumpellyite	$Ca_2Al_3(Si_2O_7)(SiO_4)(OH,O)_2 \cdot H_2O$	2680—2677	5
	Pyrope	$Mg_3Al_2Si_3O_{12}$	2710—2700	6
	Actinolite	$\square Ca_2(Mg,Fe^{2+})_5Si_8O_{22}(OH,F)_2$	2709—2701	--
	Sapphirine	$Mg_4(Mg_3Al_9)O_4(Si_3Al_9O_{36})$	2500—2448	1
	Rhodonite	$CaMn_3Mn(Si_5O_{15})$	2500—2216	--
	Osumilite	$(K,Na)(Fe^{2+},Mg)_2(Al,Fe^{3+})_3(Si,Al)_{12}O_{30}$	2485—496	1
	Humite	$Mg_9(SiO_4)_4(F,OH)_2$	2070—1950	4
	Periclase	MgO	2058—2058	4
	Coesite	SiO_2	2050—2050	6
	Jadeite	$NaAlSi_2O_6$	2038—1270	6
	Monticellite	$CaMgSiO_4$	2000—1109	3
	Spurrite	$Ca_5(SiO_4)_2(CO_3)$	1750—248	3
	Mullite	$Al_{4+2x}Si_{2-2x}O_{10-x}$ ($x \approx 0.4$)	960—248	1
	Merwinite	$Ca_3Mg(SiO_4)_2$	794—684	3
	Lawsonite	$(Ca,Sr)Al_2(Si_2O_7)(OH)_2 \cdot H_2O$	599—497	3
	Bredigite	$Ca_7Mg(SiO_4)_4$	354—248	--
	Larnite	Ca_2SiO_4	354—248	3
	Rankinite	$Ca_3Si_2O_7$	354—66	3
	Tilleyite	$Ca_5Si_2O_7(CO_3)_2$	300—300	3

1. The MED lists maximum and minimum ages for metamorphic occurrences. In many cases the age range is large because a deposit is listed, for example, as “Precambrian.” Here we cite both the greatest maximum and greatest minimum values. These two values may come from different localities.
2. Community as illustrated in Figure 1. Note that *actinolite*, *bredigite*, *spessartine, grunerite, rhodonite*, and *piemontite* were not included in Figure 1 minerals.
3. Diamond ages were provided by Shirey et al. (2013).

Earth’s first metamorphic rocks must have been thermally altered xenoliths and contact zones (hornfels and sanidinite facies) associated with early Hadean igneous activity (> 4.5 Ga). The appearance of new Hadean lithologies, including clay-rich sediments, arkosic sandstones, and carbonates, provided additional protoliths for thermal metamorphism prior to 4.0 Ga.

Indeed, the 8 oldest minerals in Table 4, all Paleoarchean or older (> 3.2 Ga), are associated with higher temperature metamorphic regimes.

Also appearing in the Meso- and Neoarcheon Eras (> 2.5 Ga) are representative minerals from regional and high-pressure metamorphic rocks (Table 4). The exposure of extensive regional metamorphic terrains by orogenesis and erosion, with lithologies corresponding to the Barrovian sequence of index mineral metamorphic zones, thus appears to have occurred significantly later in Earth history, perhaps in association with plate tectonics.

More recently, rapid subduction and rebound of crustal wedges, coupled with a shallowing geothermal gradient, has produced distinctive suites of blueschist, eclogite, and ultrahigh pressure metamorphic suites. Some of these phases, including *glacophane*, *jadeite*, *pyrope*, *staurolite*, are first recorded in the Neoarchean or Paleoproterozoic Eras (2.8 to 2.0 Ga), perhaps signaling the commencement of subduction-driven tectonics. However, a number of key high-pressure metamorphic minerals, including *coesite*, *jadeite*, and *lawsonite*, are only known since 2.05 Ga (Table 4).

The evolution of the metamorphic minerals continued into the Phanerozoic Eon (< 540 Ma). Intriguingly, 5 of the most recent (< 800 Ma) metamorphic minerals in Table 4—*bredigite*, *larnite*, *merwinite*, *rankinite*, and *tilleyite*—are all Ca-(Mg)-silicates that form by low-P contact metamorphism of limestone or dolomite. The lack of older known examples of these minerals may reflect a sparsity of dated examples, but enhanced biogenic production of carbonate lithologies may also have played a role. Indeed, the Phanerozoic Eon represents a distinctive phase in metamorphic mineral evolution. New biogenic lithologies such as coal, phosphorites, and reef carbonates were subjected to both regional and thermal metamorphism, while the

intense burning of fossil hydrocarbons in the form of coal, oil, and natural gas created new pyrometamorphic regimes—processes to be considered in a subsequent contribution to this series. The evolution of metamorphic minerals thus epitomizes the kinds of changes in physical, chemical, and ultimately biological processes in the crust and upper mantle that exemply mineral evolution over more than 4.5 billion years of Earth history.

ACKNOWLEDGMENTS

This manuscript benefited from multiple extensive and detailed reviews by John Ferry, who initially served as one of two reviewers of the submitted manuscript. His efforts fully warranted coauthorship, though he declined to be so recognized. Nevertheless, his informed and thoughtful contributions are reflected in every aspect of this contribution. We are also grateful to John Brady, Michael Brown, Douglas Rumble, Michael Walter, and Michael Wong for valuable discussions and reviews of an early version of this contribution. We also thank Associate Editor Simon Redfern and reviewer Jay Ague for their thorough, thoughtful, and constructive reviews.

FUNDING

Studies of mineral evolution have been supported by the Deep-time Digital Earth (DDE) program, the John Templeton Foundation, the NASA Astrobiology Institute ENIGMA team, a private foundation, and the Carnegie Institution for Science. Any opinions, findings, or recommendations expressed herein are those of the authors and do not necessarily reflect the views of the National Aeronautics and Space Administration.

REFERENCES

Ackermand, D., and Rasse, P. (1973) Coexisting zoisite and clinozoisite in biotite schists from the Hohe Tasuren, Austria. Contributions to Mineralogy and Petrology, 42, 333-341.

Agrell, S.O., and Langley, J.M. (1958) The dolerite plug at Tievebulliagh, near Cushendall, Co. Antrim. Part (I): The thermal metamorphism. Proceedings of the Royal Irish Academy, 59B, 93-127.

Alfors, J.T., Stinson, M.C., Matthews, R.A., and Pabst, A. (1965) Seven new barium minerals from eastern Fresno County, California. American Mineralogist, 50, 314-340.

Almende, B.V., and Contributors, Benoit Thieurmel and Titouan Robert (2021). visNetwork: Network Visualization using 'vis.js' Library. R package version 2.1.0. https://CRAN.R-project.org/package=visNetwork.

Anthony, J.W., Bideaux, R.A., Bladh, K.W., and Nichols, M.C. (1990-2003) Handbook of Mineralogy, 6 volumes. Mineral Data Publishing.

Anzolini, C., Wang, F., Harris, G.A., Locock, A.J., Zhang, D., Nestola, F., Peruzzo, L., Jacobsen, S.D., and Pearson, D.G. (2019) Nixonite, $Na_2Ti_6O_{13}$, a new mineral from a metasomatized mantle garnet pyroxenite from the western Rae Craton, Darby kimberlite field, Canada. American Mineralogist, 104, 1336-1344.

Armbruster, T., Bonazzi, P., Akasaka, M., Bermanec, V., Chopin, C., Gieré, R., Heuss-Assbichler, S., Liebscher, A., Menchetti, S., Pan, Y., and Pasero, M. (2006) Recommended nomenclature of the epidote-group minerals. European Journal; of Mineralogy, 18, 551-567.

Atherton, M.P. (1964) The garnet isograd in pelitic rocks and its relation to metamorphic rocks. American Mineralogist, 49, 1331-1349.

Augustithis, S.S. (1985) Atlas of the Textural Patterns of Metamorphosed (Transformed and Deformed) Rocks and their Genetic Significance. Theophrastus Publications.

Bai, W.J., et al. (2000) The PGE and base-metal alloys in the podiform chromitites of the Luobusa ophiolite, southern Tibet. Canadian Mineralogist,

Bai, W.J., Zhou, M.F., and Robinson, P.T. (2011) Possibly diamond-bearing mantle peridotites and chromites in the Luobusa and Dongqiao ophiolites, Tibet. Canadian Journal of Earth Sciences, 30, 1650-1659.

Ballhaus, C, *et al.* (2017) Ultra-high pressure and ultra-reduced minerals in ophiolites may form by lightning strikes. Geochemical Perspective Letters,

Banno, S., and Matsui, Y. (1965) Ecologite types and partition of Mg, Fe and Mn between clinopyroxene and garnet. Proceedings of the Japanese Academy, 41, 716-721.

Barnes, J., and Hut, P. (1986) A hierarchical O(*N* log *N*) force-calculation algorithm. Nature, 324, 446-449.

Barrow, G. (1893) On an intrusion of muscovite-biotite gneiss in the Southeast Highlands of Scotland, and its accompanying metamorphism. Journal of the Geological Society of London, 49, 330-358.

Basta, E.Z., and Shaalan, M.M.B. (1974) Distribution of opaque minerals in the Tertiary volcanic rocks of Yemen and Aden. Neues Jahrbuch fur Mineralogie—Abhandlungen, 121, 85-102.

Bilgrami, S.A. (1956) Manganese silicate minerals from Chikla, Bhandara district, India. Mineralogical magazine, 31, 236-244.

Binns, R.A. (1967) Barroisite-bearing eclogite from Naustdal, Sogn og Fjordane, Norway, Jornal of Petrology, 8, 349-371.

Bird, A., and Tobin, E. (2015) Natural Kinds. In Zalta, E.N. (ed.) The Stanford Encyclopedia of Philosophy (Spring 2015 Edition) https://plato.stanford.edu/entries/natural-kinds/

Black, P.M. (1989) High-temperature calc-silicate hornfels in Northland, New Zealand. Bulletin of the Royal Society of New Zealand, 26, 215-224.

Blondel, V.D., Guillaume, J.-L., Lambiotte, R., and Lefebvre, E. (2008) Fast unfolding of communities in large networks. Journal of Statistical Mechanics, 2008, 1–12.

Bluth, G.J.S., and Kump, L.R. (199) Phanerozoic paleogeology. American Journal of Science, 291, 284–308.

Bohlen, S.R., Montana, A., and Kerrick, D.M. (1991) Precise determinations of the equilibria kaynaite-reversible-sillimanite and kyanite-reversible-andalusite and a revised triple point for Al_2SiO_5 polymorphs. Amrican Mineralogist, 76, 677-680.

Bostock, M., Ogievetsky, V., and Heer, J. (2011). D^3 data-driven documents. IEEE transactions on visualization and computer graphics, 17(12), 2301-2309.

Botha, B.J.V. [Editor] (1983) Namaqualand Metamorphic Complex. The Geological Society of South Africa.

Boujibar, A., Howell, S., Zhang, S., Hystad, G., Prabhu, A., Liu, N., Stephan, T., Narkar, S., Eleish, A., Morrison, S.M., Hazen, R.M., and Nittler, L.R. (2021) Cluster analysis of presolar silicon carbide grains: Evaluation of their classification and astrophysical implications. Astrophysical Journal Letters. DOI: 10.3847/2041-8213/abd102

Bowen, N.L. (1928) The Evolution of the Igneous Rocks. Princeton University Press.

Bowen, N.L. (1940) Progressive metamorphism of siliceous limestone and dolomite. Journal of Geology, 48, 225-274.

Bowles, J.F.W., Howie, R.A., Vaughan, D.J., and Zussman, J. (2011) Rock-Forming Minerals. Volume 5A, Second Edition. Non-Silicates: Oxides, Hydroxides and Sulfides. The Geological Society of London.

Boyd, R. (1991) Realism, anti-foundationalism and the enthusiasm for natural kinds. Philosophical Studies, 61, 127-148.

Boyd, R. (1999) Homeostasis, species, and higher taxa. In: R. Wilson, Ed., Species: New Interdisciplinary Essays, pp.141-186. Cambridge University Press.

Brown, M. (2006) Duality of thermal regimes is the distinctive characteristic of plate tectonics since the Neoarchean. Geology, 34, 961-964.

Brown, M. (2007) Metamorphic conditions in orogenic belts: a record of secular change. International Geology Review, 49, 193–234.

Brown, M., and Johnson, T.E. (2019) Time's arrow, time's cycle: granulite metamorphism and geodynamics. Mineralogical Magazine, 83, 323-338.

Buddington, A.F. (1952) Chemical petrology of some metamorphosed Adirondack gabbroic, syenitic and quartz syenitic rocks. American Joiurnal of Science, Bowen Volume, 37-84.

Burke, E.A.J. (2006) The end of CNMMN and CCM—Long live the CNMNC! Elements, 2, 388.

Buseck, P.R., and Huang, B.-J. (1985) Conversion of carbonaceous material to graphite during metamorphism. Geochimica et Cosmochimica Acta, 49, 2003–2016.

Bustin, R.M., and Matthews, W.H. (1982) In situ gasification of coal, a natural example: history, petrology, and mechanics of combustion. Canadian Journal of Earth Sciences, 19, 514-523.

Button, A. (1982) Sedimentary iron deposits, evaporates and phosphorites: State of the art report. In H.D. Holland and M. Schidlowski, Eds., Mineral Deposits and the Evolution of the

1161 Biosphere. Springer-Verlag, pp. 259-273.

1162 Cairncross, B., and Beukes, N.J. (2013) The Kalahari Manganese Field, the Adventure Continues.
1163 Struik Nature Publishers.

1164 Carpenter, A.B. (1967) Mineralogy and petrology of the system CaO-MgO-CO_2-H_2O at
1165 Crestmore, California. American Mineralogist, 52, 1351-1363.

1166 Carswell, D.A. [Editor] (1990) Ecologite Facies Rocks. Chapman and Hall.

1167 Carswell, D.A., and Compagnoni, R. [Editor] (2003) Ultrahigh Pressure Metamorphism.
1168 European Mineralogical Union Notes in Mineralogy, 5.

1169 Chang, L.L.Y., Howie, R.A., and Zussman, J. (1996) Rock-Forming Minerals. Volume 5B, Second
1170 Edition. Sulphates, Carbonates, Phosphates and Halides. Longman Group.

1171 Chatterjee, N.D. (1970) Synthesis and upper stability of paragonite. Contributions to Mineralogy
1172 and Petrology, 27, 244-257.

1173 Chiama, K., Gabor, M., Lupini, I., Rutledge, R., Nord, J.A., Zhang, S., Boujibar, A., Morrison, S.M.,
1174 and Hazen, R.M. (2020) Garnet: A comprehensive standardized database of garnet
1175 geochemical analyses integrating provenance and paragenesis. Geological Society of
1176 America Annual Meeting 2020, 52. Doi: 10.1130/abs/2020AM-354256.

1177 Chiama, K., Gabor, M., Lupini, I., Rutledge, R., Nord, J.A., Zhang, S., Boujibar, A., Bullock, E.S.,
1178 Walter, M.J., Spear, F., Morrison, S.M., and Hazen, R.M. (2022) ESMD-Garnet dataset. Open
1179 Data Repository, https://doi.org/10.48484/camh-xy98

1180 Chopin, C. (1981) Talc-phengite: a widespread assemblage in high-grade blueschists of the
1181 Western Alps: A first record and some consequences. Journal of Petrology, 22, 628-650.

1182 Chopin, C. (1984) Coesite and pure pyrope in high-grade blueschists of the western Alps: a first

record and some consequences. Contributions to Mineralogy and Petrology, 86, 107–118.

Cleland, C.E., Hazen, R.M., and Morrison, S.M. (2021) Historical natural kinds in mineralogy: Systematizing contingency in the context of necessity. Proceedings of the National Academy of Sciences, 108, e2015370118 (8 p.)

Coleman, R.G., and Clark, J.R. (1968) Pyroxenes in the blueschist facies of California. American Journal of Science, 266, 43-59.

Coleman, R.G., and Lee, D.E. (1963) Glaucophane-bearing metamorphic rock types of the Cadazero area, California. Journal of Petrology, 4, 260-301.

Coleman, R.G., Lee, D.E., Beatty, L.B., and Brannock, W.W. (1965) Ecologites and eclogites: Their differences and similarities. Geological Society of America Bulletin, 76, 483-508.

Coombs, D.S. (1960) Lower grade mineral facies in New Zealand. Report of the 21st International Geological Congress, 13, 339-351.

Coombs, D.S. (1993) Dehydration veins in diagenetic very-low-grade metamorphic rocks: features of the crustal seismogenic zone and their significance to mineral facies. Journal of Metamorphic Geology, 11, 389-399.

Coombs, D.S., Kawachi, Y., Houghton, B.F., Hyden, G., Pringle, I.J., and Williams, J.G. (1977) Andradite and andradite-grossular solid solutions in very low-grade regionally metamorphosed rocks in southern New Zealand. Contributions to Mineralogy and Petrology, 63, 229-246.

Csardi, G., and Nepusz, T. (2006) The igraph software package for complex network research. InterJournal, Complex Systems, 1695. https://igraph.org

Daly, R.A. (1925) The geology of Ascension Island. Proceedings of the American Academy of Arts and Sciences, 60, 3–80, https://doi.org/10.2307/25130043.

Davies, G.R., Nixon, P.H., Pearson, D.G., and Obata, M. (1993) Tectonic implications of graphitized diamonds from the Ronda peridotite massif, southern Spain. Geology 21, 471–474.

Davis, S.R., and Ferry, J.M. (1993) Fluid infiltration during contact metamorphism of interbedded marble and calc-silicate hornfels, Twin Lakes area, central Sierra Nevada, California. Journal of Metamorphic Petrology, 11, 71-88.

Deer, W.A., Howie, R.A., and Zussman, J. (1982-2013) Rock-Forming Minerals. Second Edition. 11 volumes. Longman, John Wiley, and The Geological Society of London.

Deer, W.A., Howie, R.A., and Zussman, J. (1982) Rock-Forming Minerals. Volume 1A, Second Edition. Orthosilicates. Longman.

Deer, W.A., Howie, R.A., and Zussman, J. (1986) Rock-Forming Minerals. Volume 1B, Second Edition. Disilicates and Ring Silicates. John Wiley.

Deer, W.A., Howie, R.A., and Zussman, J. (1997a) Rock-Forming Minerals. Volume 2A, Second Edition. Single-Chain Silicates. The Geological Society of London.

Deer, W.A., Howie, R.A., and Zussman, J. (1997b) Rock-Forming Minerals. Volume 2B, Second Edition. Double-Chain Silicates. The Geological Society of London.

Deer, W.A., Howie, R.A., and Zussman, J. (2001) Rock-Forming Minerals. Volume 4A, Second Edition. Framework Silicates: Feldspars. The Geological Society of London.

Deer, W.A., Howie, R.A., Wise, W.S., and Zussman, J. (2004) Rock-Forming Minerals. Volume 4B, Second Edition. Framework Silicates: Silica Minerals, Feldspathoids and the Zeolites. The

Geological Society of London.

Deer, W.A., Howie, R.A., and Zussman, J. (2009) Rock-Forming Minerals. Volume 3B, Second Edition. Layered Silicates Excluding Micas and Clay Minerals. The Geological Society of London.

De Roever, W.P. (1956) Some differences between post-Paleozoic and older regional metamorphism. Geologie en Mijnbouw, New Series 18e, 123-127.

Diessel, C.F.K., Brothers, R.N., and Black, P.M. (1978) Coalification and graphitization in high-pressure schists in New Caledonia. Contributions to Mineralogy and Petrology, 68, 63–78.

Dilek, Y. (2003) Ophiolite pulses, orogeny, and mantle plumes. Geological Society of London Special Publications, 218, 9-19.

Dobrzhinetskaya, L.F., Eide, E.A, Larsen, R.B., Sturt, B.A., Trønnes, R.G., Smith, D.C., Taylor, W.R., and Posukhova, T.V. (1995) Microdiamond in high-grade metamorphic rocks of the Western Gneiss region, Norway. Geology, 23, 597– 600.

Dobrzhinetskaya, L.F., et al. (2009) High-pressure highly reduced nitrides and oxides from chromitite of a Tibetan ophiolite. Proceedings of the national Academy of Sciences USA,

Dobrzhinetskaya, L.F., O'Bannon, E.F. III, and Sumino, H. (2022) Non-cratonic diamonds from UHP metamorphic terranes, ophiolites and volcanic sources. Reviews in Mineralogy and Geochemistry, 88, 191-256.

Einaudi, M.T., and Burt, D.M. (1982) Terminology, classification and composition of skarn deposits. Economic Geology, 77, 745-754.

Einaudi, M.T., Meinert, L.D., and Newberry, R.J. (1981) Skarn deposits. Economic Geology, 75th Anniversary Volume, 317-391.

Ereshefsky, M. (2014) Species, historicity, and path dependency. Philosophy of Science, 81, 714-726.

Ernst, W.G. (1972) Occurrence and mineralogical evolution of blueschist belts with time. American Journal of Science, 272, 657-668.

Eskola, P. (1920) The mineral facies of rocks. Norsk Geolologisk Tidsskrift, 6, 143-194.

Eskola, P. (1952) On the granulites of Lapland.American Jouirnalof Science, Bowen Volume, 133-171.

Evans, B.W. (1964) Coexisting albite and oligoclase in some schists from New Zealand. American Mineralogist, 49, 173-179.

Falkowski, P., Scholes, R.J., Boyle, E., Canadell, J., Canfield, D., Elser, J., Gruber, N., Hibbard, K., Högberg, P., Linder, S., Mackenzie, F.T., Moore, B. III, Pederson, T., Rosenthal, Y., Seitzinger, S., Smetacek, V., and Steffen, W. (2000) The global carbon cycle: A test of our knowledge of Earth as a system. Science, 290, 291-296.

Ferré, E. (1989) Les gneiss à cordiérite-grenat-orthoamphibole de Topiti: témoin possible d'un soile métamorphique du Protérozoique en Corse occidentale. Compte Rendus Academie des Science Paris, Series 2, 309, 893-898.

Ferry, J.M. (1976) *P*, *T*, f_{CO_2} and f_{H_2O} during metamorphism of calcareous sediments in the Waterville-Vassalboro area, south-central Maine. Contributions to Mineralogy and Petrology, 57, 119-143.

Ferry, J.M. (1984) A biotite isograd in South-Central Maine, U.S.A.: Mineral reactions, fluid transfer, and heat transfer. Journal of Petrology, 25, 871-893.

Ferry, J.M. (1988) Infiltration-driven metamorphism in Northern New England, USA. Journal of Petrology, 29, 1121-1159.

Ferry, J.M. (1989) Contact metamorphism of roof pendants at Hope Valley, Alpine County, California, USA. Contributions to Mineralogy and Petrology, 101, 402-417.

Ferry, J.M. (1992) Regional metamorphism of the Waits River Formation, eastern Vermont: Delineation of a new type of giant metamorphic hydrothermal system. Journal of Petrology, 33, 45-94.

Ferry, J.M. (1994) Overview of the petrologic record of fluid flow during regional metamorphism in northern New England. American Journal of Science, 294, 905-988.

Ferry, J.M. (1995) Fluid flow during contact metamorphism of ophicarbonate rocks in the Bergell Aureole, Val Malenco, Italian Alps. Journal of Petrology, 36, 1039-1053.

Ferry, J.M. (1996) Prograde and retrograde fluid flow during contact metamorphism of siliceous carbonate rocks from the Ballachulish aureole, Scotalnd. Contributions to Mineralogy and Petrology, 124, 235-254.

Ferry, J.M. (2007) The role of volatile transport by diffusion and dispersion in driving biotite-forming reactions during regional metamorphism of the Gile Mountain Formation, Vermont. American Mineralogist, 92, 1288-1302.

Ferry, J.M., and Rumble III, D. (1997) Formation and destruction of periclase by fluid flow in two contact aureoles. Contributions to Mineralogy and Petrology, 128, 313-334.

Ferry, J.M., Mutti, L.J., and Zuccala, G.J. (1987) Contact metamorphism/hydrothermal alteration of Tertiary basalts from the Isle of Skye, northwest Scotland. Contributions to Mineralogy and Petrology, 95, 166-181.

Ferry, J.M., Wing, B.A., and Rumble III, D. (2001) Formation of wollastonite by chemically reactive fluid flow during contact metamorphism, Mt. Morrison Pendant, Sierra Nevada, California, USA. Journal of Petrology, 42, 1705-1728.

Ferry, J.M., Wing, B.A., Penniston-Dorland, S.C., and Rumble II, D. (2002) Direction of fluid flow during contact metamorphism of siliceous carbonate rocks: New data for the Monzoni and Predazzo aureoles, northern Italy, and a global review. Contributions to Mineralogy and Petrology, 142, 679-699.

Ferry, J.M., Rumble III, D., Wing, B.A., and Penniston-Dorland, S.C. (2005) A new interpretation of centimeter-scale variations in the progress of infiltration-driven metamorphic reactions: Case study of carbonated metaperidotite, Val d'Efra, Central Alps, Switzerland. Journal of Petrology, 46, 1725-1746.

Ferry, J.M., Stubbs, J.E., Xu, H., Guan, Y., and Eiler, J.M. (2015) ankerite grains with dolomite cores: A diffusion chronometer for low- to medium-grade regionally metaorphosed clastic sediments. American Mineralogist, 100, 2443-2457.

Fleet, M.E. (2003) Rock-Forming Minerals. Volume 3A, Second Edition. Sheet Silicates: Micas. The Geological Society of London.

Floran, R.J., and Papike, J.J. (1978) Mineralogy and petrology of the Gunflint Iron Formation, Minnesota—Ontario: Correlation of compositional and assemblage variations at low to moderate grade. Journal of Petrology, 19, 215-288.

Fortunato, S. (2010) Community detection in graphs. Physics Reports, 486, 75-174.

1311 Frondel, C. (1990) Historical overview of the development of mineralogical science at Franklin
1312 and Sterling Hill, Sussex County, N.J. In: Character and Origin of the Franklin—Sterling Hill
1313 Orebodies. Franklin—Ogdensburg Mineralogical Society, pp. 3-13.
1314 Fulignati, P., Marianelli, P., Santacroce, R., and Sharma, A. (2000) The skarn shell of the 1944
1315 Vesuvius magma chamber. Genesis and P-T-X conditions from melt and fluid inclusion data.
1316 European Journal of Mineralogy, 12, 1025-1030.
1317 Furnes, H., de Witt, M., Staudigel, H., Rosing, M., and Muehlenbachs, K. (2007) A vestige of
1318 Earth's oldest ophiolite. Science, 315, 1704-1707.
1319 Gaines, R.V., Skinner, C., Foord, E.E., Mason, B., and Rosenzweig, A. (1997) Dana's New
1320 Mineralogy. John Wiley & Sons.
1321 Ganade, C.E., Rubatto, D., Lanari, P., Hermann, J., Tesser, L.R., and Caby, R. (230 °C023) Fast
1322 exhumation of Earth's earliest ultrahigh-pressure rocks in the West Gondwana orogen, Mali.
1323 Geology, 51, 647-651.
1324 Gates, A.E., and Speer, J.A. (2022) Allochemical retrograde metamorphism in shear zones: and
1325 example in metapelites, Virginia, USA. Journal of Metamorphic Geology, 9, 581-604.
1326 Girvan, M., and Newman, M.E.J. (2002) Community structure in social and biological networks.
1327 Proceedings of the National Academy of Sciences USA, 99, 7821-7826.
1328 Godman, M. (2019) Scientific realism with historical essences: The case of species. Synthese,
1329 https://doi.org/10.1007/s11229-018-02034-3.
1330 Goldschmidt, V.M. (1911) Die Kontakmetamorphose im Kristtianiagebiet. Norske Videnskabers
1331 Selskabs Skrifter I, Mat.-Naturv. Klasse, no. 1.
1332 Grapes, R. (2006) Pyrometamorphism. Second Edition. Springer.

Gregory, D.D., Cracknell, M.J., Large, R.R., McGoldrick, P., Kuhn, S., Maslennikov, V.V., Baker, M.J., Fox, N., Belousov, I., Figueroa, M.C., Steadman, J.A., Fabris, A.J., and Lyons, T.W. (2019) Distinguishing ore deposit type and barren sedimentary pyrite using laser ablation-inductively coupled plasma-mass spectrometry trace element data and statistical analysis of large data sets. Economic Geology, 114, 771-786.

Guidotti, C.V. (1984) Micas in metamorphic rocks. Reviews in Mineralogy, 13, 357-467.

Guidotti, C.V., and Sassi, F.P. (1998) Petrogenetic significance of Na-K white mica mineralogy: Recent advances for metamorphic rocks. European Journal of Mineralogy, 10, 815-854.

Guidotti, C.V., Sassi, F.P., Sassi, R., and Selverstone, J. (1994) The paragonite-muscovite solvus. I. *P-T-X* limits derived from the Na-K compositions of natural, quasibinary paragonite-muscovite pairs. Geochimica et Cosmochimica Acta, 58, 2269-2275.

Guitard, G. (1965) Les types de métamorphisme régionale à andalousite, cordiérite et almandine, et à andalousite, cordiérite, almandine et staurotide, dans la zone axiale des Pyrénees-Orientales; contributions à l'étude des types de métamorphisme de basse pression. Compte Rendus Academie des Science, Paris, 269D, 1159-1162.

Hacker, B.R. (2006) Pressures and temperatures of ultrahigh-pressure metamorphism: Implications for UHP tectonics and H_2O in subducting slabs. International Geology Review, 48, 1053-1066.

Halferdahl, L.B. (1961) Chloritoid: Its composition, x-ray and optical properties, stability and occurrence. Journal of Petrology, 2, 49-135.

Hall, A.J., Boyce, A.J., and Fallick, A.E. (1987) Iron sulfides in metasediments; support for a retrogressive pyrrhotite to pyrite reaction. Chemical Geology, 65, 305-310.

Harker, A. (1950) Metamorphism: A Study of the Transformnations of Rock-Masses. E. P. Dutton & Co.

Harley, S.L. (2008) Refining the P-T records of UHT crustal metamorphism. Journal of Metamorphic Geology, 26, 125–154.

Harley, S.L. (2021) UHT metamorphism. In: Encyclopedia of Geology, 2nd edition. Elsevier, pp. 522-552.

Hatert, F., Mills, S.J., Hawthorne, F.C., and Rumsey, M.S. (2021) A comment on “An evolutionary system of mineralogy: Proposal for a classification of planetary materials based on natural kind clustering.” American Mineralogist, 106, 150-153.

Hawley, K., and Bird, A. (2011) What are natural kinds? Philosophical Perspectives, 25, 205-221.

Hawthorne, F.C., Griep, J.L., and Curtis, L. (1980) A three amphibole assemblage from the Talon Lake sill, Peterborough County, Ontario. Canadian Mineralogist, 18, 275-284.

Hawthorne, F.C., Oberti, R., Harlow, G.E., Maresch, W.V., Martin, R.F., Schumacher, J.C., and Welch, M.D. (2011) Nomenclature of the amphibole supergroup. American Mineralogist, 97, 2031-2048.

Hawthorne, F.C., Mills, S.J., Hatert, F., and Rumsey, M.S. (2021) Ontology, archetypes and the definition of “mineral species.” Mineralogical Magazine, 85, 125-131.

Hazen, R.M. (2019) An evolutionary system of mineralogy: Proposal for a classification based on natural kind clustering. American Mineralogist, 104, 810-816.

Hazen, R.M. (2021) Reply to “A comment on ‘An evolutionary system of mineralogy: Proposal for a classification of planetary materials based on natural kind clustering’.” American Mineralogist, 106, 154-156.

Hazen, R.M., and Ausubel, J.H. (2016) On the nature and significance of rarity in mineralogy. American Mineralogist, 101, 1245-1251.

Hazen, R.M., and Morrison, S.M. (2020) An evolutionary system of mineralogy, Part I: stellar mineralogy (>13 to 4.6 Ga). American Mineralogist, 105, 627-651.

Hazen, R.M., and Morrison, S.M. (2021) An evolutionary system of mineralogy, Part V: Planetesimal Aqueous and thermal alteration of planetesimals (4.565 to 4.550 Ga). American Mineralogist, 106, in press. https://doi.org/10.2138/am-2021-7760

Hazen, R.M., and Morrison, S.M. (2022) On the paragenetic modes of minerals: A mineral evolution perspective. American Mineralogist, 107, 1262-1287.

Hazen, R.M., Papineau, D., Bleeker, W., Downs, R.T., Ferry, J.M., McCoy, T.L., Sverjensky, D.A., and Yang, H. (2008) Mineral evolution. American Mineralogist, 93, 1693-1720.

Hazen, R.M., Morrison, S.M., and Prabhu, A. (2021) An evolutionary system of mineralogy, Part III: Primary chondrule mineralogy (4.566 to 4.561 Ga). American Mineralogist, 106, 325-350.

Hazen, R.M., Morrison, S.M., Krivovichev, S.L., and Downs, R.T. (2022) Lumping and splitting: Toward a classification of mineral natural kinds. American Mineralogist, 107, 1288-1301.

Hazen, R.M., Morrison, S.M., Prabhu, A., Walter, M.J., and Williams, J.R. (2023) An evolutionary system of mineralogy, Part VII: The evolution of the igneous minerals (> 2500 Ma). American Mineralogist, in press.

Heaney, P.J. (2016) Time's arrow in the trees of life and minerals. American Mineralogist, 101, 1027-1035.

Henry, D.J., and Dutrow, B.L. (2012) Tourmaline at diagenetic to low-grade metamorphic conditions: Its petrologic applicability. Lithos, 154, 16-32.

Henry, D.J., Novak, M., Hawthorne, F.C., Ertl, A., Dutrow, B.L., Uher, P., and Pezzotta, F. (2011) Nomenclature of the tourmaline-supergroup minerals. American Mineralogist, 96, 895-913.

Hodges, K.V., and Spear, F.S. (1982) Geothermometry, geobarometry and the Al_2SiO_5 triple point at Mt. Moosilauke, New-Hampshire. American Mineralogist, 67, 1118-1134.

Holder, R.M., Viete, D.R., Brown, M., and Johnson, T.E. (2019) Metamorphism and the evolution of plate tectonics. Nature, 572, 378-381.

Hori, F. (1962) On the load metamorphic formation of rhodonite, tephroite and manganosite. Scientific Papers of the College of General Education, Univdersity of Tokyo, 12, 117-142.

Hoschek, G. (1984) Alpine metamorphism of calcareous sediments in the Western Hohe Tauren, Tyrol: Mineral equilibria in COSH fluids. Contributions to Mineralogy and Petrology, 87, 129-137.

Hystad, G., Boujibar, A., Liu, N., Nittler, L.R., and Hazen, R.M. (2021) Evaluation of the classification of presolar silicon carbide grains using consensus clustering with resampling methods: an assessment of the confidence of grain assignments. Monthly Notices of the Royal Astronomical Society, 510, 334-350.

Iwasaki, M. (1960) Barroisitic amphibole from Bizan in eastern Sikoku, Japan. Journal of the Geological Society of Japan, 66, 6125-630.

Jacob, D.E., and Mikhail, S. (2022) Polycrystalline diamonds from kimberlites: Snapshots of rapidand episodic diamond formation in the lithospheric mantle. Reviews in Mineralogy and Geochemistry, 88, 167-190.

Jahn, B.-M., Caby, R., and Monie, P. (2001) The oldest UHP eclogites of the World: age of UHP metamorphism, nature of protoliths and tectonic implications. Chemical Geology, 178, 143–

158.

Jan, M.Q., and Symmes, R.F. (1977) Piemontite schists from Upper Swat, north-west Pakistan. Mineralogical Magazine, 41, 537-540.

Joplin, G.A. (1968) A Petrography of Australian Metamorphic Rocks. American Elsevier Publishing Company.

Kappler, A., Pasquero, C., Konhauser, K.O., and Newman, D.K. (2005) Deposition of banded iron formations by photoautotrophic Fe(II)-oxidizing bacteria. Geology, 33, 865–868.

Khalidi, M.A. (2013) Natural Categories and Human Kinds: Classification in the Natural and Social Sciences. Cambridge University Press.

Kimball, K.L., and Spear, F.S. (1984) Metamorphic petrology of the Jackson County Iron Formation, Wisconsin. Canadian Mineralogist, 22, 605-619.

Kjarsgaard, B.A., de Wit, M., Heaman, L.M., Pearson, D.G., Stiefenhofer, J., Janusczcak, N., and Shirey, S.B. (2022) A review of the geology of global diamond mines and deposits. Reviews in Mineralogy and Geochemistry, 88, 1-118.

Klein, C. (1966) Mineralogy and petrology of the metamorphosed Wabush iron formation, southwestern Labrador. Journal of Petrology, 7, 246-305.

Klein, C. (2005) Some Precambrian banded iron-formations (BIFs) from around the world: Their age, geologic setting, mineralogy, metamorphism, geochemistry, and origins. American Mineralogist, 90, 1473-1499.

Kranck, S.H. (1961) A study of phase equilibria in a metamorphic iron formation. Journal of Petrology, 2, 137-184.

1442 Krivovichev, S.V., Krivovichev, V.G., and Hazen, R.M. (2018) Structural and chemical complexity
1443 of minerals: correlations and time evolution. European Journal of Mineralogy, 30, 231-236.
1444 Kusky, T.M. [Ed.] (2004) Precambrian Ophiolites and Related Rocks. Elsevier.
1445 Kusky, T.M., Li, J.-H., and Tucker, R.D. (2001) The Archean Dongwanzi ophiolite complex, North
1446 China craton: 2.505 billion year old oceanic crust and mantle. Science, 295, 1142-1145.
1447 Lal, R.K. (1969) Retrogression of cordierite to kyanite and andalusite at Fishtail Lake, Ontario,
1448 Canada. Mineralogical Magazine, 37, 446-471.
1449 Landis, C.A. (1971) Graphitization of dispersed carbonaceous material in metamorphic rocks.
1450 Contributions to Mineralogy and Petrology, 30, 34–45.
1451 Larsen, E.S., and Foshag, W.F. (1921) Merwinite, a new cacium magnesium ortosilicate from
1452 Crestmore, Califormia. American Mineralogist, 6, 143-148.
1453 Leach, D.L., Sangster, D.F., Kelley, K.D., Large, R.R., Garven, G., Allen, C.R., Gutzmer, J., and
1454 Walters, S. (2005) Sediment-hosted lead-zinc deposits: A global perspective. Economic
1455 Geology, 100th Anniversary Volume, 561-607.
1456 Leech, M., and Ernst, G. (1998) Graphite pseudomorphs after diamond? A carbon isotope and
1457 spectroscopic study of graphite cuboids from the Maksyutov Complex, south Ural
1458 Mountains, Russia. Geochimica et Cosmochimica Acta, 62, 2143-2154.
1459 Léger, A., and Ferry, J.M. (1993) Fluid infiltrationand regional metamorphism of the Waits River
1460 Formation, north-east Vermont, USA. Journal of Metamorphic Geology, 11, 3-29.
1461 Lipp, A.G., Shorttle, O., Sperling, E.A., Brocks, J.J., Cole, D.B., Crockford, P.W., Mouro, L.D.,
1462 Dewing, K., Dornbos, S.Q., Emmings, J.F., Farrell, U.C., Jarrett, A., Johnson, B.W., Kabanov, P.,
1463 Keller, C.B., Kunzmann, M., Miller, A.J., Mills, N.T., O'Connell, B., Peters, S.E., Planavsky, N.J.,

Ritzer, S.R., Schoepfer, S.D., Wilby, P.R., and Yang, J. (2021) The composition and weathering of the continents over geologic time. Geochemical Perspectives Letters, 21–26.

Litasov, K.D., Kagi, H., and Bekker, T.B. (2019) Enigmatic super-reduced phases in corundum from natural rocks: Possible contamination from artificial abrasive materials or metallurgical slags. Lithos, 340-341, 181-190.

Luth, R.W. (2003) Mantle volatiles -- distribution and consequences. In: R.W. Carlson [Ed.], The Mantle and Core, Elsevier-Pergamon, pp. 319-361.

Magnus, P.D. (2012) Scientific Enquiry and Natural Kinds: From Mallards to Planets. Palgrave MacMillan.

Manning, C.E., and Frezzotti, M.L. (2020) Subduction-zone fluids. Elements, 16, 395-400.

Marincea, S., and Dumitras, D.-G. (2019) Contrasting types of boron-bearing deposits in magnesian skarns from Romania. Ore Geology Reviews, 112, 102952 (20 p.).

Mills, S.J., Hatert, F., Nickel, E.H., and Ferrais, G. (2009) The standardization of mineral group hierarchies: Application to recent nomenclature proposals. European Journal of Mineralogy, 21, 1073-1080.

Miyashiro, A. (1961) Evolution of metamorphic belts. Journal of Petrology, 2, 277-311.

Moore, A.C. (1973) Carbonatite and kimberlites in Australia: a review of the evidence. Mineral Science and Engineering, 5, 81-91.

Moores, E.M. (2002) Pre–1 Ga (pre-Rodinian) ophiolites: their tectonic and environmental implications. GSA Bulletin, 114, 80–95.

Morrison, S.M., and Hazen, R.M. (2020) An evolutionary system of mineralogy, part II: interstellar and solar nebula primary condensation mineralogy (> 4.565 Ga). American Mineralogist, 195, 1508-1535.

Morrison, S.M., and Hazen, R.M. (2021) An evolutionary system of mineralogy, part IV: Planetesimal differentiation and impact mineralization (4.566 to 4.560 Ga). American Mineralogist, 106, 730-761.

Morrison, S.M., Liu, C., Eleish, A., Prabhu, A., Li, C., Ralph, J., Downs, R.T., Golden, J.J., Fox, P., Hummer, D.R., Meyer, M.B., and Hazen, R.M. (2017) Network analysis of mineralogical systems. American Mineralogist, 102, 1588-1596.

Morrison, S.M., Hazen, R.M., and Prabhu, A (2023) An evolutionary system of mineralogy, part VI: Earth's earliest Hadean crust (> 4370 Ma). American Mineralogist, 107, in press.

Murdoch, J. (1951) Perovskite. American Mineralogist, 36, 573-580.

Myer, G.H. (1966) New data on zoisite and epidote. American Journal of Science, 264, 364-385.

Nakajima, Y., Uchida, E., Imai, H., and Ohno, H. (1992) Brucite-bearing white rock and the genetically related basalt dyke in the Nabeyama carbonate formation of the Kuzuu district, Tochigi Prefecture, Japan. [In Japanese]. Japanese Journal of Mineralogy and Petrology, 87, 445-459.

Newman, M.E.J. (2010) Networks: An Introduction. Oxford University Press.

Nutman, A.P., and Friend, C.R.L. (2007) Comment on "A vestige of Earth's oldest ophiolite". Science, 318, 746.

Ohnmacht, W. (1974) Petrogenesis of carbonate-orthopyroxenites (sagvandites) and related rocks from Troms, northern Norway. Journal of Petrology, 15, 303-324.

O'Reilly, S.Y., and Griffin, W.L. (2012) Mantle metasomatism. In: D.E. Harlov and H. Austrheim, Eds., Metasomatism and the Chemical Transformation of Rock, pp. 471-533. Springer.

Palin, R.M., and White, R.W. (2016) Emergence of blueschists on Earth linked to secular changes in oceanic crust composition. Nature Geoscience, 9, 60–64.

Passchier, C.W., and Trouw, R.A.J. (2005) Microtectonics, Second Edition. Springer.

Pattison, D.R.M. (2001) Instability of Al2SiO5 "triple point" assemblages in muscovite+biotite+quartz-bearing metapelites, with implications. American Mineralogist, 86, 1414-1422).

Pearson, D.G., Davies, G.R., and Nixon, P.H. (1989) Graphitized diamonds from a peridotite massif in Morocco and implications for anomalous diamond occurrences. Nature, 338, 60–62.

Penniston-Dorland, S.C., and Ferry, J.M. (2006) Development of spatial variations in reaction progress during regional metamorphism of micaceous carbonate rocks, northern New England. American Journal of Science, 306, 475-524.

Peters, S.E., and Husson, J.M. (2017) Sediment cycling on continental and oceanic crust. Geology, 45, 323–326.

Peters, S.E., Husson, J.M., and Czaplewski, J. (2018) Macrostrat: A platform for geological data integration and deep-time Earth crust research. Geochemisty Geophysics Geosystems, 19, 1393–1409.

Peters, T.A., Koestler, R.J., Peters, J.J., and Grube, C.H. (1983) Minerals of the Buckwheat dolomite, Franklin, New Jersey. Mineralogical Record, 14, 183-194.

Philpotts, A.R., and Ague, J.J. (2009) Principles of Igneous and Metamorphic Petrology. Second Edition. Cambridge University Press.

Pinger, A.W. (1950) Geology of the Franklin--Sterling area, Sussex county, New Jersey. International Geological Congress, 18, Part VII, 77--87.

Pinsent, R.H., and Hirst, D.M. (1977) The metamorphism of the Blue River ultramafic body, Cassiar, British Columbia, Canada. Journal of Petrology, 18, 567-594.

Post, J.E. (1999) Manganese oxide minerals: Crystal structures and economic and environmental significance. Proceedings of the National Academy of Sciences USA, 96, 3447-3454.

Raith, M. (1976) The Al-Fe(III) epidote miscibility gap in metamorphic profile through the Penninic series of the Tauren Window, Austria. Contributions to Mineralogy and Petrology, 57, 99-117.

Rakovan, J., and Waychunas, G. (1996) Luminescence in minerals. Mineralogical Record, 27, 7-19.

Ramberg, H. (1952) The Origin of Metamorphic and Metasomatic Rocks. University of Chicago Press.

Read, H.H. (1923) Geology of the country around Banff, Huntly, and Turiff. Memoirs of the Geological Survey of Great Britain, H. M. Stationery Office.

Reverdatto, V.V. (1970) Pyrometamorphism of limestone and the temperature opf basaltic magmas. Lithos, 3, 135-143.

Reverdatto, V.V., and Sóbolev, V.S. (1973) The Facies of Contact Metamorphism. Translated by D.A. Brown. Australian National University.

1549 Ross, J.V., Bustin, R.M., and Rouzaud, J.N. (1991) Graphitization of high rank coals the role of
1550 shear stain: experimental considerations. Organic Geochemistry, 17, 585–596.
1551 Roy, S. (1965) Compararive study of the metamorphosed manganese protores of the world—
1552 the problem of the nomenclature of the gondites and kodurites. Economic Geology, 60,
1553 1238-1260.
1554 Schertl, H.-P., Schreyer, W., and Chopin, C. (1991) The pyrope-coesite rocks and their country
1555 rocks at Parigi, Dora Maira Massif, Western Alps: detailed petrography, mineral chemistry
1556 and P-T path. Contributions to Mineralogy and Petrology, 108, 1-21.
1557 Schertl, H.-P., Mills, S.J., and Maresch, W.V. (2018) A Compendium of IMA-Approved Mineral
1558 Nomenclature. International Mineralogical Association.
1559 Schreyer, W. (1977) Whiteschists: their composition and pressure-temperature regime based
1560 on experimental, field, and petrographic evidence. Tectonophysics, 43, 127-144.
1561 Schreyer, W., Ohnmacht, W., and Mannchen, J. (1972) Carbonate-orthopyroxenites
1562 (sagvandites) from Troms, northern Norway. Lithos, 5, 345-364.
1563 Shedlock, R.J., and Essene, E.J. (1979) Mineralogy and petrology of a tactite near Helena,
1564 Montana. Journal of Petrology, 20, 71-97.
1565 Shimazaki, H. (1977) Grossular-spessartine-almandine garnets from some Japanese scheelite
1566 skarns. The Canadian Mineralogist, 15, 74-80.
1567 Shirey, S.B., Cartigny, P., Frost, D.J., Keshav, S., Nestola, F., Nimis, P., Pearson, D.G., Sobolev,
1568 N.V., and Walter, M.J. (2013) Diamonds and the geology of Mantle carbon. Reviews in
1569 Mineralogy and Geochemistry, 75, 355-421.

1570 Simmons, E.C., Lindsley, D.H., and Papike, J.J. (1974) Phase relations and crystallization
1571 sequence in a contact-metamorphosed rock from the Gunflint Iron Formation, Minnesota.
1572 Journal of Petrology, 15, 539-565.
1573 Smith, D.G.W. (1969) A reinvestigation of the pseudobrookite from Havredal (Bamble), Norway.
1574 Norsk Geologisk Tidsskrift, 49, 285-288.
1575 Spear, F.S. (1982) Phase equilibria of amphibolites from the Post Pond Volcanics, Mt Cube
1576 Quadrangle, Vermont. Jornal of Petrology, 23, 383-426.
1577 Spooner, E.T.C., and Fyfe, W.S. (1973) Sub-sea-floor metamorphism, heat and mass transfer.
1578 Contributions to Mineralogy and Petrology, 42, 287-304.
1579 Springer, R.K. (1974) Contact metamorphosed ultramafic rock in the Western Sierra Nevada
1580 foothills, California. Journal of Pterology, 15, 160-195.
1581 Spry, P.G., Plimer, I.R., and Teale, G.S. (2008) Did the giant Broken Hill (Australia) Zn-Pb-Ag
1582 deposit melt? Ore Geology Reviews, 34, 223-241.
1583 Stachel, T., Aulbach, S., and Harris, J.W. (2022) Mineral inclusions in lithospheric diamonds.
1584 Reviews in Mineralogy and Geochemistry, 88, 307-392.
1585 Stern, R.J. (2018) The evolution of plate tectonics. Philosophical Transactions of the Royal
1586 Society, 376A. https://doi.org/10.1098/rsta.2017.0406.
1587 Stewart, F.H. (1942) Chemical data on a silica-poor argillaceous hornfels and its constituent
1588 minerals. Mineralogical Magazine, 26, 260-266.
1589 Suzuki, K. (1977) Local equilibrium during the contact metamorphism of siliceous dolomites in
1590 Kasuga-Mura, Gifu-ken, Japan. Contributions to Mineralogy and Petrology, 61, 79-89.

1591 Sylvester, G.C., and Anderson, G.M. (1976) The Davis nepheline pegmatite and associated
1592 nepheline gneisses near Bancroft, Ontario. Canadian Journal of Earth Science, 13, 249-265.
1593 Thompson, J.B. Jr., and Thompson, A.B. (1976) A model system for mineral facies in pelitic
1594 schists. Contributions to Mineralogy and Petrology, 58, 243-277.
1595 Tilley, C.E. (1926) On garnet in pelitic contact zones. Mineralogicalmagazine, 21, 47-50.
1596 Tilley, C.E. (1927) Vesuvianite and grossular as products of regional metamorphism. Geological
1597 Magazine, 64, 372-376.
1598 Tilley, C.E. (1948) Earlier stages in the metamorphism of siliceous dolomites. Mineralogical
1599 Magazine, 28, 272-276.
1600 Tilley, C.E. (1951) The zoned contact skarns of the Broadford area, Skye: a study of boron-
1601 fluorine metasomatism in dolomites. Mineralogical Magazine, 29, 621-666.
1602 Tilley, C.E., and Vincent, H.C.G. (1948) The occurrence of an orthorhombic high-temperature
1603 form of Ca_2SiO_4 (bredigite) in the Scawt Hill contact-zone and as a constituent of slags.
1604 Mineralogical Magazine, 28, 255-271.
1605 Tilley, C.E., Nockolds, S.R., and Black, M. (1964) Harker's Petrology for Students, Eighth Edition.
1606 Cambridge University Press.
1607 Trouw, R.A.J., Passchier, C.W., and Wiersma, D.J. (2009) Atlas of Mylonites and Related
1608 Microstructures. Springer.
1609 Tulloch, A.J. (1979) Secondary Ca-Al silicates as low-grade alteration products of granitoid
1610 biotite. Contributions to Mineralogy and Petrology, 69, 105-117.
1611 Turner, F.J. (1967) Thermodynamic appraisal of of steps in progressive metamorphism of
1612 siliceous dolomitic limestones. Neues Jahrbuch fur Mineralogie,1967, 1-22.

Tuttle, O.F., and Harker, R.I. (1957) Synthesis of spurrite and the reaction wollastonite + calcite → spurrite + carbon dioxide. American Journal of Science, 255, 226-234.

Valkenburg, A.V. (1961) Synthesis of the humites $nMg_2SiO_4 \cdot Mg(F, OH)_2$. Journal of Research of the National Bureau of Standards - A. Physics and Chemistry, 65A, 415-428.

Vernon, R.H. (2008) Principles of Metamorphic Petrology. Cambridge University Press.

Warner, R.D., and Luth, W.C. (1973) Two-phase data for the join monticellite ($CaMgSiO_4$) - forsterite (Mg_2SiO_4): experimental results and numerical analysis. American Mineralogist, 58, 998-1008

Watters, W.A. (1958) Some zoned skarns from granite-marble contacts near Puyvalador, in the Querigut area, eastern Pyrenees, and their petrogenesis. Mineralogical Magazine, 31, 703-735.

Weeks, W.F. (1956) A thermochemical study of equilibrium relations during metamorphism of siliceous carbonate rocks. Journal of Geology, 64, 245-270.

White, A.J.R. (1959) Scapolite-bearing marbles and calc-silicate rocks from Tungkillo and Milendelia, South Australia. Geological Magazine, 96, 285-306.

Whitney, D.L. (2002) Coexisting andalusite, kyanite, and sillimanite: Sequential formation of three Al_2SiO_5 polymorphs during progressive metamorphism near the triple point, Sivrihisar, Turkey. American Mineralogist, 87, 405–416.

Wilson, M.J. (2013) Rock-Forming Minerals. Volume 3C, Second Edition. Sheet Silicates: Clay Minerals. The Geological Society of London.

1633 Wing, B.A., Ferry, J.M., and Harrison, T.M. (2003) Prograde destruction and formation of
1634 monazite and allanite during contact and regional metamorphism of pelites: petrology and
1635 geochronology. Contributions to Mineralogy and Petrology, 145, 228-250.
1636 Woodland, A.W. (1939) The petrography and petrology of the Lower Cambrian manganese ore
1637 of west Merionethshire. Quarterly Journal of the Geological Society, 95, 1-35.
1638 Zedgenizov, D.A., Shatskiy, A., Ragozin, A.L., Kagi, H., and Shatsky, V.S. (2014) Merwinite in
1639 diamond from São Luiz, Brazil: A new mineral of the Ca-rich mantle environment. American
1640 Mineralogist, 99, 547-550.
1641 Zen, E-an (1969) The stability relations of the polymorphs of aluminum silicate: A survey and
1642 some comments. American Journal of Science, 267, 297-309.
1643 Zhai, M., Zhao, G., and Zhang, Q. (2002) Is the Dongwanzi Complex an Archean ophiolite?
1644 Science, 295, 923.
1645 Zharikov, V.A., and Shmulovich, K.L. (1969) High temperature mineral equilibria in the system
1646 CaO-SiO_2-CO_2. Geochemistry International, 6, 853-869.
1647 Zheng, Y.-F., and Chen, R.-X. (2017) Regional metamorphism at extreme conditions:
1648 Implications for orogeny at convergent plate margins. Journal of Asian Earth Sciences, 145,
1649 46–73.

Table 3. Summary of 94 frequently occurring metamorphic minerals, with their compositions, abundances, and numbers of IMA species included in each mineral kind (see Supplementary Table 3).

Mineral Kind	Chemical Formula	Abundance[1]	Community[2]	#IMA[3]
Native Elements				
Diamond	C	10	6	1
Graphite	C	105	5	1
Sulfides				
Chalcopyrite	$CuFeS_2$	99	2	1
Pyrite	FeS_2	120	--	1
Pyrrhotite	Fe_7S_8	192	--	1
Pentlandite	$(Ni,Fe)_9S_8$	21	5	1
Oxides				
Rutile	TiO_2	297	--	1
Hematite	Fe_2O_3	24	--	1
Corundum	Al_2O_3	85	1	1
Periclase	MgO	34	4	1
Baddeleyite	ZrO_2	18	4	1
Magnetite	$Fe^{2+}Fe^{3+}{}_2O_4$	429	--	1
Hercynite	$Fe^{2+}Al_2O_4$	34	1	1
Spinel	$(Mg,Fe^{2+})(Al,Fe^{3+},Cr^{3+})_2O_4$	263	4	1
Chromite	$Fe^{2+}Cr^{3+}{}_2O_4$	12	5	3
Ilmenite	$Fe^{2+}Ti^{4+}O_3$	181	--	1

This is the peer-reviewed, final accepted version for American Mineralogist, published by the Mineralogical Society of America.
The published version is subject to change. Cite as Authors (Year) Title. American Mineralogist, in press.
DOI: https://doi.org/10.2138/am-2023-9004. http://www.minsocam.org/

Perovskite	$CaTi^{4+}O_3$	12	3	1
Geikielite	$MgTiO_3$	17	4	1
Pseudobrookite	$Fe^{3+}_2TiO_5$	15	1	1
Hydroxide				
Brucite	$Mg(OH)_2$	31	4	1
Carbonates				
Calcite	$CaCO_3$	645	4	1
Magnesite	$MgCO_3$	16	5	1
Dolomite	$CaMg(CO_3)_2$	152	4	2
Fe-Dolomite	$Ca(Mg,Fe)(CO_3)_2$ [0.15 < Fe/(Mg + Fe) < 0.50]	116	5	0
Aragonite	$CaCO_3$	15	2	1
Spurrite	$Ca_5(SiO_4)_2(CO_3)$	51	3	1
Tilleyite	$Ca_5Si_2O_7(CO_3)_2$	16	3	1
Phosphates				
Apatite	$Ca_5(PO_4)_3(F,OH,Cl)$	155	--	2
Nesosilicates or Orthosilicates				
Olivine Group				
Forsterite	Mg_2SiO_4	173	4	1
Fayalite	$Fe^{2+}_2SIO_4$	10	2	1
Olivine	$(Mg,Fe)_2SiO_4$ (0.3 < Fe/(Fe + Mg) < 0.7)	53	6	0
Monticellite	$CaMgSiO_4$	77	3	1
Garnet Group				
Almandine	$Fe^{2+}_3Al_2Si_3O_{12}$	367	--	1

Andradite	$Ca_3Fe^{3+}_2Si_3O_{12}$	28	2	3
Grossular	$Ca_3Al_2Si_3O_{12}$	162	2	1
Pyrope	$Mg_3Al_2Si_3O_{12}$	192	6	2
Aluminosilicate Group				
Andalusite	Al_2SiO_5	146	1	1
Kyanite	Al_2SiO_5	102	6	1
Sillimanite	Al_2SiO_5	235	1	1
Mullite	$Al_{4+2x}Si_{2-2x}O_{10-x}$ ($x \approx 0.4$)	62	1	1
Other Nesosilicates				
Larnite	Ca_2SiO_4	24	3	1
Merwinite	$Ca_3Mg(SiO_4)_2$	38	3	1
Humite	$Mg_9(SiO_4)_4(F,OH)_2$	21	4	2
Chloritoid	$Fe^{2+}Al_2O(SiO_4)(OH)_2$	46	6	3
Staurolite	$Fe^{2+}_2Al_9Si_4O_{23}(OH)$	52	1	1
Zircon	$ZrSiO_4$	66	--	1
Titanite	$CaTi^{4+}SiO_5$	186	--	1
Sorosilicates or Disilicates				
Allanite	$(CaCe)(AlAlFe^{2+})O[Si_2O_7][SiO_4](OH)$	16	5	5
Epidote	$Ca_2(Al_2Fe^{3+})[Si_2O_7][SiO_4]O(OH)$	157	--	4
Zoisite	$Ca_2Al_3[Si_2O_7][SiO_4]O(OH)$	156	6	1
Melilite	$(Ca,Na)_2(Mg,Fe^{2+},Al,Si)_3O_7$	108	3	3
Lawsonite	$(Ca,Sr)Al_2(Si_2O_7)(OH)_2 \cdot H_2O$	11	6	2
Pumpellyite	$Ca_2Al_3(Si_2O_7)(SiO_4)(OH,O)_2 \cdot H_2O$	10	5	9

Rankinite	$Ca_3Si_2O_7$	20	3	1
Vesuvianite	$(Ca,Na)_{19}(Al,Mg,Fe)_{13}(SiO_4)_{10}(Si_2O_7)_4(OH,F,O)_{10}$	15	2	10
Cyclosilicates				
Tourmaline	$(\square,Na,Ca)(Mg,Fe,Al)_3(Mg,Al)_6(Si_6O_{18})(BO_3)_3(OH,F)_3(OH,O)$	47	5	18
Cordierite	$(Mg,Fe^{2+})_2Al_4Si_5O_{18}$	395	1	2
Osumilite	$(K,Na)(Fe^{2+},Mg)_2(Al,Fe^{3+})_3(Si,Al)_{12}O_{30}$	13	1	4
Inosilicates				
Pyroxene Group				
Aegirine	$(Ca,Na)(Fe^{3+},Mg,Fe^{2+})Si_2O_6$	16	6	2
Augite	$(Ca,Mg,Fe^{2+},Fe^{3+})_2(Si,Al)_2O_6$ [0.15 < $CaSiO_3$ < 0.45]	150	--	1
Diopside	$CaMgSi_2O_6$	409	2	1
Hedenbergite	$CaFe^{2+}Si_2O_6$	16	2	1
Jadeite	$NaAlSi_2O_6$	34	6	1
Omphacite	$(Ca,Na)(Mg,Fe,Al)Si_2O_6$	151	6	1
Orthopyroxene	$(Mg,Fe^{2+})SiO_3$	281	--	2
Amphibole Group				
Actinolite	$\square Ca_2(Mg,Fe^{2+})_5Si_8O_{22}(OH,F)_2$	74	--	2
Anthophyllite	$\square Mg_2Mg_5Si_8O_{22}(OH)_2$	52	1	6
Cummingtonite	$\square Mg_2Mg_5Si_8O_{22}(OH)_2$	12	4	1
Glaucophane	$\square Na_2(Mg_3Al_2)Si_8O_{22}(OH)_2$	79	6	2
Hornblende	$(Na,K)Ca_2(Mg,Fe^{2+},Al,Fe^{3+})_5(Si,Al)_8O_{22}(OH,F,Cl)_2$	387	--	26
Richterite	$Na(CaNa)(Mg,Fe^{2+})_5(Si,Al,Fe^{3+})_8O_{22}(OH)_2$	12	6	16
Tremolite	$\square Ca_2(Mg_{5.0\text{-}4.5}Fe^{2+}{}_{0.0\text{-}0.5})Si_8O_{22}(OH)_2$	122	4	2

Other Chain Silicates					
	Wollastonite	$CaSiO_3$	158	2	1
	Sapphirine	$Mg_4(Mg_3Al_9)O_4(Si_3Al_9O_{36})$	28	1	2
Phyllosilicates					
Mica Group					
	Biotite	$KFe^{2+}_2(Fe^{2+},Mg,Mn^{2+})(Si,Al,Fe^{3+})_2Si_2O_{10}(OH,F,Cl)_2$	822	--	6
	Phlogopite	$[[KMg_2(Mg,Fe^{2+},Mn^{2+},Fe^{3+},Ti^{4+})(Si,Al,Fe^{3+})_2Si_2O_{10}(OH,F)_2]]$	78	4	6
	Muscovite	$K(Al,V,Fe^{3+},Cr)_2(Si_3Al)O_{10}(OH)_2$	515	--	3
	Phengite	$K(Al,Mg,Fe)_{2\text{-}3}(Si_3Al)O_{10}(OH)_2$	110	6	1
	Paragonite	$NaAl_2(Si_3Al)O_{10}(OH)_2$	67	6	1
Other Layer Silicates					
	Chlorite	$(Mg,Fe^{2+})_5(Al,Fe^{3+})(Si_3AlO_{10})(OH)_8$	339	5	3
	Serpentine	$(Mg,Fe)_2Al(AlSiO_5)(OH)_4$	68	4	5
	Talc	$Mg_3Si_4O_{10}(OH)_2$	73	5	1
	Prehnite	$Ca_2Al(Si_3Al)O_{10}(OH)_2$	16	5	1
Tectosilicate					
Silica Group					
	Quartz	SiO_2	1353	--	1
	Tridymite	SiO_2	44	1	1
	Coesite	SiO_2	23	6	1
	Cristobalite	SiO_2	10	1	1
Feldspar Group					
	Albite	$NaAlSi_3O_8$	177	--	1

This is the peer-reviewed, final accepted version for American Mineralogist, published by the Mineralogical Society of America.
The published version is subject to change. Cite as Authors (Year) Title. American Mineralogist, in press.
DOI: https://doi.org/10.2138/am-2023-9004. http://www.minsocam.org/

Anorthite	$CaAl_2Si_2O_8$	78	2	1
Plagioclase	$(Na,Ca)Al(Al,Si)_3O_8$	809	--	0
Kspar	$KAlSi_3O_8$	411	--	1
Sanidine	$KAlSi_3O_8$	102	1	1
Other Framework Silicates				
Scapolite	$(Na,Ca)_4(Al,Si)_{12}O_{24}(CO_3,SO_4,Cl)$	33	2	3
Silicate Glass	(Si,Al,Ca,Mg,Fe,O; SiO_2 < 70 wt %)	68	1	0

[1] Number of occurrences in a survey of the modes of 2785 metamorphic rocks; see Supplementary Table 3.

[2] The Community Number refers to the 6 communities illustrated in Figure 1A, based on a survey of 73 minerals.

[3] The number of IMA-approved mineral species lumped into this mineral kind (see Supplementary Table 2). For example, *tourmaline* (which is not an IMA-approved mineral name) includes 18 IMA species. Note that *biotite, chlorite, Fe-dolomite, kspar, melilite, olivine, phengite, plagioclase, scapolite, serpentine*, and *silicate glass* are not IMA-approved names and do not correspond to any single IMA species.

This is the peer-reviewed, final accepted version for American Mineralogist, published by the Mineralogical Society of America.
The published version is subject to change. Cite as Authors (Year) Title. American Mineralogist, in press.
DOI: https://doi.org/10.2138/am-2023-9004. http://www.minsocam.org/

APPENDIX I. SYSTEMATIC MINERALOGY OF METAMORPHIC MINERALS

Appendix I presents a systematic mineralogy of the 94 most frequently encountered metamorphic minerals. Supplementary Table 1 provides a list of 1220 metamorphic mineral species, the corresponding 755 metamorphic mineral kinds, and the distribution of these phases among 8 major groups of metamorphic rocks. This conversion of 1220 metamorphic minerals into 755 natural kinds requires several modifications to the IMA list, as detailed in Hazen et al (2022). In 568 instances, the IMA species name (e.g., augite) is identical to the natural kind name (*augite*). Note that in this contribution we *italicize* the names of mineral natural kinds to distinguish them from IMA-CNMNC-approved mineral species. In the case of 652 IMA-approved species, we lump groups of two or more IMA species into single natural kinds. These numerous examples, resulting in a reduction from 652 species to 187 root natural kinds, are detailed in Supplementary Table 2 (see also Supplementary Read-Me File 2). For example, *pumpellyite* combines 9 IMA-approved species of the pumpellyite group. In 18 instances, the name assigned to the natural kind is a group name that is not itself an approved IMA species name. Thus, *hornblende* lumps 26 IMA-approved species of calcic amphiboles, while *biotite* encompasses 6 species of Fe-bearing trioctahedral micas.

We include five phases that do not correspond to an IMA-CNMNC-approved species in Supplementary Table 1. In the instance of *plagioclase*, we recognize intermediate compositions of the albite ($NaAlSi_3O_8$)—anorthite ($CaAl_2Si_2O_8$) solid solution with $0.15 < Ca/(Ca + Na) < 0.85$ as a separate natural kind. Similarly, *olivine* refers to intermediate compositions of the forsterite (Mg_2SiO_4)—fayalite (Fe_2SiO_4) solid solution for which $0.3 < Fe/(Fe + Mg) < 0.7$. *Fe-Dolomite* refers to intermediate compositions of the dolomite-ankerite solid solution, where $0.15 <$

Fe/(Fe + Mg) < 0.50, many examples of which are incorrectly described as ankerite (Ferry et al. 2015). *Phengite* is a fine-grained variety of muscovite [$K(Al,Mg,Fe)_{2-3}(AlSi_3)O_{10}(OH)_2$], typically with excess Si, that is common in high-pressure metamorphic deposits. We also introduce *silicate glass*, an important amorphous phase in some pyrometamorphic lithologies, as a natural kind.

Of the 755 mineral kinds recorded in Supplementary Tables 1 and 2, 94 phases are relatively common based on their occurrence in at least 10 rocks in 2785 metamorphic rocks (Table 3; Supplementary Table 3). Supplementary Table 3 also records a literature reference for each rock mode, the rock's locality, and information on the type of metamorphism, the metamorphic facies, and its protolith. Here we present brief descriptions of these 94 mineral kinds, arranged according to the New Dana Classification (Gaines et al. 1997).

Native Elements

Two polymorphs of carbon (C), *graphite* and *diamond*, with 105 and 10 occurrences in Supplementary Table 3, respectively, are the only native element minerals that occur in any significant abundance in metamorphic rocks, though more than two dozen rare native elements and metal alloys are listed in Supplementary Table 1. *Graphite* most frequently occurs in carbon-rich metapelites (Landis 1971; Diessel et al. 1978; Buseck and Huang 1985). However, *graphite* is also reported to occur as a product of retrograde metamorphism of *diamond*, at times as euhedral pseudomorphs (Pearson et al. 1989; Ferry 1992; Davies et al. 1993; Leech and Ernst 1998). In addition, Ross et al. (1991) reported an occurrence of *graphite* formed by the shearing of coal—an example of Phanerozoic metamorphism of a biotic protolith.

Most *diamond* formation occurs in the mantle by precipitation from carbon-rich fluids (Jacob and Mikhail 2022; Kjarsgaard et al. 2022). However, in some instances, micrometer-scale *diamond* forms during subduction, ultra-deep metamorphism, and subsequent rebound of carbon-bearing crustal wedges (Dobrzhinetskya et al. 1995, 2022).

Sulfides

More than 50 sulfide and other chalcogenide minerals have been reported from metamorphic rocks (Supplementary Table 1). However, only four iron-bearing sulfides, *pyrite* (FeS_2), *pyrrhotite* (Fe_7S_8), *chalcopyrite* ($CuFeS_2$), and *pentlandite* [$(Ni,Fe)_9S_8$], are relatively common. *Pyrrhotite* is the most commonly observed sulfide in our survey, occurring in 192 metamorphic rocks. It frequently occurs with *graphite* in higher-grade regional metamorphic rocks (Hoscheck 1984; Ferry 1992), and it may form by solid-state transformation of *pyrite* coupled with sulfur loss (Bowles et al. 2011). It is also a common sulfide mineral associated with skarn deposits (Einaudi and Burt 1982).

Pyrite (FeS_2) is the next most frequently reported metamorphic sulfide, with 120 occurrences in Supplementary Table 3. *Pyrite* is found in all metamorphic grades, including high-pressure regimes, and may form through solid-state transformation of *pyrrhotite* (Hall et al. 1987). *Pyrite* also occurs via contact metamorphism associated with skarn formation (Einaudi et al. 1981), and in shear zones (e.g., Harker 1950).

Chalcopyrite, the only copper-bearing mineral among the most common metamorphic phases, is reported from 99 rocks in our survey. Most occurrences are as minor grains in regionally metamorphosed igneous and sedimentary lithologies (Ferry 1984, 1992, 1994; Ferry

et al. 2001). It is likely that chalcopyrite, as an opaque and often micrometer-scale phase, is underrepresented in our study.

The 21 occurences of *pentlandite*, the only common nickel-bearing metamorphic minerals, are recorded exclusively from ultramafic lithologies (Ferry 1995; Ferry et al. 2005).

In addition, it should be noted that *sphalerite* (ZnS) occurs in 9 of the rocks surveyed—a number that likely significantly underestimates the frequency of this opaque and typically minute zinc-bearing phase.

Oxides

Oxide minerals occur in the entire range of metamorphic rocks. More than 50 species, most of them relatively rare, have been reported (Supplementary Table 1). We list 13 mineral kinds among the most frequently encountered metamorphic minerals.

The simple oxide *rutile* (TiO_2) is reported in 297 of the metamorphic rocks from our study (Supplementary Table 3), most often in regional metamorphic rocks by transformation of prior Ti-bearing phases, including *titanite*, *ilmenite*, and titaniferous micas and *magnetite* (Bowles et al. 2011), but also in a range of pyrometamorphic (Grapes 2006), contact metamorphic (Reverdatto and Sóbolev 1973), and shear zone (Harker 1950) rocks.

Additionally, among the more common simple oxides is c*orundum* (Al_2O_3; 85 occurrences), observed most frequently in silica-poor lithologies subjected to high temperature, notably in contact metamorphic zones. Al-rich lithologies with prominent *corundum*, often in association with *spinel, mullite, cordierite*, and/or *sanidine*, are known as “emery.” *Corundum* also occurs in

pyrometamorphosed limestone xenoliths (Joplin 1968; Grapes 2006), as well as in high-grade regional metamorphic rocks (Harker 1950; Augustithus 1985).

Periclase (MgO) is a common mineral in *calcite/dolomite* marbles, often in association with *brucite* (Carpenter 1967; Bowles et al. 2011). As early as 1940, Bowen described *periclase* as part of an evolutionary thermal metamorphic sequence (Bowen 1940). We record 36 occurences of *periclase*, primarily in limestone xenoliths and contact metamorphic environments (Augustithus 1985; Grapes 2006; Ferry and Rumble 2007).

Hematite (Fe_2O_3), represented by 24 occurrences in our tabulation, forms from Fe-rich protoliths in oxidized environments. Contexts of metamorphic *hematite* include xenoliths, contact environments, iron formations, and regional metamorphism (Bowles et al. 2011).

We record 18 occurrences of the zirconium oxide baddeleyite (ZrO_2) in both contact and regional metamorphic contexts (Ferry and Rumble 2007). That number that may underrepresent the frequency of baddeleyite because of its typical low modal abundance and small grain size.

The most frequently encountered metamorphic oxides are members of the spinel group, which occur in 672 (24 %) of the 2785 metamorphic rocks we tabulated. With the general formula $[(Mg,Fe^{2+})(Al,Fe^{3+},Cr^{3+},Ti)_2O_4]$, the spinel group encompasses a complex range of solid solutions (Bowles et al. 2011), of which four end-members are among the most commonly reported metamorphic minerals: *magnetite* ($Fe^{2+}Fe^{3+}{}_2O_4$), *spinel* ($MgAl_2O_4$; although "spinel" may also refer to the mineral group rather than the species in some modes), *chromite* ($Fe^{2+}Cr^{3+}{}_2O_4$), and *hercynite* ($Fe^{2+}Al_2O_4$). In addition, several reports cite "pleonaste," which

refers to Fe^{2+}-bearing intermediate compositions of the spinel-hercynite solid solution—examples that we include with *spinel*.

Magnetite is by far the most frequently reported metamorphic oxide, occurring in 429 (15 %) of the 2785 metamorphic rocks we compiled, and in a wide range of metamorphic contexts (Joplin 1968; Reverdatto and Sóbolev 1973; Grapes 2006). *Magnetite* often forms by thermal alteration of ferric iron oxide/hydroxides, as well as through the introduction of Fe-rich fluids—a situation in which the distinction between metamorphism and metasomatism may be blurred.

The Mg-Al oxide *spinel*, with 263 occurrences in our list, is found in numerous contact and regional metamorphic contexts, principally as a high-temperature mineral in metacarbonates and Al-rich protoliths (Harker 1950; Botha 1983; Carswell 1990; Grapes 2006).

Hercynite, which forms in high-grade metamorphic environments, often in association with *corundum*, *mullite*, and/or *sillimanite*, is represented by 34 examples in Supplementary Table 3. Metamorphic contexts include xenolith, contact, and regional environments (Harker 1950; Grapes 2006; Bowles et al. 2011).

We list 12 occurrences of metamorphic *chromite*—a number that likely underestimates this most common chromium mineral because it is opaque and easily mistaken for other Fe-bearing oxides. *Chromite* is most often associated with ultramafic lithologies, particularly ophiolites.

Four titanium-bearing double oxides are listed among the 94 most common metamorphic phases. We record *Ilmenite* ($FeTiO_3$) from 181 xenoliths, contact metamorphic rocks, or regional metamorphic formations, notably forming via alteration of mafic and Fe-bearing lithologies (Reverdatto and Sóbolev 1973; Carswell 1990; Grapes 2006). *Geikielite* ($MgTiO_3$), the

magnesium analog of ilmenite, occurs in 17 contact and regional metasedimentary rocks in Supplementary Table 3. Geikeilite protoliths include carbonates, calc silicates, pelites, and sandstones. *Perovskite* ($CaTiO_3$) is reported from 12 rocks, primarily in xenoliths and contact metamorphic environments with impure limestone (Murdoch 1951; Fulignati et al. 2000; Grapes 2006). *Pseudobrookite* ($Fe^{3+}_2TiO_5$), which we record in 15 primarily xenolith and contact metamorphic rocks, forms most often by the high-temperature oxidation of *ilmenite* (Agrell and Langley 1958; Smith 1969; Basta and Shaalan 1974).

Brucite [$Mg(OH)_2$], the only relatively common hydroxide mineral in metamorphic rocks, occurred in 31 rocks of our survey. It is typically the consequence of hydration of *periclase* in altered Ca-Mg carbonates (Nakajima et al. 1992; Ferry et al. 2002; Ferry and Rumble 2007; Bowles et al. 2011).

Carbonates

At least 70 carbonate minerals have been reported from metamorphic rocks (Supplementary Table 1), though only seven species occur with any significant frequency. By far the most abundant carbonates are *calcite* ($CaCO_3$), *dolomite* [$CaMg(CO_3)_2$], and the intermediate composition *Fe-dolomite* [*dolomite* with a significant *ankerite* $CaFe(CO_3)_2$ component], with 645, 152, and 116 occurrences in our compilation, respectively. *Calcite* and *dolomite* most often occur in metamorphosed limestones and other carbonate-bearing protoliths (Harker 1950; Reverdatto and Sóbolev 1973; Chang et al. 1996; Grapes 2006). In many instances, these phases form through recrystallization of prior carbonates to form a marble (Chang et al. 1996; Philpotts and Ague 2009). *Fe-dolomite* (often reported as “ankerite” in the petrologic literature) is found

primarily in regionally metamorphosed sediments (Ferry 1992, 1994, 2007; Ferry et al. 2015) where it formed through carbonation reactions during metamorphism/metasomatism (Spooner and Fyfe 1973).

Metamorphic *magnesite* ($MgCO_3$) with 16 occurrences is characteristic of altered ophiolites, where it occurs in association with talc and serpentine. It typically forms via the carbonation of Mg-bearing oxides and silicates (Chang et al. 1996).

Aragonite, a high-pressure form of $CaCO_3$, was recorded in 15 rocks of eclogite, blueschist, and ultrahigh-pressure facies carbonate rocks (Carswell 1990; Carswell and Compagnoni 2003; Philpotts and Ague 2009).

Two silicate carbonates, s*purrite* [$Ca_5(SiO_4)_2(CO_3)$] with 51 examples and *tilleyite* [$Ca_5Si_2O_7(CO_3)_2$] with 16 examples, arise when *calcite* and *wollastonite* react at high temperature (Tuttle and Harker 1957; Zharikov and Shmulovich 1969).

Phosphates

Of the more than 50 metamorphic phosphates recorded in Supplementary Table 1, only the calcium phosphate *apatite* [$Ca_5(PO_4)_3(F,OH)$] is widely reported, with 155 occurrences in Supplementary Table 3. We lump two common species, fluorapatite and hydroxylapatite, which are rarely differentiated in reports of metamorphic mineral modes. The majority of these *apatite* occurrences are in high-grade metamorphosed mafic igneous rocks, including granulites and eclogites (Harker 1950; Joplin 1968; Carswell 1990). In addition, *apatite* has been reported from contact metamorphic and shear environments (Harker 1950; Joplin 1968).

This is the peer-reviewed, final accepted version for American Mineralogist, published by the Mineralogical Society of America.
The published version is subject to change. Cite as Authors (Year) Title. American Mineralogist, in press.
DOI: https://doi.org/10.2138/am-2023-9004. http://www.minsocam.org/

Silicates

Silicates constitute the majority of metamorphic minerals, both volumetrically and in terms of diversity. In Supplementary Tables 1 and 2 we record 746 silicate mineral species, corresponding to 418 root natural kinds, of which 66 are frequently encountered metamorphic phases. In the following sections we review these more common silicates.

Nesosilicates or Orthosilicates

Orthosilicates, with silicon exclusively in insular SiO_4^{4-} structural groups, are characteristic minerals in environments with relatively low Si, notably those associated with carbonate, calc-silicate, or aluminous protoliths (Deer et al. 1982). We detail 21 orthosilicates in addition to the orthosilicate-carbonate mineral *spurrite*, described above. Of these 22 phases, 16 contain essential Ca and/or Al.

Olivine Group: We recognize four members of the olivine group [$(Mg,Fe,Ca)_2SiO_4$] as important metamorphic minerals (Deer et al. 1982). The Mg olivine *forsterite* (ideally Mg_2SiO_4) is reported in 173 of the rocks we surveyed, notably via contact, regional, or high-pressure metamorphism of silica-poor ultramafic (Springer 1974; Pinsent and Hirst 1977) or carbonate-bearing (Weeks 1956; Schreyer et al. 1972; Suzuki 1977) protoliths. We also distinguish *olivine* as intermediate Mg-Fe compositions with $0.3 < Fe/(Fe + Mg) < 0.7$, which are common in metamorphosed mafic and ultramafic rocks (53 occurrences; Reverdatto and Sóbolev 1973; Ferry et al. 1987).

Fayalite (ideally Fe_2SiO_4) is much less common, occurring in 10 rocks with Fe-rich protoliths, including mafic rocks and iron formations (Joplin 1968; Simmons et al. 1974; Floran and Papike

1978; Carswell 1990). Note that metamorphic Fe-dominant olivines with intermediate compositions are less common than examples close to either end-member (Deer et al. 1982).

Monticellite ($CaMgSiO_4$), with 77 occurrences, is commonly found in contact metamorphic environments with siliceous carbonate lithologies, often forming with increasing temperature at the expense of *diopside*, *forsterite*, and/or *wollastonite* (Bowen 1940; Turner 1967; Deer et al. 1982). *Monticellite* frequently co-occurs with *forsterite*, as the solid solution between these two olivine group minerals is limited (Warner and Luth 1973).

Garnet Group: The garnet group is represented by four relatively common metamorphic phases, occurring in 745 (27 %) of 2785 rocks in our survey. Garnets collectively display a significant compositional range, typically with solid solutions among two or three end-members (Deer et al. 1982; Chiama et al. 2020, 2022). Ideal end-members of these minerals are *almandine* [$Fe^{2+}_3Al_2(SiO_4)_3$], *andradite* [$Ca_3Fe^{3+}_2(SiO_4)_3$], *grossular* [$Ca_3Al_2(SiO_4)_3$], and *pyrope* [$Mg_3Al_2(SiO_4)_3$], often with a significant *spessartine* [$Mn^{2+}_3Al_2(SiO_4)_3$] component, as well, though true Mn-dominant *spessartine* is recorded in only 9 occurrences in our compilation (Woodland 1938; Roy 1965; Jan and Symmes 1977).

In some instances, such as *pyrope-almandine-spessartine* ("pyralspite") from ecologites and other high-grade metamorphic rocks, *grossular-andradite* ("grandite") from the contact metamorphism of carbonate-bearing sediments, and contact metamorphic garnets in the *grossular-spessartine-almandine* field (Shimazaki 1977), the compositional ranges among end-members may be continuous, thus warranting lumping of species into a single metamorphic mineral kind. However, until cluster analysis (Gregory et al. 2019; Boujibar et al. 2021; Hystad et

al. 2021) can be performed on a wide range of garnet compositions from known paragenetic environments, we will treat these five types of metamorphic garnet separately.

Almandine, with 367 occurrences in Supplementary Table 3, is the commonest garnet in metamorphic rocks (Harker 1950; Joplin 1968; Reverdatto and Sóbolev 1973; Botha 1983; Augustithus 1985). Most *almandine* forms in a regional metamorphic context, derived from mafic or pelitic protoliths (Atherton 1964; Deer et al. 1982), including high-pressure examples from blueschist (Coleman and Lee 1963; Banno and Matsui 1965), eclogite (Coleman et al. 1965), and granulite (Buddington 1952; Eskola 1952) facies. In addition, *almandine* from contact metamorphism of pelites is not uncommon (Tilley 1926; Stewart 1942), while it also occurs in some metamorphosed iron formations (Klein 1966).

Pyrope's 192 entries are overwhelmingly from high-pressure metamorphic environments, in many instances from ecologite-grade rocks with mafic precursors, most commonly in association with *omphacite* (Carswell 1990). Metamorphic *pyrope* typically has a significant *almandine* component (Deer et al. 1982).

The great majority of 162 *grossular* occurrences in Supplementary Table 3 arise from contact metamorphism of calcareous rocks, often in association with *diopside* and/or *wollastonite* (Watters 1958; Reverdatto and Sóbolev 1973), or in regional metamorphic formations, also with carbonate-bearing protoliths (Tilley 1927; Sylvester and Anderson 1976). In addition, 28 occurrences of the Ca-Fe^{3+} garnet *andradite* arise predominantly from contact and regional metamorphism of calc-silicate rocks (Harker 1950; White 1959; Shedlock and Essene 1979). In several instances, contact metamorphic garnets have so-called "grandite" compositions intermediate between *grossular* and *andradite* (Coombs et al. 1977; Tulloch 1979).

This is the peer-reviewed, final accepted version for American Mineralogist, published by the Mineralogical Society of America.
The published version is subject to change. Cite as Authors (Year) Title. American Mineralogist, in press.
DOI: https://doi.org/10.2138/am-2023-9004. http://www.minsocam.org/

Three additional Ca-Mg orthosilicates, *bredigite* [$Ca_7Mg(SiO_4)_4$] with 6 occurrences (Tilley and Vincent 1948; Grapes 2006), *larnite* (Ca_2SiO_4) with 24 occurrences (Deer et al. 1986), and *merwinite* [$Ca_3Mg(SiO_4)_2$] with 38 occurrences (Larsen and Foshag 1921; Reverdatto and Sóbolev 1973), are frequently found in contact metamorphosed calc-silicate protoliths, often in association with the calc-silicates *melilite*, *rankinite*, and *spurrite* (Joplin 1968; Deer et al. 1986; Grapes 2006). *Merwinite* is also reported as an ultrahigh pressure mantle phase (Zedgenizov et al. 2014).

We lump three compositionally similar IMA species—humite, clinohumite, and hydroxylclinohumite—into *humite* [$Mg_{7-9}(SiO_4)_4(F,OH)_2$]. Members of the humite group differ in the ratios of two structural modules, one of forsterite composition [$Mg_2(SiO_4)$] and the other of brucite composition [$Mg(OH,F)_2$]. Reports of metamorphic mineral modes seldom distinguish between humite [$Mg_9(SiO_4)_4(OH,F)_2$] and clinohumite [$Mg_7(SiO_4)_4(OH,F)_2$], nor between the OH- and F-dominant species. We record 21 occurrences of *humite*, all of which are characteristic of the contact metamorphism of dolomite-bearing sediments (Tilley 1951; Joplin 1968; Deer et al. 1982). Note that two other members of the humite group (Van Valkenburg 1961), *norbergite* [$Mg_3(SiO_4)_4(OH,F)_2$] and *chondrodite* [$Mg_5(SiO_4)_4(OH,F)_2$], are also contact metamorphic minerals, but did not appear as common phases in our tabulations of metamorphic rock modes.

Three aluminosilicate (Al_2SiO_5) polymorphs, *andalusite*, *kyanite*, and *sillimanite*, are abundant constituents of many metapelites, with 146, 102, and 235 occurrences in Supplementary Table 3, respectively. These phases, which can coexist at their invariant triple point (approximately 500 °C and 0.4 GPa; Hodges and Spear 1982; Bohlen et al. 1991; Pattison 2001), have received special attention for their ability to document the pressure-temperature

regimes of their host rocks (Barrow 1893; Zen 1969; Deer et al. 1982; Whitney 2002; Philpotts and Ague 2009). *Sillimanite*, the high-temperature, low-pressure polymorph, is a common phase in a variety of metapelites subjected to hornblende hornfels, granulite, and pyrometamorphic (sanidinite) conditions (Reverdatto and Sóbolev 1973; Botha 1983; Grapes 2006). *Mullite* [$Al_{4+2x}Si_{2-2x}O_{10-x}$ ($x \approx 0.4$)] is also a high-temperature, low-pressure orthosilicate that we record from 62 pyrometamorphic rocks, often in association with *sillimanite* (Grapes 2006).

Andalusite forms in pelitic protoliths at low pressure and moderate temperature (< 770 °C), notably from albite-epidote hornfels and hornblende hornfels facies (Read 1923; Guitard 1965; Reverdatto and Sóbolev 1973). *Kyanite*, the highest-pressure crustal polymorph of Al_2SiO_5, is frequently encountered in regional and high-pressure metamorphic rocks with aluminous precursors (Carswell 1990; Carswell and Compagnoni 2003). The aluminosilicates may record either prograde or retrograde metamorphism. For example, Lal (1969) described *andalusite* and *kyanite* formed via retrograde metamorphism from cordierite-bearing rocks, and Gates and Speer (2022) record retrograde *kyanite* after *sillimanite* in metapelite shear zones.

Chloritoid [$(Fe^{2+},Mg,Mn^{2+})Al_2O(SiO_4)(OH)_2$], with 46 occurrences in our tabulation, is most commonly formed by regional or high-pressure metamorphism of pelitic rocks (Joplin 1968; Carswell 1990). We lump three IMA-CNMNC-approved species, chloritoid [$Fe^{2+}Al_2O(SiO_4)(OH)_2$], magnesiochloritoid [$MgAl_2O(SiO_4)(OH)_2$], and ottrelite [$Mn^{2+}Al_2O(SiO_4)(OH)_2$], because they form a continuous solid solution and they are rarely differentiated in reports of metamorphic rock modes. The broad pressure-temperature stability field of *chloritoid* leads to a wide range

of assemblages, from low-grade, clay-mineral- and *phengite*-bearing facies to high-grade rocks with *kyanite*, *pyrope-almandine*, and/or *staurolite* (Halferdahl 1961).

Staurolite [$(Fe^{2+},Mg)_2Al_9Si_4O_{23}(OH)$] is another common phase derived by regional or high-pressure metamorphism of pelitic sediments. Its 52 occurrences in Supplementary Table 3 reflect a range of *P-T* conditions of formation, from low-grade assemblages with *chloritoid* and *quartz*, medium-grade assemblages with *almandine* and *kyanite*, and high-grade assemblages with *sillimanite* and *plagioclase* (Deer et al. 1982; Augustithus 1985; Carswell 1990). *Staurolite* is also observed in the contact metamorphism of pelites (Reverdatto and Sóbolev 1973; Grapes 2006).

Titanite ($CaTiSiO_5$; commonly reported as "sphene") occurs as a minor phase in 186 metamorphic rocks in our survey in a variety of contexts (Harker 1950; Joplin 1968; Reverdatto and Sóbolev 1973; Carswell 1990). *Zircon* ($ZrSiO_4$), another volumetrically minor phase, is listed in 66 of 2785 rocks in our tabulation, including a wide range of contact and regional metamorphic lithologies (Joplin 1968; Carswell 1990; Grapes 2006). *Titanite* and *zircon* are particularly durable accessory minerals that are widespread in igneous and sedimentary formations; therefore, their occurence in metamorphic rocks sometimes derives from protolith minerals that have been little altered.

Though not among the more common metamorphic orthosilicates, *willemite* (Zn_2SiO_4) is an important mineral in some metamorphosed Pb-Zn deposits, such as the sillimanite-grade deposits at Franklin, New Jersey (Pinger 1950; Frondel 1990). In this case, which may be relevant to minerals in many metamorphic environments, *willemite* occurs both as a major phase in the ore and as a secondary phase in thin hydrothermal veins. These two generations of

This is the peer-reviewed, final accepted version for American Mineralogist, published by the Mineralogical Society of America.
The published version is subject to change. Cite as Authors (Year) Title. American Mineralogist, in press.
DOI: https://doi.org/10.2138/am-2023-9004. http://www.minsocam.org/

willemite, furthermore, have distinct properties: both forms are fluorescent, but only the secondary *willemite* has persistent luminescence as a consequence of its greater arsenic content (Rakovan and Waychunas 1996). With their distinct modes of formation and attributes, these coexisting forms of willemite represent two different mineral kinds in our evolutionary system.

Sorosilicates or Disilicates

Sorosilicates incorporate the double-tetrahedron pyrosilicate group ($Si_2O_7^{6-}$). We find eight sorosilicate root natural kinds, corresponding to at least 35 IMA-CNMNC-approved species, among the 94 most frequently encountered metamorphic mineral kinds. All of these phases, in addition to the disilicate-carbonate mineral *tilleyite* described earlier, are calcium-bearing minerals that occur most frequently in the contact metamorphic zones of limestone and dolomite.

The most common metamorphic sorosilicates are from the diverse epidote group (Deer et al. 1986; Armbruster et al. 2006). We lump 4 monoclinic species (including Fe^{3+}-bearing clinozoisite) into *epidote* [$Ca_2(Al_2Fe^{3+})[Si_2O_7][SiO_4]O(OH)$] with 149 occurrences; 5 rare-earth element-bearing epidote group minerals into *allanite* [$(CaCe)(AlAlFe^{2+})O[Si_2O_7][SiO_4](OH)$] with 16 occurrences (though certainly under-reported); and orthorhombic *zoisite* [$Ca_2Al_3[Si_2O_7][SiO_4]O(OH)$] with 156 occurrences. In addition, Mn-bearing *piemontite* [$Ca_2Al_2Mn^{3+}(Si_2O_7)(SiO_4)O(OH)$] is an important phase in metamorphosed manganese deposits, though we record only 7 occurrences. Metamorphic *epidote* is found most commonly via contact metamorphism of carbonate-bearing sediments and mafic igneous rocks (Joplin 1968;

Reverdatto and Sóbolev 1973), but also in regional (Harker 1950), high-pressure (Carswell 1990), and xenolith (Grapes 2006) contexts. Note, however, that it may be difficult to distinguish metamorphic *epidote* and *zoisite* (see below) from examples formed by metasomatism (Joplin 1968).

Zoisite generally forms at lower metamorphic grades than *epidote*, though it can coexist with *epidote* in medium-grade regional metamorphic rocks derived from calcareous sediments or mafic igneous rocks (Myer 1966; Ackermand and Rasse 1973; Raith 1976). *Zoisite* is also common in *kyanite*-bearing ecologite (Carswell and Compagnoni 2003), where it may form by a prograde reaction from *lawsonite* (Deer et al. 1986).

We lump two species, lawsonite and itoigawaite, into the root kind *lawsonite* [$(Ca,Sr)Al_2(Si_2O_7)(OH)_2{\cdot}H_2O$], with 11 occurrences in Supplementary Table 3. *Lawsonite* forms exclusively in high-pressure blueschist or eclogite facies rocks (Philpotts and Ague 2009), commonly in association with *glaucophane* and an epidote group mineral, either *zoisite* or *epidote* (Coleman et al. 1965; Carswell 1990).

Rankinite ($Ca_3Si_2O_7$), with 20 occurrences, is found exclusively in contact metamorphic rocks, commonly in association with *larnite*, *melilite*, *spurrite*, and/or *wollastonite* (Reverdatto and Sóbolev 1973; Grapes 2006).

The melilite group includes the solid solution between åkermanite [$Ca_2(Al_2SiO_7)$] and gehlenite [$Ca_2(MgSi_2O_7)$], as well as alumoåkermanite [$(Ca,Na)_2(Al,Mg,Fe^{2+})(Si_2O_7)$]—minerals that we lump into the root mineral kind *melilite*. With 108 occurrences in Supplementary Table 3, *melilite* is a common mineral in pyrometamorphosed siliceous limestone and dolomite,

2123 particularly at pyroxene hornfels and sanidinite facies (Reverdatto and Sóbolev 1973; Grapes
2124 2006), often forming at the expense of *diopside* or *anorthite* (Bowen 1940; Reverdatto 1970).

2125 *Pumpellyite* [$Ca_2(Al,Fe^{2+},Fe^{3+})_3(Si_2O_7)(SiO_4)(OH,O)_2 \cdot H_2O$] lumps 9 closely-related species of
2126 Ca-Al-Fe sorosilicates that are found most frequently in the low-grade zeolite and pumpellyite-
2127 prehnite facies of regional metamorphism. We list 10 occurrences, all of which occur in low-
2128 grade metapelites (Joplin 1968; Botha 1983; Augustithus 1985). However, Deer et al. (1986)
2129 note that Al-rich *pumpellyite* also occurs in blueschist facies, and Fe- and Mn-rich pumpellyite
2130 may occur in mineralized skarn zones.

2131 We lump 10 IMA-CNMNC-approved species, most of which are rare compositional variants,
2132 into *vesuvianite* [$(Ca,Na)_{19}(Al,Mg,Fe)_{13}(SiO_4)_{10}(Si_2O_7)_4(OH,F,O)_{10}$]. We record 15 occurrences in
2133 contact metamorphosed limestone, in which it is a characteristic skarn mineral, commonly in
2134 association with *diopside*, *grossular*, and/or *wollastonite* (Harker 1950). *Vesuvianite* occurs less
2135 commonly in regional metamorphosed limestones (Tilley 1927; Deer et al. 1982). Note that, as
2136 with the example of *epidote*, it may be difficult to distinguish *vesuvianite* formed by
2137 metamorphism versus metasomatism (Joplin 1968).

2138

2139 **Cyclosilicates**

2140 Members of the cordierite, tourmaline, and osulmilite groups are relatively common
2141 metamorphic cyclosilicates. We lump the species cordierite (with Mg) and sekaninaite (with
2142 Fe^{2+}) into the root mineral kind *cordierite* [$(Mg,Fe^{2+})_2Al_4Si_5O_{18}$], which, with 395 occurrences in
2143 Supplementary Table 3, is among the most common minerals in contact and regionally
2144 metamorphosed pelites (Joplin 1968; Reverdatto and Sóbolev 1973; Botha 1983; Grapes 2006).

Deer et al. (1986) detail a wide range of *cordierite* parageneses, including pyrometamorphosed xenoliths, contact metamorphosed argillaceous sediments, and a range of regional metamorphic facies, including low-pressure, high-temperature assemblages with *andalusite*; moderate-pressure assemblages with *sillimanite* and garnet; and high-pressure assemblages with *kyanite*.

Tourmaline [$(Na,Ca,\square)(Mg,Al,Fe^{2+},Fe^{3+},Ti^{4+})_3(Al,Fe^{3+},Mg)_6(Si_6O_{18})(BO_3)_3(OH)_3(O,F)$] is the only common boron-bearing mineral in metamorphic rocks (Deer et al. 1986; Henry et al. 2011; Henry and Dutrow 2012). We lump 18 IMA-CNMNC-approved species of the tourmaline group (Supplementary Table 1), all of which have been reported from regional metamorphic environments. The 47 *tourmaline* occurrences listed in Supplementary Table 3, including several examples of *tourmaline*-dominant tourmalinites, are from metapelites (Harker 1950; Joplin 1968). Joplin (1968) suggests that metamorphic tourmaline occurs in 3 distinct ways: as a remnant mineral of the protolith, through metamorphism of a borate-containing lithology, or as the result of boron metasomatism.

Osumilite [$(K,Na)(Fe^{2+},Mg)_2(Al,Fe^{3+})_3(Si,Al)_{12}O_{30}$] was reported in 13 of our mineral modes, typoically from ultrahigh temperature metamorphosed pelites, in which it commonly occurs with *cordierite*, *orthopyroxene*, *sanidine*, and/or *sillimanite* (Harley 2021).

Inosilicates

Among the 94 relatively common metamorphic minerals listed in Table 2, 16 are chain silicates, including several members of the pyroxene (7 kinds) and amphibole (7 kinds) groups

This is the peer-reviewed, final accepted version for American Mineralogist, published by the Mineralogical Society of America.
The published version is subject to change. Cite as Authors (Year) Title. American Mineralogist, in press.
DOI: https://doi.org/10.2138/am-2023-9004. http://www.minsocam.org/

(Deer et al. 1997a, 1997b). Inosilicates are one of the most common classes of metamorphic minerals, occurring in 1387 (50 %) of the 2785 metamorphic rocks in Supplementary Table 3.

Pyroxene Group: We consider 7 root kinds of pyroxene group single-chain silicates, most of which lie in or near the [$(Ca,Mg,Fe)_2Si_2O_6$] quadrilateral (Deer et al. 1997a).

Orthopyroxene lumps 281 occurrences of orthorhombic pyroxenes, most often described as enstatite (the Mg end-member) or "hypersthene" (with Mg ~ Fe^{2+}) but sometimes "bronzite" (with Mg > Fe^{2+}) or ferrosilite (the Fe^{2+} end-member), always lying close to the $MgSiO_3$—$Fe^{2+}SiO_3$ binary. *Orthopyroxene* most often occurs in granulite, ecologite, and UHT facies of metamorphosed ultramafic and mafic igneous rocks, in which it is often the most abundant mafic phase (Joplin 1968; Augustithus 1985; Carswell and Compagnoni 2003). It also occurs in lower-grade regional metamorphic rocks (Joplin 1968; Botha 1983), with iron-rich examples in metamorphosed iron formations (Kranck 1961; Simmons et al. 1974). *Orthopyroxene* is not uncommon in contact metamorphic environments, including pyrometamorphosed xenoliths (Reverdatto and Sóbolev 1973; Grapes 2006). In some instances, Mg-rich *orthopyroxene* is associated with carbonate minerals (Schreyer et al. 1972; Ohnmacht 1974).

Three Ca-bearing clinopyroxenes, *diopside* [$Ca(Mg,Fe^{2+})Si_2O_6$; 409 occurrences in Supplementary Table 3), *hedenbergite* ($CaFe^{2+}Si_2O_6$; 16 occurrences), and the ternary solid solution *augite* [$(Ca,Mg,Fe^{2+})_2Si_2O_6$, typically with $0.5 < Ca/(Mg+Fe) < 0.9$; 150 occurrences], are common in a wide variety of metamorphic rocks (Deer et al. 1997a). Pyroxenes close to the continuous CaMg—$CaFe^{2+}$ solid solution between *diopside* and *hedenbergite* are most typical of thermally metamorphosed carbonate and calc-silicate rocks, occurring in xenolithes and

2188 contact metamorphic contexts (Grapes 2006). We define *diopside* broadly to include most
2189 intermediate Mg-Fe compositions (e.g., "salite" and "ferrosalite"), as well as Al-bearing
2190 "fassaite." More than 80% of occurrences of *diopside*, the most abundant pyroxene in our
2191 survey, arise from contact metamorphism. Diopside also occurs in regional and high-pressure
2192 metamorphic rocks, with several examples from amphibolite facies (Harker 1950; Augustithus
2193 1985) and eclogite facies (Carswell 1990; Carswell and Compagnoni 2003).

2194 *Hedenbergite* displays much the same parageneses as *diopside*, but with Fe-rich protoliths
2195 (Joplin 1968; Augustithus 1985). We debated whether to lump these two end-members, but
2196 *hedenbergite* appears to form a discrete cluster of metamorphic clinopyroxenes with low Mg.
2197 Cluster analysis of igneous and metamorphic clinopyroxenes represents an important future
2198 research goal.

2199 The IMA-CNMNC-approved species augite, including clinopyroxenes in the
2200 $[(Ca,Mg,Fe^{2+})_2Si_2O_6]$ system with Ca occupying between ~25 and ~45 atom percent of the Ca-
2201 Mg-Fe sites, is equivalent to our root kind *augite*. The 150 occurrences in Supplementary Table
2202 3, while mostly from contact metamorphism or pyrometamorphism of ultramafic/mafic
2203 lithologies (Reverdatto and Sóbolev 1973; Grapes 2006), also include representatives derived
2204 by regional metamorphism of mafic and intermediate igneous protoliths (Harker 1950; Joplin
2205 1968; Ferry 1987).

2206 Three Na-bearing clinopyroxenes, *Aegirine* $[(Ca,Na)(Fe^{3+},Mg,Fe^{2+})Si_2O_6$; 16 occurrences],
2207 *jadeite* ($NaAlSi_2O_6$; 34 occurrences), and *omphacite* $[(Ca,Na)(Mg,Fe,Al)Si_2O_6$; 151 occurrences]
2208 are especially characteristic of high-pressure metamorphic environments. *Aegirine*, in which we
2209 lump two IMA-CNMNC-approved species aegirine ($NaFe^{3+}Si_2O_6$) and aegirine-augite

2210 [(Ca,Na)(Fe^{3+},Mg,Fe^{2+})Si_2O_6], is the least common of these phases in metamorphic rocks, being
2211 found primarily in the context of mafic and intermediate igneous rocks subjected to ultrahigh
2212 pressure and ecologite facies (Carswell 1990), though *aegirine* also occurs via contact
2213 metamorphism of alkaline rocks (Reverdatto and Sóbolev 1973). A complication is the
2214 formation of *aegirine* through sodium metasomatism of prior pyroxenes (Moore 1973; Deer et
2215 al. 1997a).

2216 *Jadeite* is a diagnostic phase found exclusively in high-pressure metamorphic environments,
2217 including blueschist facies, eclogite facies, and ultrahigh pressure metamorphic rocks (Carswell
2218 1990). It often forms through the iconic reaction *albite* → *jadeite* + *quartz* (Deer et al. 1997a,
2219 and references therein). *Jadeite* commonly incorporates up to 15 mol % of an
2220 *aegirine*/*omphacite* component; however, a significant compositional gap separates *jadeite*
2221 from these phases, which often coexist in high-pressure assemblages (Coleman and Clark 1968).

2222 *Omphacite*, which represents a solid solution among *aegirine*, *diopside*, and *jadeite*, is a
2223 relatively common phase in high-pressure metamorphic rocks. All 151 occurrences in our
2224 tabulation were reported from blueschist, eclogite, or ultrahigh-pressure environments, most
2225 often with ultramafic or mafic protoliths and often in association with *glaucophane*,
2226 *pyrope/almandine*, and *quartz/coesite* (Carswell 1990; Carswell and Compagnoni 2003).

2227

2228 <u>*Pyroxenoid Group:*</u> Two members of the inosilicate pyroxenoid group, *wollastonite* ($CaSiO_3$;
2229 158 occurrences) and the Mn-bearing *rhodonite* [$CaMn_3Mn(Si_5O_{15})$; 8 occurrences, not listed
2230 among the top 94 phases], are most commonly associated with skarn zones. Almost all

wollastonite reports are from carbonate or calc-silicate protoliths subjected to pyroxene hornfels or sanidinite facies metamorphism (Reverdatto and Sóbolev 1973; Grapes 2006).

Rhodonite, which lumps 4 closely-related species of Mn pyroxenoids, is most frequently encountered in the high-pressure metamorphic environments of Mn-rich protoliths (Carswell 1990), notably by reaction of *rhodochrosite* ($MnCO_3$; Hori 1962), though it can also form through Mn metasomatism (Bilgrami 1956).

Amphibole Group: The amphibole group of double-chain silicates, which boasts more than 110 IMA-CNMNC-approved species (https://rruff.info/ima; accessed January 13, 2023), is likely the most diverse of all mineral structure types (Deer et al 1997b; Hawthorne et al. 2011). Here, we provisionally lump 55 amphibole species known to occur in metamorphic rocks into 7 root mineral kinds. It should be noted, however, that the variety of amphibole parageneses, coupled with the extensive and complex solid solutions and miscibility gaps among many species, render any suggestion of amphibole mineral kinds tentative, at best. In the context of metamorphism, we have yet to determine if different facies, different protoliths, effects of metasomatism, prograde versus retrograde formation, and other factors may yield numerous distinct combinations of paragenesis and attributes. We require data resources with analyses of tens of thousands of well-characterized amphibole specimens, coupled with advanced methods of cluster analysis (Boujibar et al. 2021; Hystad et al. 2021). Such an epic endeavor could represent a lifetime of fruitful study for an ambitious young mineralogist.

Anthophyllite [$\square(Mg,Fe^{2+})_2(Mg,Fe^{2+},Fe^{3+},Al)_5(Si,Al)_8O_{22}(OH)_2$; with 52 occurrences in Supplementary Table 3], lumps 6 species of the complex anthophyllite/ferro-

This is the peer-reviewed, final accepted version for American Mineralogist, published by the Mineralogical Society of America.
The published version is subject to change. Cite as Authors (Year) Title. American Mineralogist, in press.
DOI: https://doi.org/10.2138/am-2023-9004. http://www.minsocam.org/

anthophyllite/gedrite/ferro-gedrite solid solution of orthorhombic amphiboles (Ferré 1989). An unresolved question regards the possible presence of a miscibility gap in this system between Al-rich (at times with Na) and Al-poor orthoamphiboles (Hawthorne et al. 1980; Spear 1982). If so, then at least two root mineral kinds would be warranted. Most of the examples in our compilation arise from hornblende-hornfels or pyroxene-hornfels facies contact metamorphism of ultramafic/mafic igneous rocks or pelitic sediments, often in association with *biotite*, *cordierite*, and *quartz* (Reverdatto and Sóbolev 1973). We also record a number of instances of *anthophyllite* in regional metamorphic settings, including amphibolite and granulite facies metamorphism of pelites and ultramafic rocks (Joplin 1968).

The closely-related clinopyroxenes *cummingtonite* [$\square Mg_2Mg_5Si_8O_{22}(OH)_2$; with 12 occurrences] and *grunerite* [$\square Fe^{2+}{}_2Fe^{2+}{}_5Si_8O_{22}(OH)_2$; with 8 occurrences, hence not listed among the top 94] are the monoclinic polymorphs of anthophyllite and ferro-anthophyllite. All but one of the *cummingtonite* examples in our tabulation, with Mg/(Mg+Fe) generally > 0.4 (i.e., in some instances with Fe > Mg), are from metapelites subjected to hornblende-hornfels facies contact metamorphism (Reverdatto and Sóbolev 1973). The more iron-rich *grunerite* examples, by contrast, are primarily from amphibolite or granulite facies regionally metamorphosed iron formations (Joplin 1968; Kimball and Spear 1984). Therefore, we provisionally distinguish these two closely-related mineral kinds based on paragenetic mode, even though they may display continuous solid solution between the Mg and Fe^{2+} end-members. It should be noted that as a result of miscibility gaps, *cummingtonite* and *grunerite* often occur in assemblages with multiple amphiboles, including calcic *hornblende*, Al-bearing *anthophyllite*, and/or a sodic amphibole (Deer et al. 1997b).

This is the peer-reviewed, final accepted version for American Mineralogist, published by the Mineralogical Society of America.
The published version is subject to change. Cite as Authors (Year) Title. American Mineralogist, in press.
DOI: https://doi.org/10.2138/am-2023-9004. http://www.minsocam.org/

Several calcic clinoamphiboles are common constituents of metamorphic rocks. *Tremolite* [□$Ca_2(Mg_{5.0\text{-}4.5}Fe^{2+}_{0.0\text{-}0.5})Si_8O_{22}(OH,F)_2$; with 122 occurrences] is typically an almost pure Ca-Mg phase (i.e., low Fe^{2+}) formed from ultramafic/mafic igneous or calc-silicate sediments in contact, regional, and high-pressure metamorphic environments. Most of the examples in Supplementary Table 3 are from muscovite-hornfels, hornblende-hornfels, or pyroxene-hornfels contact metamorphic zones, in which *tremolite* is associated with *diopside*, *dolomite*, *grossular*, *talc*, and/or other Ca-Mg phases (Reverdatto and Sóbolev 1973). We lump the OH^-- and F^--bearing species, which display a complete solid solution and share the same paragenesis.

Actinolite [□$Ca_2(Mg,Fe^{2+})_5Si_8O_{22}(OH,F)_2$; with 74 occurrences] lumps the species actinolite and ferro-actinolite, spanning a range 0.9 > Mg/(Mg + Fe^{2+}) > 0 (Deer et al. 1997b). Though chemically and structurally similar to *tremolite*, *actinolite* is distinguished both by its greater Fe^{2+} content and by its common association in metapelites or metabasites with *biotite, epidote* or *zoisite*, and/or *quartz* in high-pressure, regional, or contact metamorphic settings (Harker 1950; Joplin 1968; Botha 1983; Carswell 1990).

We lump 26 IMA-CNMNC-approved metamorphic species of Ca-(+/-Na,K)-clinoamphiboles into *hornblende* [$(Na,K)Ca_2(Mg,Fe^{2+},Al,Fe^{3+})_5(Si,Al)_8O_{22}(OH,F,Cl)_2$; with 387 occurrences]. This complex group displays significant compositional plasticity, with solid solutions among Na, K, and vacancies in alkali sites; Mg-Fe^{2+}-Fe^{3+}-Al in octahedral sites; and Al-Fe^{3+}-Si in tetrahedral sites, as well as among OH, F, and Cl (Deer et al. 1997b; Hawthorne et al. 2011; see Supplementary Tables 1 and 2). *Hornblende*, a defining phase in hornblende-hornfels and amphibolite facies rocks, appears in numerous metamorphic environments, including contact metamorphism (albite-epidote to sanidinite facies; Reverdatto and Sóbolev 1973; Grapes

2006), regional metamorphism (greenschist to granulite facies; Harker 1950; Joplin 1968), and high-pressure metamorphism (blueschist to eclogite facies; Reverdatto and Sóbolev 1973; Carswell 1990). *Hornblende* protoliths, similarly, span a wide range of igneous, sedimentary, and metamorphic rocks. *Hornblende* in metamorphic rocks commonly coexists with other amphiboles, including *anthophyllite*, *cummingtonite*, and *grunerite* (Deer et al. 1997b). Given the complexity of this mineral group, cluster analyses of numerous hornblende samples based on composition, paragenesis, and mineral associations, would doubtless reveal many distinct kinds of *hornblende*.

We lump a wide range of Na-Ca clinoamphiboles into *richterite*, defined here as $[(\square,Na)(NaCa)(Mg,Fe^{2+},Al,Fe^{3+})_5(Si,Al,Fe^{3+})_8O_{22}(OH)_2]$. Although we record only 12 occurrences in Supplementary Table 3, most of which were originally described as barroisite [nominally $(\square NaCa)(Mg_3Al_2)(Si_7Al)O_{22}(OH)_2$] or winchite $[(\square NaCa)(Mg_4Al)Si_8O_{22}(OH)_2]$, we lump 16 IMA-CNMNC-approved species into the root natural kind *richterite*, while acknowledging that much more work is needed to fully characterize these minerals and their associated parageneses. Most of the *richterite* occurrences that we record are metamorphosed mafic rocks from eclogite facies, almost always in association with *omphacite*, *pyrope*, and *rutile* (Binns 1967; Carswell 1990), though it is reported from regionally metamorphosed basalt, as well (Iwasaki 1960).

The sodium amphibole *glaucophane* $[\square Na_2(Mg,Fe^{2+})_3Al_2Si_8O_{22}(OH)_2$; with 79 occurrences] lumps 2 species, glaucophane and ferro-glaucophane, which form a Mg-Fe^{2+} solid solution. All of the examples in Supplementary Table 3 are from high-pressure metamorphism (most

This is the peer-reviewed, final accepted version for American Mineralogist, published by the Mineralogical Society of America.
The published version is subject to change. Cite as Authors (Year) Title. American Mineralogist, in press.
DOI: https://doi.org/10.2138/am-2023-9004. http://www.minsocam.org/

commonly blueschist or eclogite facies, but also ultrahigh-pressure facies) of mafic/intermediate igneous rocks or Mg-bearing sediments (Augustithus 1985; Carswell 1990).

One additional inosilicate group, *sapphirine* [$(Mg,Fe^{2+},Al,Fe^{3+})_8O_2(Al,Si)_6O_{18}$, 28 occurrences], is important as a key indicator of the temperature (> 900 °C) of ultrahigh temperature metamorphic rocks formed from ultramafic protoliths (Monchoux 1972; Deer et al. 1997a; Carswell and Compagnoni 2003; Harley 2021). It commonly occurs in association with *orthopyroxene* and *sillimanite*.

Phyllosilicates

Mica Group: With 1244 occurrences in Supplementary Table 3 (45% of the 2795 rocks surveyed), the mica minerals are prominent constituents of many metamorphic lithologies (Guidotti 1984; Fleet 2003). We lump 15 IMA-CNMNC-approved species into five root mineral kinds of micas: *biotite*, *phlogopite*, *phengite*, *muscovite*, and *paragonite*. However, there undoubtedly exist many more kinds of metamorphic micas, the identification of which will require the construction of extensive mica databases and application of cluster analysis (Hazen 2019). In paticular, widely occurring metamorphic *biotite* and *muscovite* will likely be split into multiple natural kinds.

We define the familiar group of dark-colored, Fe^{2+}-bearing trioctahedral mica species as *biotite* [$KFe^{2+}_2(Fe^{2+},Mg,Mn^{2+})(Si,Al,Fe^{3+})_2Si_2O_{10}(OH,F,Cl)_2$; 822 occurrences]. We lump 6 IMA-CNMNC-approved species, which are themselves rarely identified in the petrographic literature. Few minerals occur in as a diverse array of metamorphic environments as *biotite*, which we record from low-pressure pyrometamorphic, contact, regional, and high-pressure

This is the peer-reviewed, final accepted version for American Mineralogist, published by the Mineralogical Society of America.
The published version is subject to change. Cite as Authors (Year) Title. American Mineralogist, in press.
DOI: https://doi.org/10.2138/am-2023-9004. http://www.minsocam.org/

metamorphism, typically of pelites, but also of ultramafic, mafic, intermediate, acidic, and (rarely) agpaitic igneous rocks, as well as Fe-bearing impure carbonate and calc-silicate protoliths (Harker 1950; Joplin 1968; Reverdatto and Sóbolev 1973; Botha 1983; Carswell 1990; Fleet 2003; Grapes 2006).

We also lump 6 Mg-dominant species of trioctahedral micas, which are generally lighter in color than *biotite*, as *phlogopite* [$KMg_2(Mg,Fe^{2+},Mn^{2+},Fe^{3+},Ti^{4+})(Si,Al,Fe^{3+})_2Si_2O_{10}(OH,F)_2$; with 78 occurrences]. Though often combined with *biotite* in some descriptions of mica (e.g., Fleet 2003), and consequently sometimes reported as *biotite* in the petrologic literature, *phlogopite* displays distinct mineral associations in metamorphosed high-Mg, low-Fe environments, including ultramafic and dolomitic carbonate protoliths (Joplin 1968; Reverdatto and Sóbolev 1973). Owing to their diverse parageneses and compositional range, trioctahedral micas represent yet another mineral group that is ripe for investigation by cluster analysis.

The dioctahedral aluminous mica *muscovite* [$K(Al,Fe^{3+},Cr)_2(Si_3Al)O_{10}(OH)_2$; 515 occurrences], commonly reported with the varietal names illite, phengite, or sericite, is most characteristic of regionally and contact metamorphosed pelites (Reverdatto and Sóbolev 1973; Philpotts and Ague 2009), which represent most of the occurrences recorded in Supplementary Table 3. *Muscovite*, among the first phases to form during diagenesis of clay minerals (Fleet 2003), also occurs in a wide range of other contexts, including contact and regional metamorphosed arkosic, calc-silicate, and impure carbonate sediments (Philpotts and Ague 2009), as well as a variety of igneous protoliths (Harker 1950; Carswell 1990).

This is the peer-reviewed, final accepted version for American Mineralogist, published by the Mineralogical Society of America.
The published version is subject to change. Cite as Authors (Year) Title. American Mineralogist, in press.
DOI: https://doi.org/10.2138/am-2023-9004. http://www.minsocam.org/

We also include the fine-grained, Si-rich white mica *phengite* (110 occurrences) as a separate kind, even though it falls under IMA's definition of muscovite. Phengite is most commonly associated with high-pressure metamorphism (Carswell 1990).

The sodium trioctahedral mica *paragonite* [$NaAl_2(Si_3Al)O_{10}(OH)_2$; 67 occurrences] is characteristic of high-pressure eclogite facies metamorphism of mafic igneous rocks, often in association with *glaucophane, kyanite, omphacite*, and/or *pyrope* (Carswell 1990). *Paragonite*, often intimately intermixed with *phengite* (with which it has limited solid solution; e.g., Thompson and Thompson 1976; Guidotti et al. 1994), also occurs in low- and medium-grade metapelites, in which it can form by both prograde and retrograde reactions (Chatterjee 1970; Guidotti 1984; Guidotti and Sassi 1998; Fleet 2003). *Paragonite* also frequently co-occurs with the so-called "brittle mica" *margarite* [$CaAl_2(Si_2Al_2)O_{10}(OH)_2$] in a wide range of metamorphic grades of metasediments (Guidotti 1984; Fleet 2003); however, *margarite* is relatively rare in comparison to the micas described above, being reported from only one of the metamorphic rocks in our survey (Carswell and Compagnoni 2003, their Table 2).

Other phyllosilicates: More than 30 other IMA-CNMNC-approved layer silicates occur in metamorphic rocks (Supplementary Table 1). Most of these minerals (e.g., apophyllite group, *gillespite, pyrophyllte, stilpnomelane, zussmanite*) occur only rarely in metamorphic rocks. Note that we do not list diagenetically-formed clay minerals as metamorphic phases (Wilson 2013); they will be considered further in Part IX of this series. However, *chlorite*, *prehnite*, *serpentine*, and *talc* are included in our list of 94 relatively common metamorphic phases (Deer et al. 2009).

This is the peer-reviewed, final accepted version for American Mineralogist, published by the Mineralogical Society of America.
The published version is subject to change. Cite as Authors (Year) Title. American Mineralogist, in press.
DOI: https://doi.org/10.2138/am-2023-9004. http://www.minsocam.org/

Chlorite [$(Mg,Fe^{2+})_5(Al,Fe^{3+})(Si_3AlO_{10})(OH)_8$; 339 occurrences] encompasses 3 IMA-CNMNC-approved species of Mg-Fe^{2+}-Al-(Fe^{3+}) layer silicates: chamosite, clinochlore, and sudoite. *Chlorite* is common in pelites subjected to greenschist and amphibolite facies metamorphism (Harker 1950; Joplin 1968; Botha 1983), as well as from muscovite-, hornblende-, and pyroxene-hornfels facies contact metamorphism of pelites and basic igneous rocks (Joplin 1968; Reverdatto and Sóbolev 1973), often in association with *albite, biotite, muscovite*, and/or *quartz.* In addition, Coleman et al. (1965) and Carswell (1990) record more than a dozen examples of *chlorite* in eclogite facies high-pressure metamorphism. *Chlorite* forms through a variety of pathways, including prograde and retrograde metamorphism, both with and without external aqueous fluids. As such, *chlorite* represents a mineral whose often uncertain parageneses grade continuously from regional or "burial" metamorphism to metasomatism to hydrothermal alteration (Deer et al. 2009).

We lump 5 IMA-CNMNC-approved species, including three structural variants of $Mg_3Si_2O_5(OH)_4$ (antigorite, chrysotile, and lizardite), aluminous amesite, and Fe-bearing greenalite, into *serpentine* [$(Mg,Fe^{2+},Al,Fe^{3+})_3(Al,Si)Si(OH)_4$; 68 occurrences]. Most examples in Supplementary Table 3 are from low- to moderate-grade regional metamorphism of ultramafic/mafic igneous or pelitic protoliths (Joplin 1968; Philpotts and Ague 2009), in which they form primarily by retrograde/hydrothermal reactions from olivine and Mg-rich pyroxene or by prograde metamorphism of serpentinite (Deer et al. 2009, and references therein). Given its varied modes of formation, coupled with multiple polymorphs, cluster analysis of metamorphic *serpentine* is warranted.

Talc [$Mg_3Si_4O_{10}(OH)_2$; 73 occurrences] is characteristic of Mg-rich protoliths over a wide range of pressure-temperature condition. Examples include thermal metamorphism of *dolomite*-bearing sediments (Tilley 1948; Reverdatto and Sóbolev 1973; Augustithus 1985), high-pressure (blueschist and eclogite facies) metamorphism of basic igneous rocks (Chopin 1981; Carswell 1990), and greenschist to amphibolite grade regional metamorphism of ultramafic rocks (Harker 1950; Joplin 1968). Of special note are high-pressure to ultrahigh pressure (> 0.6 GPa) *talc-kyanite*-(*quartz/coesite*) assemblages known as "whiteschists" (Schreyer 1977), which form in the Mg-Al-Si-H ("MASH") system, at times with P_{H_2O} approximately equal to the total pressure.

Prehnite [$Ca_2Al(Si_3Al)O_{10}(OH)_2$; 16 occurrences], though most familiar as a hydrothermal phase associated with zeolites in amygdaloidal basalt, is also common in the eponymous prehnite-pumpellyite facies of low-grade regional metamorphism (Coombs 1960; Philpotts and Ague 2009). *Prehnite*, often in association with *chlorite* and *quartz*, is also present occasionally in metamorphosed basic igneous and pelitic sedimentary rocks from zeolite to lower amphibolite grades (Harker 1950; Joplin 1968; Botha 1983), at times the result of retrograde reactions (Coombs 1993).

Tectosilicates

A wide range of framework silicates, including the silica group, feldspars, feldspathoids, and zeolites (Deer et al. 2001, 2004), occur in metamorphic rocks, with one or more examples reported in 1595 (67 %) of the 2785 rocks surveyed in Supplementary Table 3. We focus attention on 10 mineral kinds that occur most frequently.

This is the peer-reviewed, final accepted version for American Mineralogist, published by the Mineralogical Society of America.
The published version is subject to change. Cite as Authors (Year) Title. American Mineralogist, in press.
DOI: https://doi.org/10.2138/am-2023-9004. http://www.minsocam.org/

2424

2425 *Silica Group:* Four silica group minerals—*quartz*, high-pressure *coesite*, and high-
2426 temperature *cristobalite* and *tridymite*—span the entire range of metamorphic environments,
2427 occurring in all but the most Si-deficient rocks (Deer et al. 2004).

2428 *Quartz* (SiO_2), with 1353 occurrences in our study (49 % of rocks in Supplementary Table 3),
2429 is the most common metamorphic mineral. It occurs in pyrometamorphosed xenoliths, contact
2430 metamorphic rocks, metamorphosed iron-manganese formations, high-pressure and regional
2431 metamorphic settings, metasomatized rocks, and shear zones (Supplementary Table 3 and
2432 references therein), often by recrystallization of protolith *quartz* (Deer et al. 2004). *Quartz* is
2433 stable in all crust and upper mantle pressure-temperature regimes except above ~2.7 GPa,
2434 where it transforms to *coesite*, or at low pressure above ~850 °C, where *cristobalite* and
2435 *tridymite* are the stable silica phases.

2436 *Coesite* (SiO_2; 23 occurrences) is restricted to ultrahigh pressure (> 2.7 GPa) metamorphic
2437 environments, where it is typically associated with *kyanite*, *omphacite*, and/or *pyrope* (Carswell
2438 and Compagnoni 2003). Several reports describe *coesite* as inclusions in upper mantle phases,
2439 including *pyrope* (Chopin 1984; Schertl et al. 1991) and *diamond* (Stachel et al. 2022, and
2440 references therein).

2441 *Cristobalite* (10 occurrences) and *tridymite* (44 occurrences) are high-temperature, low-
2442 pressure polymorphs of SiO_2 that occur almost exclusively in sedimentary rocks that have been
2443 thermally metamorphosed (pyroxene hornfels or sandinite facies) by basic igneous rocks (Agrell
2444 and Langley 1958; Reverdatto and Sóbolev 1973; Black 1989; Grapes 2006). These two minerals
2445 co-occur in 7 of the 10 reported rocks with *cristobalite*. *Tridymite* and *cristobalite* also are

associated in some burning coal deposits with temperatures that may exceed 1100 °C (Bustin and Matthews 1982; Grapes 2006), and therefore are the consequence of Phanerozoic biological precursors (to be considered in Part XII).

Feldspar Group: Metamorphic feldspar group minerals display compositions close to two binary solid solutions (Deer et al. 2001): the Na-Ca plagioclase feldspars and the Na-K alkali feldspars. In both instances we suggest modifications of the nomenclature approved by the IMA-CNMNC.

In the case of the plagioclase series [$(CaAl,NaSi)AlSi_2O_8$], we identify *albite* as compositions close to $NaAlSi_3O_8$ [Na/(Na+Ca) > 0.85 and often with > 10 mol % $KAlSi_3O_8$], *anorthite* as close to $CaAl_2Si_2O_8$ [Ca/(Ca+Na) > 0.85], and *plagioclase* as having intermediate compositions between ~An_{20} and ~An_{70} as valid root mineral kinds. We justify this division based on the existence of the so-called peristerite and Huttenlocker miscibility gaps between ~$An_{2\text{-}17}$ and $An_{65\text{-}88}$, respectively. As a consequence, several authors have recorded coexiting *albite-plagioclase* and *plagioclase-anorthite* pairs (Evans 1964; Botha 1983).

Albite, with 177 occurrences in Supplementary Table 3, is observed in a wide range of thermal, regional, and high-presssure metamorphic environments, with both igneous and sedimentary protoliths (Harker 1950; Joplin 1968; Reverdatto and Sóbolev 1973; Philpotts and Ague 2009). *Anorthite* (78 occurrences) is more restricted in its occurrences, being found primarily as a contact metamorphic mineral derived from calc-silicate and carbonate-bearing sediments (Grapes 2006), though it is also found in regionally metamorphosed mafic and calc-silicate rocks from amphibolite to granulite facies (Joplin 1968). *Plagioclase* (809 occurrences),

This is the peer-reviewed, final accepted version for American Mineralogist, published by the Mineralogical Society of America.
The published version is subject to change. Cite as Authors (Year) Title. American Mineralogist, in press.
DOI: https://doi.org/10.2138/am-2023-9004. http://www.minsocam.org/

like *quartz*, *albite*, and *kspar* (see below) is not a particularly diagnostic phase in metamorphic rocks because it occurs across the full spectrum of thermal, regional, and high-pressure metamorphic environments, with an equally broad range of igneous, sedimentary, and metamorphic protoliths. For a given protolith, the anorthite content of plagioclase tends to increase with metamorphic grade (Deer et al. 2001). Note that most reports of "plagioclase" in the older metamorphic literature lack compositional information; thus, some of these occurrences may fit our definitions of *albite* or *anorthite*.

The alkali feldspars are complicated by the existence of three K-rich ($KAlSi_3O_8$) variants—the higher-temperature (> 500 °C) monoclinic *sanidine* and two lower-temperature triclinic phases, microcline and orthoclase, which are often reported as "kspar" in the literature of metamorphic petrology. An additional consideration is that alkali feldspars of intermediate compositions often exsolve Na- and K-rich phases, typically reported as "perthite." In our study, we adopt the name *kspar* for microcline and orthoclase, and record both *albite* and *kspar* for perthite.

Sanidine (102 occurrences) is most commonly found in thermally metamorphosed rocks of pyroxene hornfels or sanidinite grade (Grapes 2006), though it also has been reported from ultrahigh pressure metamorphism of pelites (Carswell 1990; Carswell and Compagnoni 2003) and ultrahigh temperature regimes (Harley 2021).

Kspar (411 occurrences) has been reported from thermal (zeolite to pyroxene hornfels facies), regional (amphibolite to granulite facies), and high-pressure (eclogite to ultrahigh pressure facies) metamorphic environments. Protoliths for *kspar* include mafic, acidic, and agpaitic igneous rocks and arkosic, pelitic, and carbonate-bearing sedimentary rocks (Harker 1950; Joplin 1968; Reverdatto and Sóbolev 1973; Carswell 1990; Deer et al. 2001).

This is the peer-reviewed, final accepted version for American Mineralogist, published by the Mineralogical Society of America.
The published version is subject to change. Cite as Authors (Year) Title. American Mineralogist, in press.
DOI: https://doi.org/10.2138/am-2023-9004. http://www.minsocam.org/

2490 At the temperatures of UHT metamorphism (> 900 °C), an additional complication is the
2491 occurrence of Ca-Na-K ternary feldspars, which typically exsolve to a perthite with coexisting
2492 plagioclase and alkali feldspar lamellae (Harley 2008; Harley 2021, their Figure 20).
2493
2494 *Scapolite Group:* Three species of the scapolite group are lumped as *scapolite*
2495 [$(Na,Ca)_4Al_3(Al,Si)_3Si_6O_{24}(CO_3,SO_4,Cl)$, with 33 occurrences]. *Scapolite* is not infrequently
2496 observed in medium- to high-grade contact (hornblende-hornfels and pyroxene hornfels facies)
2497 and regional (amphibolite and granulite facies) metamorphosed pelites and calc-silicate
2498 sediments (Joplin 1968; Reverdatto and Sóbolev 1973), and has also been reported from the
2499 albite-epidote hornfels facies contact metamorphism of amygdaloidal basalt (Joplin 1968).
2500
2501 *Zeolite Group:* The zeolite facies is the lowest pressure-temperature regime of
2502 metamorphism, with temperatures < 200 °C at pressures < 0.3 GPa (Philpotts and Ague 2009).
2503 Most zeolite minerals form via low-temperature aqueous processes, including fluid interactions
2504 with cooling basalt and authigenesis (Deer et al. 2004). Nevertheless, some zeolite occurrences
2505 are attributed to metamorphism, *sensu stricto.* Though not sufficiently abundant to include
2506 among the most common metamorphic phases, *analcime* (2 occurrences), *laumontite* (1), and
2507 *wairakite* (2), as well as 6 undifferentiated reports of "zeolite," were listed in modes of low-
2508 grade metamorphosed mafic igneous rocks and pelites (Joplin 1968).
2509
2510 *Feldspathoid Group:* None of the members of the sub-silicic feldspathoid framework silicate
2511 group is common in metamorphic rocks. Nevertheless, *kalsilite*, *leucite*, and *nepheline* (with 5,

2, and 4 occurrences, respectively) are representative of undersaturated pyrometamorphosed calc-silicates (Grapes 2006).

To these framework silicates, we add *silicate glass* [(Si,Al,Ca,Mg,Fe)O; SiO_2 > 70 wt %; with 68 occurrences] as an important yet often poorly characterized metamorphic phase in thermal metamorphic environments, particularly of arkosic sandstones and pelites (Reverdatto and Sóbolev 1973; Grapes 2006). Two varietal names of metamorphic glass are "buchite," which forms when a silica-rich pelitic rock is altered by igneous contact, and "porcellanite," a glass derived from pyrometamorphosed clay, marl, shale, or bauxite (Grapes 2006). Melting and glass formation may occur as low as ~650 °C at 0.5 GPa in a granite protolith, or > 1000 °C at low pressure and dry conditions. Grapes (2006) details how "Si-rich glass" in many pyrometamorphic zones typically contains significant Al_2O_3 and alkalis, a consequence of quartz-feldspar melting. Note that pure SiO_2 melts at 1700 °C—a temperature only attainable by lightning strikes or bolide impacts.

Rarer Metamorphic Minerals: In addition to the 94 mineral kinds outlined above, 661 other mineral kinds occur rarely as trace phases in metamorphic rocks, as documented by reports in numerous primary sources and compilations, notably Anthony et al. (1990-2003) and references cited in https://mindat.org and https://rruff.info/ima (both accessed 20 January 2023). Most of these scarce minerals, which are listed in Supplementary Table 1, were not recorded from any of the 2785 metamorphic rock modes in Supplementary Table 3.

2533 However, a few of the less common minerals in Supplementary Table 1, were also noted in
2534 one or more metamorphic rock modes. Among these minor minerals, listed alphabetically, are
2535 *alleghanyite* (1 occurrence), *analcime* (2), *anhydrite* (2), *ankerite* (6), *ardennite* (1), *arsenopyrite*
2536 (1), *axinite* (4), *bornite* (1), *braunite* (7), *bredigite* (6), *brownmillerite* (5), *bustamite* (4), *calzirtite*
2537 (3), *celestine* (1), *chondrodite* (4), *cuspidine* (2), *deerite* (2), *diaspore* (1), *fluorite* (1),
2538 *fluormayenite* (5), *friedelite* (1), *galaxite* (1), *giuseppeite* (1), *grunerite* (8), *hausmannite* (1),
2539 *hillbrandite* (1), *högbomite* (2), *ilvaite* (2), *jacobsite* (1), *kalsilite* (5), *kornerupine* (1), *kutnohorite*
2540 (1), *laumontite* (1), *leucite* (2), *margarite* (1), *monazite* (3), *nepheline* (4), *norbergite* (1),
2541 *piemontite* (7), *pigeonite* (2), *pyrophanite* (1), *pyroxmangite* (2), *qandilite* (3), *rhodocrosite* (2),
2542 *rhodonite* (8), *riebeckite* (4), *scawtite* (1), *siderite* (9), *sonolite* (1), *sphalerite* (9), *spessartine* (9),
2543 *stilpnomelane* (3), *suenoite* (5), *tephroite* (1), *thompsonite* (3), *uvarovite* (2), *wairakite* (2), and
2544 "zeolite" (6).

A

Community 1
High-T, Low-P

Community 2
Ca-Silicates, High T

Community 3
Contact Ca-Si

Community 4
Contact Mg-Si

Community 5
Regional Lower T

Community 6
High P

Mullite
Si-Glass
Cristobalite
Corundum
Tridymite
Pseudobrookite
Sillimanite
Cordierite
Sanidine
Anorthite
Andalusite
Hercynite
Perovskite
Spurrite
Larnite
Sapphirine
Hedenbergite
Merwinite
Osumilite
Fayalite
Spinel
Monticellite
Rankinite
Staurolite
Tilleyite
Wollastonite
Melilite
Andradite
Scapolite
Vesuvianite
Grossular
Periclase
Tourmaline
Calcite
Diopside
Cummingtonite
Allanite
Humite
Olivine
Anthophyllite
Phlogopite
Coesite
Forsterite
Pyrope
Chalcopyrite
Fe-Dolomite
Brucite
Diamond
Baddeleyite
Graphite
Prehnite
Zoisite
Geikielite
Pumpellyite
Kyanite
Aegirine
Aragonite
Serpentine
Chloritoid
Tremolite
Jadeite
Dolomite
Phengite
Lawsonite
Chlorite
Pentlandite
Omphacite
Talc
Paragonite
Richterite
Chromite
Magnesite
Glaucophane

B

Dolostone
Sanidinite
Facies

Sillimanite-
Cordierite
Gneiss

Wollastonite
Marble

Calcite Skarn

UHP
Eclogite

Prehnite-
Pumpellyite
Facies

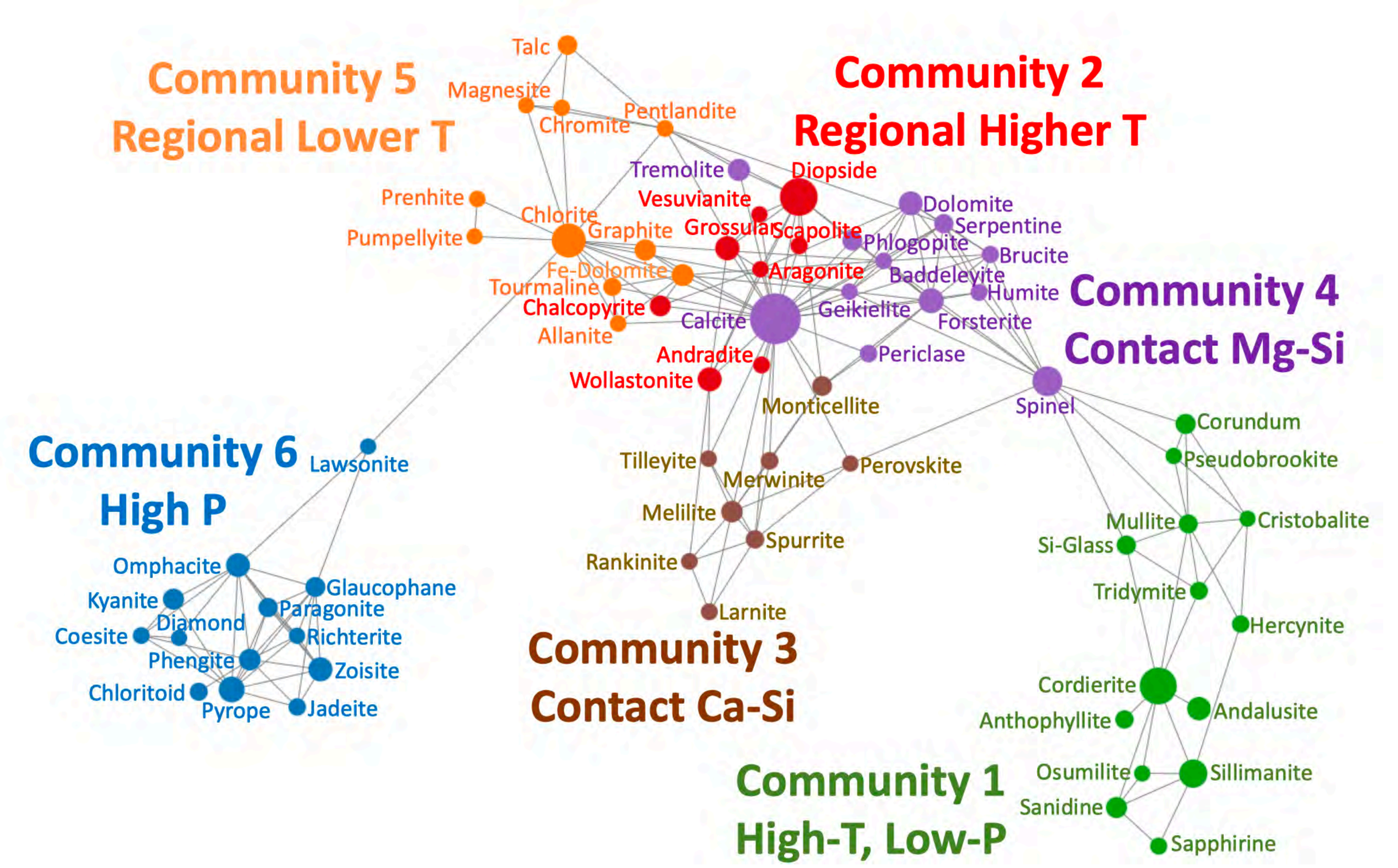
Community 5
Regional Lower T
Talc
Magnesite
Chromite
Pentlandite
Community 2
Regional Higher T
Tremolite
Diopside
Prenhite
Vesuvianite
Dolomite
Chlorite
Graphite
Grossular
Scapolite
Serpentine
Pumpellyite
Phlogopite
Brucite
Fe-Dolomite
Aragonite
Baddeleyite
Tourmaline
Humite
Community 4
Contact Mg-Si
Chalcopyrite
Calcite
Geikielite
Forsterite
Allanite
Andradite
Periclase
Wollastonite
Monticellite
Spinel
Corundum
Community 6
High P
Lawsonite
Tilleyite
Merwinite
Perovskite
Pseudobrookite
Omphacite
Melilite
Mullite
Cristobalite
Glaucophane
Kyanite
Paragonite
Spurrite
Si-Glass
Diamond
Rankinite
Tridymite
Coesite
Richterite
Hercynite
Phengite
Zoisite
Larnite
Community 3
Contact Ca-Si
Cordierite
Chloritoid
Andalusite
Anthophyllite
Pyrope
Jadeite
Community 1
High-T, Low-P
Osumilite
Sillimanite
Sanidine
Sapphirine

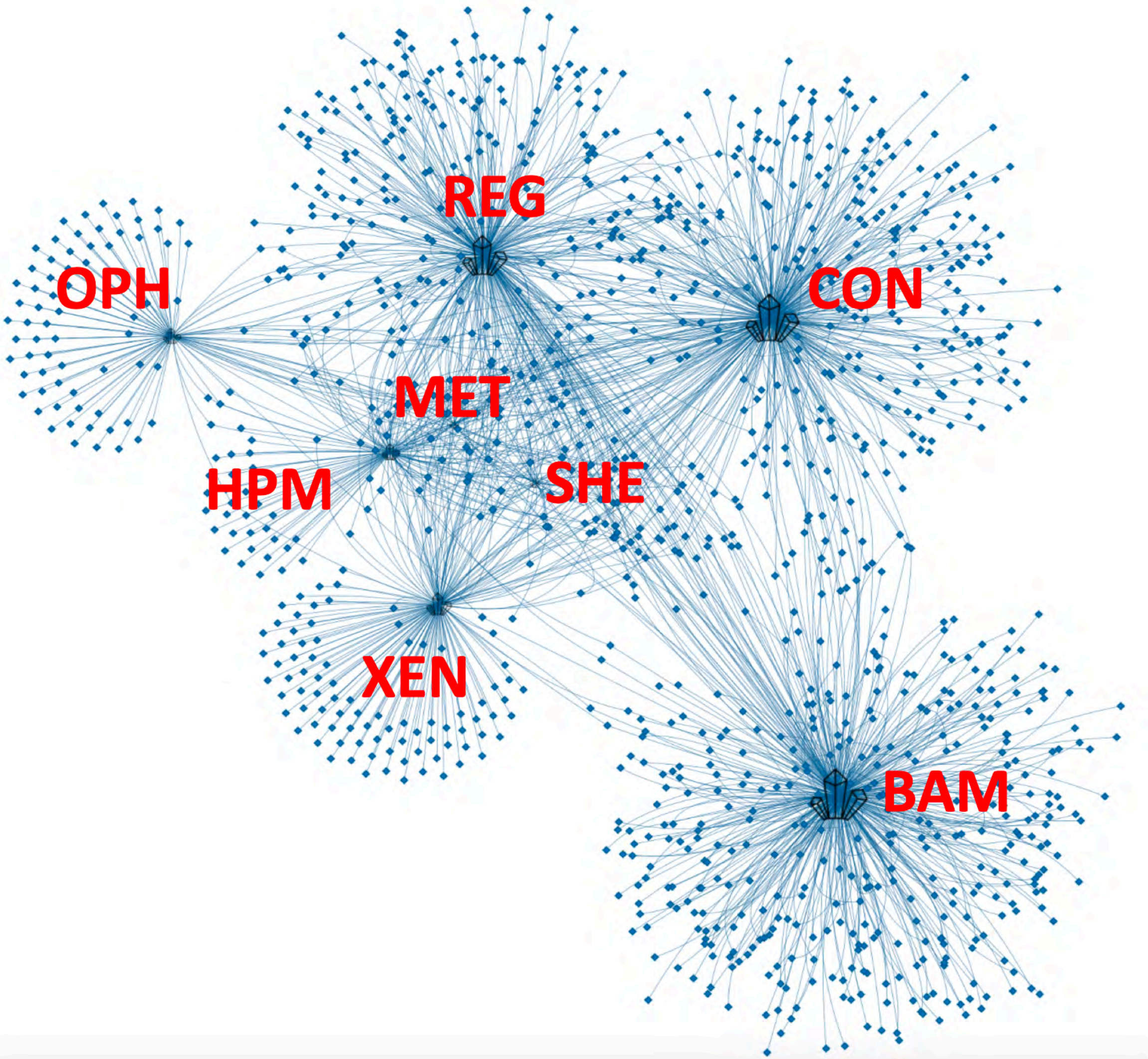
REG
OPH
CON
MET
HPM
SHE
XEN
BAM